A Dissertation

entitled

The AIB interneurons are modulated by excitatory and inhibitory signaling pathways to shape aversive behaviors in response to 1-octanol

by

Robert Layne

Submitted to the Graduate Faculty as partial fulfillment of the requirements for the

Doctor of Philosophy Degree in

Biology

_____
Dr. Bruce Bamber, Committee Chair

_____
Dr. Richard Komuniecki, Committee Member

_____
Dr. Robert Steven, Committee Member

_____
Dr. Guofa Liu, Committee Member

_____
Dr. Scott Molitor, Committee Member

_____
Dr. John Bellizzi, Committee Member

_____
Dr. Patricia Komuniecki, Dean
College of Graduate Studies

The University of Toledo

September 2015

Copyright 2015, Robert Layne

This document is copyrighted material. Under copyright law, no parts of this document may be reproduced without the expressed permission of the author.

An Abstract of

The AIB interneurons are modulated by excitatory and inhibitory signaling pathways to shape aversive behaviors in response to 1-octanol

by

Robert Layne

Submitted to the Graduate Faculty as partial fulfillment of the requirements for the Doctor of Philosophy Degree in
Biology

The University of Toledo

September 2015

Dysfunctional integration of sensory information is associated with numerous pathological conditions in the human nervous system, including autism spectrum disorders, attention deficit hyperactivity disorder (ADHD), and schizophrenia. In the model organism *Caenorhabditis elegans*, the noxious odorant 1-octanol is primarily sensed by the ASH sensory neurons, and presentation of the odorant causes animals to initiate an aversive response that is modulated by the presence of food or serotonin (5-HT). However, in the present study we found that presentation of 1-octanol to animals activates, inhibits, and has no effect on the glutamatergic ASH, AWC, and ASE right (ASER) sensory neurons, respectively. The ASHs, AWCs, and ASER all synapse onto a common postsynaptic pair of interneurons, the AIB interneurons.

The AIB interneurons profoundly affect animal behavior. Based on indirect evidence, the leading hypothesis states that some of the upstream glutamatergic sensory neurons signal onto the AIBs through receptors containing the AMPA-type subunit GLR-1. Using whole-cell patch clamp electrophysiology and calcium imaging, we found that glutamate evokes both an anionic current mediated by the glutamate-gated Cl^- (GluCl)

channel subunit AVR-14, and a cationic GLR-1-dependent current in the AIBs. Similarly, previous work has shown that tonic glutamate release from the AWCs and ASER onto GLR-1 and AVR-14 on the AIBs, respectively, differentially modulate 1-octanol-evoked aversive behaviors. Additionally, the L-type voltage-gated calcium channel (VGCC) subunit EGL-19 amplifies glutamate-evoked increases in AIB intracellular Ca^{2+} (iCa^{2+}). In addition to glutamate, acetylcholine also evokes an inhibitory current in the AIBs that is partially mediated by the acetylcholine-gated Cl^- (AChCl) channel subunit ACC-1. Interestingly, the AIA interneurons are cholinergic, direct much of their synaptic output onto the AIBs, are thought to inhibit the AIBs, and are also innervated by the ASHs, AWCs, and ASER. In order to correlate neuronal activity with animal behavior, we used calcium imaging to investigate the effects of the noxious odorant 1-octanol the AIAs and AIBs. Presentation of 1-octanol activates and inhibits the AIA and AIB interneurons, respectively, and odorant inhibition of the AIBs is partially dependent on both AVR-14 and cholinergic transmission from the AIAs. Together, these data demonstrate how multiple signaling pathways modulate a pair of interneurons to differentially shape animal behavior.

My dissertation is dedicated to my two sons, Maximus Penn Layne and Aaron Forbes Layne. You two are the most important people in my life, and I love you both, immensely.

Acknowledgements

First and foremost, I'd like to thank my advisor, Dr. Bruce Bamber, as his patience and guidance were of paramount importance to this project, my development as a scientist, and my maturation as an adult. I'd also like to thank Dr. Richard Komuniecki, Dr. Komuniecki's graduate student Philip Summers, and Dr. Komuniecki's lab technician Amanda Ortega for their constructive input and collaborative efforts. I would also like to thank Dr. Scott Molitor for his invaluable insights on this project, and his willingness to explain or clarify mathematical concepts. Additionally, I'd like to thank the various faculty members in the Department of Biological Sciences at the University of Toledo, especially Dr. Robert Steven, Dr. John Gray, Dr. Scott Leisner, Dr. Malathi Krishnamurthy, and Dr. Anthony Quinn for their willingness to help with questions relevant to their area of expertise. Finally, I'd like to thank thank my fellow lab members and friends at the University of Toledo, including Dr. Jeffrey Zahratka, Paul Williams, Dr. Holly Mills, Mitchell Oakes, Deanna Filppi, Tobias Clarke, Rahul Prasad, Brianne Gillespie, and Dr. Michael Bekier.

Table of Contents

List of Figures

List of Abbreviations

5-HT.....Serotonin

ACh.....Acetylcholine
AChCl.....Acetylcholine-gated Cl^-
ADHD.....Attention-deficit hyperactivity disorder
ADRA1B.....Adrenoreceptor alpha 1B
AMPA.....α-amino-3-hydroxy-5-methyl-4-xazolepropionic acid
ARS.....Area-restricted search
ASEL.....ASE left sensory neuron
ASER.....ASE right sensory neuron
Aversive behaviors.....Off food, animals reverse ~10 seconds after presentation of 30% 1-octanol, reverse a long distance (~2.5 body bends), and turn away from the odorant after completing backward locomotion

BDNF.....Brain-derived neurotrophic factor
bHLH.....Basic helix-loop-helix
BK.....Big potassium channel
BL.....Backward locomotion

Ca^{2+}.....Calcium ion with a net charge of +2
CADPS.....Ca^{2+}-dependent secretion activator
cAMP.....Cyclic adenosine monophosphate
Cd^{2+}.....Cadmium ion with a net charge of +2
cGMP.....Cyclic guanosine monophosphate
Cl^-.....Chloride ion with a net charge of -1
CNG.....Cyclic nucleotide-gated
CNGA1.....Cyclic nucleotide-gated alpha 1
CNGB1.....Cyclic nucleotide-gated beta 1
CNTF.....Ciliary neurotrophic factor
CPG.....Central pattern generator
Cu^{2+}.....Copper ion with a net charge of +2

DA.....Dopamine
DAT.....Dopamine transporter

DCV(s) ..... Dense-core vesicle(s)

Dilute IAA/1-octanol mixture ..... A mixture of 40% IAA and 30% 1-octanol diluted in ethanol (vol/vol)

EEG ..... Electroencephalogram

Enhanced aversive behaviors ..... Animals reverse ~5 seconds after presentation of 30% 1-octanol, reverse a short distance (~1.5 body bends), and continue moving forward after completing backward locomotion; food, 5-HT, ASER-specific *eat-4* overexpression, AIB-specific *avr-14* overexpression, heterologous inhibition of AIB signaling, animals presented with a dilute IAA/1-octanol mixture, and animals that experience a salt downstep prior to assaying aversive behaviors all display enhanced aversive behaviors

Enhanced initial aversive behavior ..... Animals reverse ~5 seconds after presentation of 30%; food, 5-HT, ASH-specific *eat-4* overexpression, ASER-specific *eat-4* overexpression, AIB-specific *avr-14* overexpression, heterologous inhibition of AIB signaling, animals presented with a dilute IAA/1-octanol mixture, and animals that experience a salt downstep prior to assaying aversive behaviors all display enhanced initial aversive behavior; animals off food presented with 100% 1-octanol also display enhanced initial aversive behavior

Enhanced postinitiation behaviors ..... After initiating a reversal following presentation of 30% 1-octanol, animals reverse a short distance (~1.5 body bends), and continue moving forward after completing backward locomotion; food, 5-HT, ASER-specific *eat-4* overexpression, AIB-specific *avr-14* overexpression, heterologous inhibition of AIB signaling, animals presented with a dilute IAA/1-octanol mixture, and animals that experience a salt downstep prior to assaying aversive behaviors all display enhanced aversive behaviors

fMRI ..... Functional magnetic resonance imaging

GABA ..... γ-aminobutyric acid
GAD ..... Glutamic acid decarboxylase
gf ..... *Gain-of-function* allele
Glu ..... Glutamate
GluCl ..... Glutamate-gated Cl^-
GPCRs ..... G protein-coupled receptors

HA ..... Histamine
HisCl1 ..... Histamine-gated Cl^- channel subunit 1

IAA .....Isoamyl alcohol
iCa^{2+} .....Intracellular Ca^{2+}
IGF .....Insulin-like growth factor
Initial aversive
behavior.....Off food, animals initiate an aversive response ~10 seconds after presentation with 30% 1-octanol

K^+ .....Potassium ion with a net charge of +1

LIF.....Leukemia inhibitory factor

MRI .....Magnetic resonance imaging

Na^+ .....Sodium ion with a net charge of +1
NaCl .....Sodium chloride salt
NPY .....Neuropeptide Y
NGM .....Nematode growth medium
NMDA .....N-methyl-D-aspartate
OA.....Octopamine

PAS .....Period circadian protein, aryl hydrocarbon receptor nuclear translocator protein, single-minded protein
PDE(s).....Phosphodiesterase(s)
PET .....Positron emission tomography
PI3 .....Phosphoinositide 3-kinase
Postinitiation
behavior.....After initiating a reversal following presentation of 30% 1-octanol, animals reverse a long distance (~2.5 body bends) and turn away from the odorant after completing backward locomotion
PUFA(s) .....Polyunsaturated fatty acid(s)

QRFPR.....Pyroglutamylated RFamide peptide receptor

RGC(s) .....Receptor guanylate cyclases
RGS.....Regulator of G protein signaling

Salt downstep .....Exposing an animal to a higher concentration of salt and then transferring animals/switching a solution to a lower concentration of salt
Salt upstep.....Exposing an animal to a lower concentration of salt and then transferring animals/switching a solution to a higher concentration of salt
SST.....Somatostatin
SV(s) .....Clear synaptic vesicle(s)

TA .....Tyramine
TH .....Tyrosine hydroxylase
TRP .....Transient receptor potential
TRPV .....Transient receptor potential vanilloid
TRPV1 .....Transient receptor potential cation channel subfamily V member 1
TRPV4 .....Transient receptor potential cation channel subfamily V member 4

VGCC(s) .....Voltage-gated Ca^{2+} channel
VIP .....Vasoactive intestinal peptide

List of Symbols

A.....Ampere
^{O}C.....Degrees celsius
F_0.....Baseline fluorescence
F_t.....Fluorescence at time t
m .....Meter
M.....Molar concentration
n.....Nano, 10^{-9}
p.....Pico, 10^{-12}
t_{abs}.....Time when trace averaged $\Delta F_t/F_0$ is greatest before either the maximum $\Delta F_t/F_0$ following a trace-averaged decrease or the minimum $\Delta F_t/F_0$ after a trace-averaged increase
t_{max}.....Time when $\Delta F_t/F_0$ is greatest after the trace averaged decrease
t_{min} .....Time when $\Delta F_t/F_0$ is least after the trace averaged increase

α.....Greek alpha, G protein subunit
γ.....Greek gamma, amino group is bound to the gamma carbon
Δ.....Greek delta, change in
μ .....Greek mu, micro, 10^{-6}

Chapter 1

Significance

An overarching goal in neuroscience is to understand how neurons integrate information from a variety of inputs and accordingly adjust neurotransmission to postsynaptic targets to produce a situationally appropriate behavioral response. A variety of nervous system pathologies result from dysfunctional integration of sensory inputs, including autism-spectrum disorders, schizophrenia, posttraumatic stress disorder, ADHD, and depression (Kantrowitz and Javitt 2010, Ghanizadeh 2011, Mueller-Pfeiffer, Schick et al. 2013). Neurons process information regarding various and potentially unrelated intrinsic and extrinsic sensory stimuli to modulate behavioral responses. Indeed, recent work supports that thousands of excitatory and inhibitory inputs compose recurrent networks that both dictate neuronal responsiveness and maintain persistent activity in the absence of sensory stimulation (Haider, Duque et al. 2006). These networks are functionally dependent on balanced excitatory and inhibitory signaling to maintain neurons at a noisy, depolarized level near their threshold of firing, despite changes in total membrane conductance (Haider, Duque et al. 2006). Novel therapies to correct excitatory and inhibitory signaling imbalances may be possible with a comprehensive understanding of neuronal integration, its effects on neurotransmission,

and the subsequent effects on neural network activity.

Approximately 86 billion neurons and 100 trillion synapses compose the human central nervous system, thereby presenting a barrier of complexity that makes focused examinations into structure-function relationships extraordinarily difficult (Azevedo, Carvalho et al. 2009). Traditionally, much of our understanding of the brain has derived from correlation of behavioral defects caused by lesions (e.g. tumors, strokes, mechanical damage, etc.) with the location of the afflicted area using magnetic resonance imaging (MRI). While this provides some insight into the function of neuroanatomical structures, it does not provide insight into the signaling mechanisms employed by a dynamic network of convergent and divergent pathways to respond to stimuli. Although advanced imaging techniques, such as positron emission tomography (PET) and functional magnetic resonance imaging (fMRI) indicate what regions of the brain are active during the performance of a given task, they do not offer direct insight into the mechanisms responsible for the neuronal signaling occurring within a given structure. Single electrode electrophysiology recordings have been employed to investigate the temporal lobe and the anterior cingulate gyrus, and implanted electrodes have been used to record the intra-cortical electroencephalogram (EEG) in the prefrontal cortex. However, when such techniques are employed in surgical patients, the amount of attainable information is limited by time constraints and, as in the case of multi-electrode arrays, the clinical needs of the patient (Ojemann, Schoenfield-McNeill et al. 2002, Williams, Bush et al. 2004, Rizzuto, Mamelak et al. 2005). Furthermore, it is not possible to completely understand the connectivity of every individual neuron because of the billions of neurons and trillions of synapses in the human brain. Therefore, it is impossible to know how an

individual neuron integrates every presynaptic input to modulate its output to every postsynaptic partner, how every postsynaptic partner's activity is in turn then modulated, and, most importantly, correlate these observations with behavioral consequences. Even in *Drosophila melanogaster*, whose brain consists of approximately 100,000 neurons, only recently has a mesoscopic map of the brain been developed by deconstructing the brain into approximately 16,000 individual neurons and reconstructing them into a framework in an effort to produce a virtual fly brain (Chiang, Lin et al. 2011). Therefore, an organism with a simple and anatomically defined nervous system is essential for understanding how an intact neural network functions to govern animal behavior.

The nematode *C. elegans* is an excellent model organism to investigate how neurons in a neural network sense, integrate, and transduce information regarding internal and external sensory cues to produce context-dependent behavioral responses because the hermaphrodite has only 302 neurons, and the web of neuronal interconnectivity has been reconstructed in a "wiring diagram" (White, Southgate et al. 1983). Furthermore, there are only 302 neurons, which makes it possible to record the activity of a specific, identified neuron. In addition, the wiring diagram allows for predictions and examinations of interactions between two or more specific neurons in the nervous system. Furthermore, *C. elegans* exhibits complex, quantifiable behavioral responses to a variety of sensory stimuli, including chemoattractants, chemorepellants, mechanical stimuli, and temperature gradients (Mori and Ohshima 1995, Gray, Hill et al. 2005, Bargmann 2006, Bergamasco and Bazzicalupo 2006, Kahn-Kirby and Bargmann 2006, O'Hagan and Chalfie 2006, Kuhara, Okumura et al. 2008, Chatzigeorgiou, Yoo et al. 2010, Ohnishi, Kuhara et al. 2011, Liu, Schulze et al. 2012). Therefore, *C. elegans* also

offers the ability to correlate the effects of a specific neuron's activity to behavioral responses exhibited by the animal. Finally, advanced genetic techniques allow for cell-specific changes in gene expression, and subsequent examination of the perturbation in network function on physiologic and behavioral scales. Currently, neurobiology research has exploited the benefits of *C. elegans* to correlate sensorimotor coupling at both molecular and cellular levels with animal behavior. As a result, *C. elegans* is a useful system for elucidating the mechanisms by which neurons sense and integrate multiple inputs to modulate neuronal output to modify behavior to a specific stimulus or mosaic of stimuli.

1.1 The *C. elegans* nervous system is structurally well-defined and uses neurotransmission pathways that are conserved in humans

The adult hermaphrodite *C. elegans* somatic nervous system is composed of 282 neurons, and the pharyngeal nervous system is composed of 20 neurons (Ward, Thomson et al. 1975, Sulston and Horvitz 1977, Sulston, Schierenberg et al. 1983, White, Southgate et al. 1986). The 302 neurons in the adult hermaphrodite are grouped into 118 classes; 39 classes are sensory neurons, 27 classes are motor neurons, and 52 classes are interneurons (Ward, Thomson et al. 1975, Ware, Clark et al. 1975, de Bono and Maricq 2005). Many sensory neurons likely function as interneurons, as they are extensively innervated, and some motor neurons also likely function as sensory and/or interneurons (White, Southgate et al. 1986, Tavernarakis, Shreffler et al. 1997, de Bono and Maricq 2005, O'Hagan and Chalfie 2006, Leinwand and Chalasani 2013). Most sensory neurons and interneurons exist as left and right pairs, many of which are linked by gap junctions.

Unlike traditional mammalian synapses that consist of a presynaptic nerve terminus innervating a postsynaptic partner, chemical synapses between processes in *C. elegans* are formed by *en passant* synapses. E*n passant* synapses are synaptic varicosities in neighboring process that are formed along the length of a neuronal process. In the presynaptic varicosity, *C. elegans en passant* synapses are characterized by an electron-rich presynaptic density (~50 nm wide and 100-400 nm long) that is in close proximity to docked and reserve pool vesicles (the active zone) (Weimer and Jorgensen 2003, Rostaing, Weimer et al. 2004, Zhen and Jin 2004, Nakata, Abrams et al. 2005, Altun and Hall 2011). Near the active zone are molecules responsible for the growth and organization of synapses, as well as sites of vesicle membrane recovery by endocytosis (the periactive zone) (Jin 2002, Rostaing, Weimer et al. 2004, Nakata, Abrams et al. 2005, Altun and Hall 2011). Presynaptic inputs may terminate onto one or more postsynaptic partners (Altun and Hall 2011). An individual neuron can have upwards of 30 synaptic partners and up to 19 synapses between any two neurons (~5 on average) (de Bono and Maricq 2005). In total, there are approximately 6400 chemical synapses, 900 gap junctions, and 1500 neuromuscular junctions in the *C. elegans* nervous system (Altun and Hall 2011). *C. elegans* utilizes many of the same neurotransmitter pathways as the human nervous system, including 5-HT, γ-aminobutyric acid (GABA), glutamate (Glu), acetylcholine (ACh), dopamine (DA), and neuropeptides. Furthermore, many of the proteins involved in these neurotransmission pathways demonstrate conservation with human homologs (Troemel, Chou et al. 1995, Bargmann 1998, Bargmann and Kaplan 1998, Chalasani, Kato et al. 2010). Finally, unlike mammalian neurons, there are no voltage-gated Na^+ channels in *C. elegans*, and thus, *C. elegans* does utilize classical

action potentials to mediate neurotransmission (Bargmann 1998, Goodman, Hall et al. 1998). However, due to the small size and high input resistances of *C. elegans* neurons, the calculated length constants (distance from a point of current injection where the passive propagation of a change in membrane potential decays 63% relative to the change in membrane potential at the point of current injection) are much longer than the neurons themselves (Goodman, Hall et al. 1998). Consequently, *C. elegans* neurons are functionally isopotential, meaning that passive propagation of a current will cause a uniform change in membrane potential, with negligible to no decay in magnitude, thereby circumventing the need for classical action potentials (Goodman, Hall et al. 1998).

1.2 The layer 1 neurons integrate sensory information from numerous sensory neurons to alter animal behavior

A primary focus of *C. elegans* neurobiology research has been to perform extensive analysis and quantification of locomotory behaviors exhibited by freely moving worms on either solid surfaces (e.g. NGM plates), or in swimming/thrashing behavior in liquid media. On solid surfaces, worms move by laying on either their left or right side and produce sinusoidal waves by contracting and relaxing body wall muscles (de Bono and Maricq 2005). A total of 113 *C. elegans* motor neurons mediate crawling and swimming behaviors and motility of the alimentary and reproductive systems (Altun and Hall 2011). The locomotory musculature consists of 95 longitudinally projecting body-wall muscle cells that are innervated by A- and B-type excitatory cholinergic motor neurons (VA, VB, DA, DB, AS), and D-type inhibitory GABAergic motor neurons (VD, DD) (Altun and Hall 2011). Forward locomotion is controlled by stimulatory B-type motor neurons,

backward locomotion is controlled by stimulatory A-type motor neurons, and A- and B-type motor neurons innervate inhibitory D-type motor neurons that project to the contralateral musculature. Thus, cholinergic stimulation of dorsal or ventral muscles results in simultaneous GABAergic inhibition of the contralateral musculature (White, Southgate et al. 1976, White, Southgate et al. 1986, McIntire, Jorgensen et al. 1993, Altun and Hall 2011). Additionally, multiple neurotransmitters are expressed in the VC motor neurons, which primarily innervate vulval muscle (Altun and Hall 2011). Rather than coordinating locomotory behavior using a central pattern generator (CPG), proprioceptive elements of motor neurons are activated by local bending and passive propagation of electrical activity between adjacent motor neurons via gap junctions, thereby stimulating contraction of adjacent musculature (Altun and Hall 2011).

The command interneurons regulate forward and backward locomotion. Two AVB and PVC command interneurons synapse onto and stimulate DB and VB motor neurons, thereby promoting forward locomotion, and the AVA, AVD, and AVE command interneurons synapse onto and stimulate DA and VA motor neurons, thereby promoting backward locomotion (Von Stetina, Treinin et al. 2006, Altun and Hall 2011). For example, laser ablation of the AVAs and AVDs impairs anterior touch avoidance behavior and backward movement, supporting their role in mediating backward movement (Chalfie, Sulston et al. 1985, White, Southgate et al. 1986, de Bono and Maricq 2005). In contrast, laser ablation of the AVBs and PVCs impairs posterior touch avoidance behavior and forward locomotion (Chalfie, Sulston et al. 1985, White, Southgate et al. 1986, de Bono and Maricq 2005). Additionally, laser ablation of the AVEs decreases anterior touch avoidance behavior, while laser ablation of the AVAs,

AVDs, and AVEs abolishes anterior touch avoidance behavior (Li, Kang et al. 2011). However, even though the command interneurons determine locomotory direction, laser ablation studies demonstrate that their contribution to locomotory behaviors are not equivalent. For instance, laser ablation of AVAs or AVBs causes uncoordinated spontaneous changes in locomotory direction, but animals exhibit normal touch-evoked behavioral responses (Chalfie, Sulston et al. 1985, Altun and Hall 2011). In contrast, laser ablation of the PVCs or AVDs alters touch-evoked avoidance behaviors, but does not affect spontaneous locomotory behavior (Chalfie, Sulston et al. 1985, Altun and Hall 2011). Additionally, transgene-induced necrotic cell death of the command interneurons, in addition to other neurons, decreases touch-evoked avoidance behaviors and cause bidirectional locomotory impairment (Maricq, Peckol et al. 1995, de Bono and Maricq 2005). An animal on food will move forward for an extensive period of time, then briefly move back, and a subsequently change locomotory direction, and expression of a gain-of-function (*gf*) AMPA receptor in the command interneurons causes rapid switching between forward and backward locomotion, despite not altering locomotion itself (Zheng, Brockie et al. 1999, de Bono and Maricq 2005, Croll 2009). These data imply that the command interneurons make the decision for the animal to either move forward or backward, but do not coordinate g forward or backward locomotion. Thus, a primary focus in *C. elegans* neurobiology research is to elucidate the transduction mechanisms sensory neurons use to transform sensory stimuli into an electrical signal, identify the signaling pathways sensory neurons use to transmit information to interneurons, determine how interneurons integrate information from multiple sensory inputs, and, subsequently, how interneurons modulate the command interneurons to alter locomotory

behavior.

The amphid sensory neurons comprise the layer 0 neurons and direct ~50% of their synaptic output onto the layer 1 AIA, AIB, AIY, and AIZ interneurons (Gray, Hill et al. 2005). The layer 1 neurons in turn direct a large portion of their output onto the layer 2 RIA and RIB interneurons, RIM and SMB head motor neurons, and the command interneurons (Gray, Hill et al. 2005). Layer 2 neurons innervate some musculature, but >50% of their output innervates head interneurons, the head layer 3a SAA, RIV, RMD, SMD, SIA, and SIB head motor neurons, and the layer 3b command interneurons (Gray, Hill et al. 2005).

Laser ablation of individual pairs of the layer 1 neurons reveals that the AIAs, AIBs, AIYs, and AIZs shape animal behavior (Wakabayashi, Kitagawa et al. 2004, Gray, Hill et al. 2005). Immediately after an animal is removed from food, it engages in an area-restricted foraging strategy (area-restricted search; ARS) (Bell 1991, Hills, Brockie et al. 2004). Initially after being removed from food, animals frequently change their direction of movement and are more likely to perform high-angle turns; however, after being off food for 15 minutes, animals predominantly move forward and are less likely to perform high-angle turns (Shingai 2000, Tsalik and Hobert 2003, Hills, Brockie et al. 2004, Wakabayashi, Kitagawa et al. 2004, Gray, Hill et al. 2005). Laser ablation of either the AIBs or AIZs results in animals that predominantly move forward immediately after removal from food, implicating the AIBs and AIZs in stimulating reversal behavior during ARS. Conversely, laser ablation of the AIAs or AIYs results in animals that spend less time moving forward immediately after removal from food, implicating the AIAs and AIYs in inhibiting reversal behavior during ARS (Tsalik and Hobert 2003,

Wakabayashi, Kitagawa et al. 2004, Gray, Hill et al. 2005). Additionally, the AIAs extensively innervate the AIBs, and the AIYs extensively innervate the AIZs, suggesting that the AIAs and AIYs inhibit the AIBs and AIZs, respectively (White, Southgate et al. 1986). Together, the extensive innervation of the layer 1 neurons by the amphid sensory neurons and the profound effect each pair of layer 1 neurons has on animal behavior indicate that the layer 1 neurons are an important point of sensorimotor integration.

1.3 The structure and function of the *C. elegans* amphid sensory organ

Polymodal sensory neurons with ciliated terminal dendrites compose the amphid sensory organ (Inglis, Ou et al. 2007). Most eukaryotic organisms use cilia (microtubule based sub-cellular organelles) to move (motile cilia; e.g. eukaryotic flagella) or sense extracellular chemical and/or physical stimuli (non-motile/primary cilia) (Inglis, Ou et al. 2007). Only *C. elegans* sensory neurons have cilia, and *C. elegans* sensory neurons only have not-motile/primary cilia (Inglis, Ou et al. 2007). In all organisms, cilia nucleate from a basal body (modified centriolar structure), and a basal body is typically located near the cell membrane region from which its cilia protrude (Inglis, Ou et al. 2007). Most organisms have basal bodies that exhibit a circular triplet microtubule arrangement, whereas *C. elegans* basal bodies exhibit a circular array of doublet microtubules (transition zones) (Perkins, Hedgecock et al. 1986, Inglis, Ou et al. 2007). In *C. elegans* amphid sensory neurons, the middle segment (circular arrangement of nine doublet microtubules) follows the transition zone, and the distal segment (circular arrangement of singlet microtubules) follows the middle segment (Inglis, Ou et al. 2007). Vertebrate pancreatic, renal, and olfactory cells possess cilia that are composed of an array of

doublets transitioning into an array of singlets at distal segments, suggesting that all sensory cilia possess this conserved structural motif (Reese 1965, Webber and Lee 1975, Hidaka, Ashizawa et al. 1995, Inglis, Ou et al. 2007).

The soma of *C. elegans* amphid sensory neurons are situated near the anterior end of the posterior pharyngeal bulb, project axons into the nerve ring, and project ciliated dendrites to the anterior end of the animal (Inglis, Ou et al. 2007). Amphid sensory neuron dendritic extensions project through a channel formed by socket cells, partially exposing their termini to the external environment, and a sheath cell protects proximal amphid cilia (Inglis, Ou et al. 2007). Amphid sensory neuron cilia are shaped like a single rod (ASE, ASG, ASH, ASI, ASJ, and ASK sensory neurons), pairs of rods (ADF and ADL sensory neurons), a 'winged' morphology (AWA, AWB, and AWC sensory neurons), or a 'finger' morphology, in which approximately 50 villi surround the cilium (AFD sensory neurons) (Inglis, Ou et al. 2007). Winged and finger cilia terminate within a sheath cell that prevents their exposure to the external environment (Inglis, Ou et al. 2007). For cilia that terminate in a sheath cell, odorants reach the cilia either by being transported by the sheath cell, or by passively diffusing through the cuticle.

1.4 The AWCs produce chemotactic behaviors to volatile odorants by modulating the layer 1 neurons

The AWCs sense the presence of food, volatile chemoattractants (e.g. benzaldehyde, butanone, trimethylthiazole, isoamyl alcohol [IAA], 2,3-pentanedione) and temperature (Bargmann, Hartwieg et al. 1993, Bargmann 2006, Chalasani, Chronis et al. 2007, Kuhara, Okumura et al. 2008, Ohnishi, Kuhara et al. 2011). The AWCs stimulate

turning probability during ARS (Gray, Hill et al. 2005). Furthermore, the AWCs are functionally distinct from one another, whereby AWC^{ON} senses butanone, benzaldehyde, and IAA, and AWC^{OFF} senses 2,3-pentanedione, benzaldehyde, and IAA (Wes and Bargmann 2001, Bargmann 2006, Chalasani, Chronis et al. 2007). There is not a consistent left versus right association with AWC^{ON} and AWC^{OFF}, just coordinated AWC^{ON} and AWC^{OFF} generation in every animal (Troemel, Sagasti et al. 1999, Bargmann 2006). Therefore, the AWCs mediate sensation of various sensory stimuli to alter animal behavior.

Numerous odorant-specific pathways mediate chemosensation in the AWCs. For example, the $G\alpha_i$-like subunit encoded by *odr-3* (only expresses in cilia) is required for wild-type chemotactic responses to benzaldehyde, butanone, trimethylthiazole, and IAA (Roayaie, Crump et al. 1998, Bargmann 2006). Interestingly, *odr-3* mutants exhibit a filamentous morphology like AWA cilia, instead of the fan-like morphology typically exhibited by AWC cilia (Roayaie, Crump et al. 1998). The $G\alpha_i$-like subunit encoded by *gpa-3* expresses in cilia and axons, and weak olfactory responses that persist in *odr-3* mutants are completely abolished in *odr-3;gpa-3* double-mutants, suggesting that ODR-3 and GPA-3 function redundantly (Lans, Rademakers et al. 2004, Bargmann 2006). The AWCs also express the $G\alpha_i$-like subunit encoded by *gpa-2* in both cilia and axons, and *odr-3;gpa-2* double-mutants are significantly more defective for butanone chemotaxis than *odr-3* or *gpa-2* mutants, suggesting that the two $G\alpha_i$-like subunits function redundantly in butanone sensation (Roayaie, Crump et al. 1998, Bargmann 2006). However, *odr-3;gpa-2* double-mutants exhibit enhanced chemotactic responses to 2,3-pentadione and benzaldehyde relative to *odr-3* mutants, suggesting that GPA-2

antagonizes 2,3-pentadione and benzaldehyde sensation (Lans, Rademakers et al. 2004, Bargmann 2006). The $G\alpha_i$-like subunit encoded by *gpa-13* only expresses in cilia, and plays a minor role in positively regulating chemotaxis behaviors mediated by the AWCs (Lans, Rademakers et al. 2004, Bargmann 2006). Together, these data demonstrate that numerous $G\alpha_i$-like subunits interact in the AWCs to tailor behavioral responses to a variety of volatile chemoattractants.

The AWC chemotransduction pathway is similar to the mammalian phototransduction pathway (Xiong, Solessio et al. 1998, Fu and Yau 2007, Liu, Ward et al. 2010). The AWCs express the cyclic nucleotide-gated beta 1 (CNGB1) channel subunit *tax-2* and the cyclic nucleotide-gated alpha 1 (CNGA1) channel subunit *tax-4*, and *tax-2* and *tax-4* mutants are defective for AWC-mediated chemotaxis to volatile odors (Coburn and Bargmann 1996, Komatsu, Mori et al. 1996, Bargmann 2006). The AWCs strongly express *tax-2* in cilia and axons, but weakly express *tax-2* in cell bodies and dendrites (Coburn and Bargmann 1996). Conversely, the AWCs strongly express *tax-4* in cilia, and slightly express *tax-4* in dendrites (Komatsu, Mori et al. 1996). The channel formed by the TAX-4 and TAX-2 subunits is highly sensitive to cGMP and is relatively insensitive to cAMP, much like the mammalian phototransduction channel (Komatsu, Jin et al. 1999, Bargmann 2006). Although TAX-4 can form a functional channel on its own, the TAX-2 subunit enhances TAX-4 activity 25-fold (Komatsu, Jin et al. 1999, Bargmann 2006). In the mammalian visual system, light absorption by rhodopsin family G protein-coupled receptors (GPCRs) activates the G protein transducin (Fu and Yau 2007). In turn, transducin positively regulates phosphodiesterases (PDEs) to decrease intracellular cGMP, resulting in closure of cyclic-nucleotide gated (CNG)

channels (Fu and Yau 2007). Conversely, vertebrate parietal eye photoreceptor cells inhibit PDEs to increase intracellular cGMP levels, thereby opening CNG channels (Xiong, Solessio et al. 1998). However, the *C. elegans* light-sensitive ASJs require the receptor-like guanylate cyclases (RGCs) DAF-11 and ODR-1, and do not require PDEs (Liu, Ward et al. 2010). Furthermore, DAF-11 and ODR-1 function downstream of G protein signaling and upstream of CNG channels; however, it is unclear whether G protein signaling directly or indirectly modulates RGCs (Liu, Ward et al. 2010). The AWCs express *daf-11* and *odr-1*, and *daf-11* and *odr-1* mutants are defective for chemotaxis to odorants sensed by the AWCs (Birnby, Link et al. 2000, L'Etoile and Bargmann 2000). Therefore, DAF-11 and ODR-1 may function downstream of G protein signaling and upstream of RGCs to mediate odor sensation in the AWCs. Since AWC chemotransduction and mammalian phototransduction pathways are similar, regulatory pathways important for AWC-mediated sensory responses may be conserved in the mammalian phototransduction system.

Animals with laser ablated AWCs exhibit decreased turning behavior during ARS, indicating that the presence of odor promotes forward locomotion and inhibits turning behavior by inhibiting the AWCs, whereas odor removal promotes turning behavior and inhibits forward locomotion by activating the AWCs (Wakabayashi, Kitagawa et al. 2004, Gray, Hill et al. 2005, Chalasani, Chronis et al. 2007, Chalasani, Kato et al. 2010, Ohnishi, Kuhara et al. 2011). The AWCs are odor-OFF neurons, meaning that odor presentation and removal inhibits and activates the AWCs, respectively (Chalasani, Chronis et al. 2007, Chalasani, Kato et al. 2010). The AWCs exhibit graded iCa^{2+} increases in a concentration- and time-dependent manner, with odor-evoked iCa^{2+}

increasing in amplitude with longer pre-exposure for 1 to 5 minutes (Chalasani, Chronis et al. 2007). Since *C. elegans* neurons express VGCCs, iCa^{2+} increases are associated with depolarization (Kerr, Lev-Ram et al. 2000, Jospin, Jacquemond et al. 2002, Chalasani, Chronis et al. 2007). Together, these data demonstrate that the AWCs significantly affect animal behavior, indicating that the AWC chemosensory circuit is an adequate model for investigating sensorimotor coupling.

Glutamatergic signaling from the AWCs differentially modulates the layer 1 neurons. The AWCs activate the AIBs by releasing glutamate onto GLR-1-containing receptors (Maricq, Peckol et al. 1995, Chalasani, Chronis et al. 2007, Ohnishi, Kuhara et al. 2011). In support of this, odor presentation inhibits AIB iCa^{2+}, whereas sustained glutamate release from the AWCs following odorant removal increases AIB iCa^{2+}, with near maximal increases lasting for two minutes or longer (Chalasani, Chronis et al. 2007). Conversely, tonic glutamate release due to basal AWC activity inhibits the AIAs and AIYs by activating a GLC-3-containing GluCl receptor (Horoszok, Raymond et al. 2001, Chalasani, Chronis et al. 2007, Chalasani, Kato et al. 2010, Ohnishi, Kuhara et al. 2011). Therefore, odor presentation disinhibits the AIAs and AIYs, resulting in neurite iCa^{2+} increases (Chalasani, Chronis et al. 2007, Chalasani, Kato et al. 2010). Similar to the AWCs, rod and cone photoreceptors are inhibited and activated by the presentation and removal of light, respectively, tonically release glutamate, and release glutamate in a graded fashion (Zhang and Cote 2005). Furthermore, like AWC modulation of the layer 1 neurons, photoreceptor cells provide contrast-enhancement in the mammalian visual system by releasing glutamate that activates and inhibits off and on bipolar cells, respectively (Schiller, Sandell et al. 1986, Yang 2004). Therefore, the AIAs, AIBs, and

AIYs may have a function analogous to the off and on bipolar cells in chemosensation, and the circuit as a whole may be useful for understanding sensorimotor coupling.

Odor-evoked behavioral dynamics are modulated by inhibitory peptidergic feedback from the AIAs onto the AWCs. The AWCs release buccalin-related *nlp-1* encoded peptides that activate the human pyroglutamylated RFamide peptide receptor (QRFPR) ortholog NPR-11 on the AIAs; however, it is uncertain whether the AWCs tonically release *nlp-1* encoded peptides or only while activated following odor removal (Chalasani, Kato et al. 2010). The AWCs release *nlp-1* encoded peptides that activate NPR-11 on the AIAs to both enhance odor presentation-evoked increases of AIA neurite iCa^{2+} and stimulate the release of insulin-related peptides encoded by *ins-1* (Kodama, Kuhara et al. 2006, Chalasani, Kato et al. 2010). The *ins-1* encoded peptides released from the AIAs inhibit turning behaviors during ARS in an *eat-4*-dependent manner (Chalasani, Kato et al. 2010). Additionally, *ins-1* encoded peptides released from the AIAs both decrease the duration of odor removal-evoked AWC iCa^{2+} increases and are required for AWC-dependent olfactory adaptation (Chalasani, Kato et al. 2010). Similarly, *D. melanogaster* interneurons inhibit presynaptic olfactory neurons by releasing tachykinin peptides, and modulation of pain afferent neurons is prevalent in pain sensing pathways (Ignell, Root et al. 2009, Stein, Clark et al. 2009). Importantly, these data reveal the mechanisms by which experience and environmental conditions provide an elementary form of decision-making.

Cell-selective activation or inhibition of an individual neuron allows for the investigation of how the activity state of one neuron affects the activity of other neurons in the neural network. Histamine (HA) is not used as a neurotransmitter in *C. elegans*,

and heterologous expression of a *D. melanogaster* HA-gated Cl^- channel subunit 1(HisCl1) allows for specific inactivation of one or more neurons (Pokala, Liu et al. 2014). The HisCl1 allows for manipulation of the activity state of downstream layer 1 neurons and command interneurons during odorant application, thereby allowing investigation of the effect of neural network state on the responses of multiple neurons to an odorant stimulus (Gordus, Pokala et al. 2015). When the AIBs, RIMs, and AVAs are all activated (predominant activity pattern; ~65%), there is a variable delay in response of these neurons to odorant presentation, but silencing either the RIMs or AVAs increases the speed and reliability of responses in the AIBs and RIMs/AVAs (whichever was not being manipulated) (Gordus, Pokala et al. 2015). Additionally, silencing the RIMs decreases correlations in activity between the AIBs and AVAs, indicating that the RIMs are crucial for synchronizing the AIBs and AVAs activity (Gordus, Pokala et al. 2015). Furthermore, activation of the AVAs with the red light-sensitive cation channel Chrimson results in synchronous increases of RIM and AIB activity (Gordus, Pokala et al. 2015). Silencing the AIBs has little effect on initial odor responses, but decreases the duration of RIM and AVA activation following odorant-removal, indicating that the AIBs stabilize odor removal-induced activation of the RIMs and AVAs (Gordus, Pokala et al. 2015). Together, these data show that the responsiveness of neurons downstream from the sensory neurons exhibit variable responsiveness due to the activity state of the neural network at the time of stimulus presentation (Gordus, Pokala et al. 2015). The AWCs differentially modulate the AIAs, AIBs, and AIYs with glutamatergic signaling to regulate chemotactic behaviors . Furthermore, inhibitory peptidergic feedback from the AIAs onto the AWCs may represent a rudimentary pathway for decision-making.

Finally, the responsiveness of neurons in the AWC olfactory circuit is determined in part by the activity of other neurons in the circuit at the time of stimulus presentation. Together, these data demonstrate that the AWC olfactory circuit is extensively modulated at several levels to fine-tune behavioral responses, and is a useful circuit for investigating sensorimotor coupling. Figure 1-1 illustrates how the AWCs sense stimuli (Figure 1-1A), and how AWC signaling modulates the AIAs, AIBs, and AIYs (Figure 1-1B).

1.5 The ASEs produce chemotactic behaviors to water soluble attractants by modulating the layer 1 neurons

The ASEs sense water-soluble attractants like Na^+, Cl^-, cAMP, biotin, lysine, 5-HT, and heavy metals (e.g. Cu^{2+} and Cd^{2+}) (Bargmann and Horvitz 1991, Sambongi, Nagae et al. 1999, Bargmann 2006, Altun and Hall 2011). Like the AWCs, the ASEs exhibit left versus right asymmetry; however, unlike the AWCs, there is consistent left versus right asymmetry, with ASER preferentially sensing Cl^-, Na^+, and decreases in salt concentration (salt downstep) and ASE left (ASEL) preferentially sensing Na^+ and increases in salt concentration (salt upstep) (Pierce-Shimomura, Faumont et al. 2001, Bargmann 2006). For example, the ASEs express the Na^+-sensitive multipass integral membrane membrane protein *tmc-1* (Chatzigeorgiou, Bang et al. 2013). Similar to the AWCs, the ASEs express *tax-2* and *tax-4*, and mutants for these genes are defective for sensory modalities mediated by the ASEs (Coburn and Bargmann 1996, Okochi, Kimura et al. 2005). Additionally, *daf-11* mutants are also defective for chemotaxis to water-soluble attractants (Vowels and Thomas 1994). Therefore, it is likely that the ASEs use a

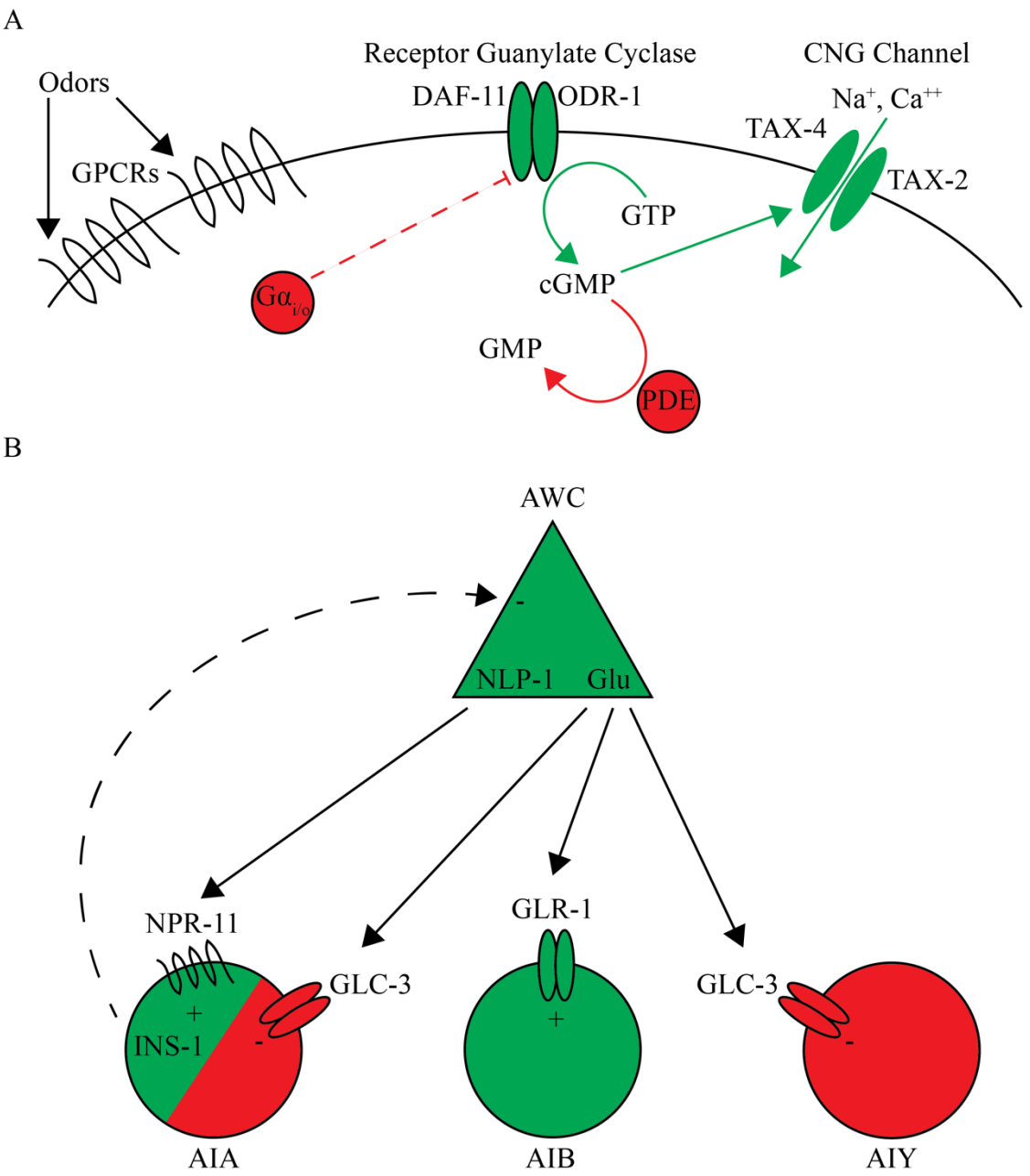

Figure 1-1. Odorants modulate the AWCs, which in turn modulates the layer 1 neurons. A. A likely model for AWC sensory transduction, based off ASJ sensory transduction (Liu, Ward et al. 2010). An odorant binds to a GPCR to activate a $G\alpha_{i/o}$ subunit (i.e. ODR-3, GPA-3, GPA-2, GPA-2, GPA-13). The $G\alpha_{i/o}$ subunit inhibits the RGC composed of DAF-11 and ODR-1, preventing cGMP. A PDE cleaves cGMP into

GMP, reducing cGMP levels. As cGMP levels drop, the CNG channel composed of TAX-4 and TAX-2 closes, preventing the influx of excitatory cations. Odorant removal relieves inhibition, activating the AWCs. B. The AWCs release *nlp-1* encoded peptides that activate NPR-11 on the AIAs. The AIA-release of *ins-1* encoded peptides provides inhibitory feedback onto the AWCs. The AWCs also activate the AIBs with tonic and evoked glutamate release onto GLR-1. Conversely, the AWCs inhibit the AIAs and AIYs with tonic and evoked glutamate release onto GLC-3.

similar sensory transduction pathway to the ASJs.

similar sensory transduction pathway.

In *C. elegans*, ASE-mediated chemotaxis responses are modulated by prior experiences. For example, salt downstep activates the ASER, whereas salt upstep both activates and inhibits the ASEL and ASER, respectively (Suzuki, Thiele et al. 2008, Ortiz, Faumont et al. 2009, Oda, Tomioka et al. 2011, Leinwand and Chalasani 2013). Animals freely moving on a salt concentration gradient stimulate forward locomotion and decrease reversal probability when moving up the gradient, whereas animals decrease forward probability and increase reversal behavior when moving down the gradient (Miller, Thiele et al. 2005, Suzuki, Thiele et al. 2008, Leinwand and Chalasani 2013). Similarly, cell-specific activation of ASEL increases forward locomotion, while cell-specific activation of ASER increases turning probability (Suzuki, Thiele et al. 2008). Conversely, animals can also learn to associate a high salt concentration with starvation (salt conditioned), causing animals to increase turning behavior when moving up a salt gradient, and enhance forward locomotion when moving down a salt gradient (Miller, Thiele et al. 2005). Therefore, the ASE gustatory circuit allows for the development of learned behaviors.

Learned ASE gustatory behaviors are in part due to the regulation of ASE responsiveness by neuromodulators. Relative to mock conditioned animals, salt conditioned animals have enhanced salt downstep-evoked ASER iCa^{2+} increases and reduced salt upstep-evoked ASEL iCa^{2+} increases (Oda, Tomioka et al. 2011). Enhanced salt-downstep-evoked ASER iCa^{2+} responses are dependent on *ins-1* encoded peptides, the mammalian insulin IGF receptor tyrosine kinase DAF-2, and the PI3-kinase homolog that functions downstream of DAF-2, AGE-1, but independent of the mammalian

Munc13 homolog UNC-13 (required for clear synaptic vesicle/SVs release) (Dorman, Albinder et al. 1995, Oda, Tomioka et al. 2011). Additionally, the reduction of salt upstep-evoked ASEL iCa^{2+} increases in salt conditioned animals is dependent on *ins-1* encoded peptides (Oda, Tomioka et al. 2011). In contrast to iCa^{2+}, salt conditioned animals have reduced salt downstep-evoked ASER synaptic vesicle release that is dependent on INS-1, DAF-2, and AGE-1, whereas salt upstep-evoked ASEL synaptic vesicle release is not significantly different from mock conditioned animals (Oda, Tomioka et al. 2011). Furthermore, naive animals increase and decrease AIB iCa^{2+} following salt downstep and upstep, respectively, whereas salt conditioned animals show no changes in AIB iCa^{2+} (Oda, Tomioka et al. 2011). In support of these data, ASER-specific activation evokes iCa^{2+} increases in the AIBs (Oda, Tomioka et al. 2011). Conversely, relative to salt conditioned animals, mock conditioned animals exhibit prolonged AIA iCa^{2+} increases following salt upstep, while salt downstep has no effect on either salt or mock conditioned animals (Oda, Tomioka et al. 2011). These data are consistent with the AIBs and AIAs effects on turning behavior, as animals increase turning probability moving down a salt gradient, and increase forward movement moving up a salt gradient (Wakabayashi, Kitagawa et al. 2004, Gray, Hill et al. 2005, Oda, Tomioka et al. 2011). One possible explanation for the dichotomy between ASER iCa^{2+} and ASER synaptic release is that reduced ASER synaptic release may result in less stimulation of postsynaptic inputs that provide inhibitory feedback of ASER iCa^{2+} using dense-core vesicles (DCVs) (Oda, Tomioka et al. 2011). Another possible explanation is that enhanced ASER iCa^{2+} increases may activate the calcium-activated BK potassium channel SLO-1, which mediates a hyperpolarizing outward K^+ current, thereby shunting

depolarization, resulting in decreased synaptic transmission (Zahratka, Williams et al. 2015, Williams Unpublished, Zahratka Unpublished). Together, these data begin to reveal how insulin signaling regulates sensory neuron responsiveness. Moreover, these data begin to elucidate the molecular mechanisms responsible for learning.

Unique behavioral responses to high and low salt gradients are due to remodeling of the salt-sensitive chemosensory circuit by the release of extrasynaptic neuropeptides from the ASEL. For example, a 50-mM salt upstep stimulates release of insulin-related *ins-6* encoding peptides processed by the proprotein convertase BLI-4 from the ASEL (Leinwand and Chalasani 2013). Despite lacking synaptic outputs onto AWC^{ON}, release of *ins-6* encoded peptides from ASEL activates DAF-2 on the AWC^{ON}, thereby activating intracellular AGE-1 signaling, resulting in increases of AWC^{ON} iCa^{2+} (Leinwand and Chalasani 2013). However, a 10-mM salt upstep does not effect AWC^{ON} iCa^{2+} (Leinwand and Chalasani 2013). Relative to a 10-mM salt upstep, activation of AWC^{ON} results in enhanced AIA iCa^{2+} increases (Leinwand and Chalasani 2013). Additionally, animals require this signaling pathway for salt chemotaxis up a steep salt concentration gradient, but not a shallow salt concentration gradient (Leinwand and Chalasani 2013). These data demonstrate how a sensory neuron not involved in sensing a stimulus to be recruited by another sensory neuron to differentially modulate behavior. Similarly, lateral signaling between olfactory receptor neurons modifies sensory output in certain olfactory contexts in *D. melanogaster* (Su, Menuz et al. 2012). Together, these results demonstrate that connectivity alone does not provide a complete description of the functional interactions between neurons. Neuromodulators also alter gastric rhythms in *Cancer borealis* by differentially regulating individual motor neurons, as well as inhibit

the modulation of bipolar cells by rod photoreceptor cells in the mammalian retinal system (Hooper and Moulins 1989, Weimann, Meyrand et al. 1991, Baldridge, Vaney et al. 1998, Xia and Mills 2004). However, the mechanisms by which neuromodulators are released and detected in *C. borealis* and the mammalian retinal system are poorly understood. Therefore, the ASE gustatory circuit is useful for elucidating the mechanisms by which neuromodulators alter neural network activity.

The ASEs differentially modulate the AIAs and AIBs to produce salt chemotactic behaviors. Additionally, insulin-like signaling modulates ASE responsiveness to generate learned salt behaviors. Finally, altered behavioral responses on a high salt gradient relative to a low salt gradient are due to the release of extrasynaptic insulin-like peptides from the ASEL that activate the AWC^{ON}, resulting in enhanced activation of the AIAs. Together, these data demonstrate that the ASE gustatory circuit alters the activity of the layer 1 neurons to mediate chemotactic behaviors, and that neuromodulators alter the ASE gustatory circuit to elicit experience- and magnitude-dependent behaviors. Therefore, the ASE gustatory circuit provides an excellent model for investigating the molecular mechanisms of sensorimotor coupling. Figure 1-2 illustrates how the ASEs sense stimuli (Figure 1-2A), and how ASE signaling modulates the AWC^{ON}, AIAs, and AIBs (Figure 1-2B).

1.6 The ASHs mediate aversive behaviors to noxious stimuli by modulating the layer 1 neurons and command interneurons

The polymodal ASHs are a pair of nociceptive sensory neurons that sense noxious stimuli, such as anterior touch, high osmolarity, odors, heavy metals (e.g. Cu^{2+} and Cd^{2+}),

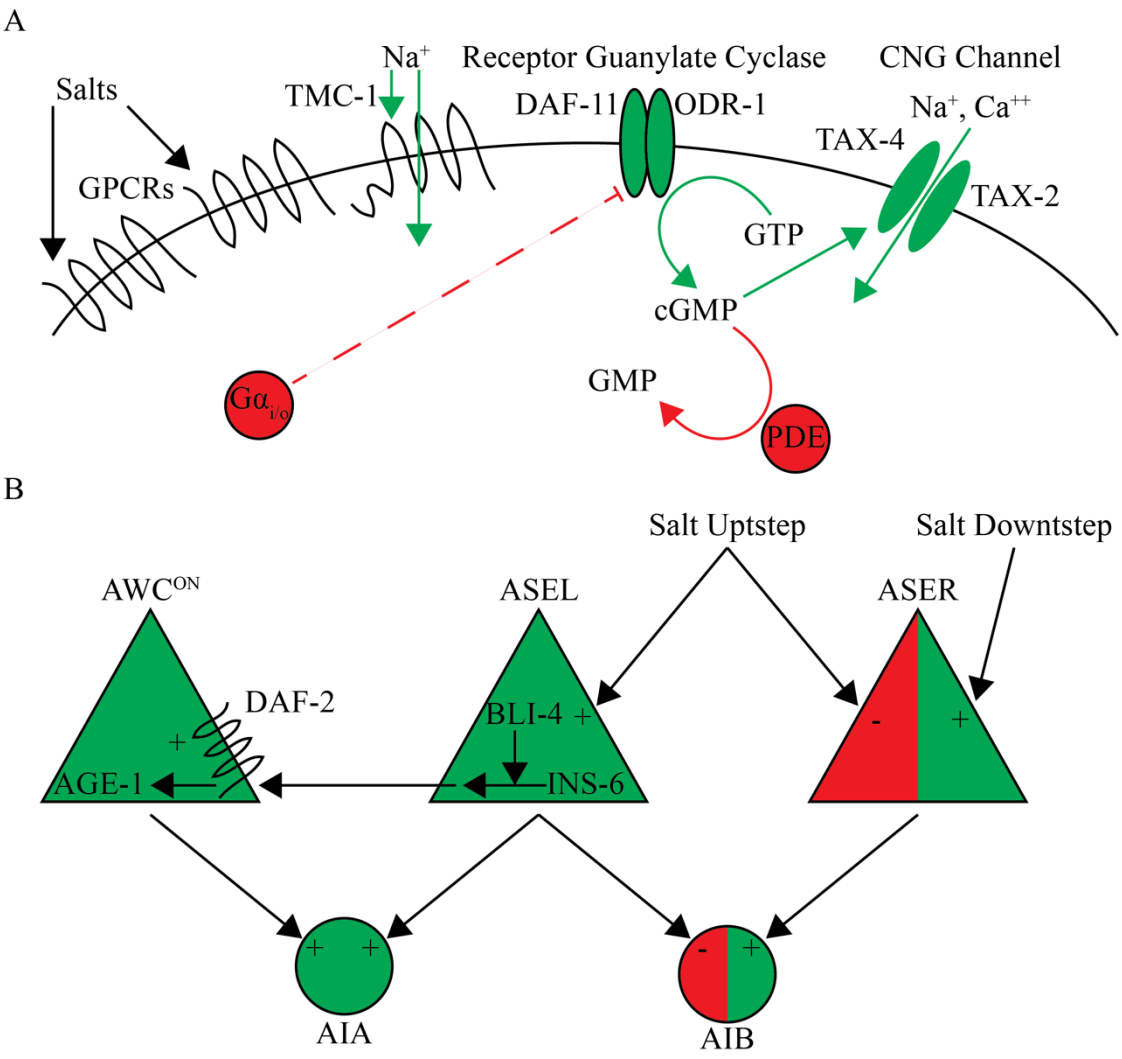

Figure 1-2. Changes in salt concentration differentially modulate the ASEL and ASER, which in turn modulate the layer 1 neurons. A. A likely model for ASE sensory transduction, based off ASJ sensory transduction (Liu, Ward et al. 2010). Differential activation of GPCRs by shifts in NaCl concentration activate a $G\alpha_{i/o}$ subunit. The $G\alpha_{i/o}$ subunit inhibits the RGC composed of DAF-11 and ODR-1, preventing cGMP. A PDE cleaves cGMP into GMP, reducing cGMP levels. As cGMP levels drop, the CNG channel composed of TAX-4 and TAX-2 closes, preventing the influx of excitatory cations. Additionally, the Na^+-activated TMC-1 mediates an inward depolarizing Na^+

current (permeability, Na^{+}>Ca^{++}>>>K^{+}) (Chatzigeorgiou, Bang et al. 2013). B. Salt upstep (<20-mM) activates and inhibits the ASEL and ASER, respectively, resulting in excitation and inhibition of the AIAs and AIBs. Additionally, salt upstep (>20-mM) evokes release of BLI-4-processed peptides encoded by *ins-6* from ASEL onto DAF-2 on the AWC^{ON}, leading to AWC^{ON} activation through an AGE-1 intracellular signaling cascade. In turn, AWC^{ON} then activates the AIAs. Conversely, salt downstep activates the ASER and AIBs, but has no effect on ASEL or AIAs activity.

NaCl, low pH, alkaloids (e.g. quinine), and detergents (Culotti and Russell 1978, Bargmann, Thomas et al. 1990, Kaplan and Horvitz 1993, Troemel, Chou et al. 1995, Colbert, Smith et al. 1997, Sambongi, Nagae et al. 1999, Sambongi, Takeda et al. 2000, Hilliard, Bargmann et al. 2002, Hilliard, Bergamasco et al. 2004, de Bono and Maricq 2005, Hilliard, Apicella et al. 2005, Bargmann 2006, Thiele, Faumont et al. 2009, Aoki, Yagami et al. 2011, Chatzigeorgiou, Bang et al. 2013). ASH-mediated aversive responses require the transient receptor potential vanilloid (TRPV)-related proteins OSM-9 and OCR-2 (Colbert, Smith et al. 1997, Tobin, Madsen et al. 2002, de Bono and Maricq 2005, Bargmann 2006). Noxious stimuli sensed by the ASHs depolarize and increase ASH iCa^{2+}, and responses are absent in animals lacking the *C. elegans* ortholog of the mammalian TRPV4 OSM-9 (de Bono and Maricq 2005, Hilliard, Apicella et al. 2005, Bargmann 2006, Piggott, Liu et al. 2011, Zahratka, Williams et al. 2015, Zahratka Unpublished). Expression of the rat TRPV4 in the ASH sensory neurons is capable of restoring osmotic avoidance and nose-touch responses in *osm-9* mutants, whereas expression of the rat TRPV1 does not; however, expression of rat TRPV1 in the ASHs does induce avoidance to the TRPV1 agonist capsaicin (Tobin, Madsen et al. 2002, Liedtke, Tobin et al. 2003, de Bono and Maricq 2005, Bargmann 2006). Additionally, the $G\alpha_i$-like subunit encoded by *odr-3* (only expressed in cilia) is required for ASH sensation of anterior touch and osmotic avoidance, the $G\alpha_i$-like subunit encoded by *gpa-3* (localized in cilia, cell bodies, and axons) is the primary Gα-protein involved in Cu^{2+} and quinine avoidance, and the biosynthetic enzymes responsible for making polyunsaturated fatty acids (PUFAs) are required for all ASH-mediated sensory responses (Roayaie, Crump et al. 1998, Jansen, Thijssen et al. 1999, Hilliard,

Bergamasco et al. 2004, Kahn-Kirby, Dantzker et al. 2004, Lans, Rademakers et al. 2004, de Bono and Maricq 2005, Hilliard, Apicella et al. 2005, Bargmann 2006). The ASHs also express the $G\alpha_i$-like subunit *gpa-11*, which is required for food- and 5-HT enhancement of aversive responses to 30% (volume/volume, diluted in ethanol) 1-octanol (Chao, Komatsu et al. 2004, Bargmann 2006). Animals expressing the rat TRPV1 in the ASHs exhibit capsaicin-evoked aversive responses in the absence of ODR-3 and PUFA signaling, suggesting that TRP channels function downstream of Gα-proteins and PUFAs (Kahn-Kirby, Dantzker et al. 2004, de Bono and Maricq 2005, Bargmann 2006). These data support an ASH intracellular signaling cascade whereby $G\alpha_i$-proteins, particularly ODR-3 and GPA-3, generate PUFA-containing lipids that in turn activate a TRPV receptor composed of OSM-9 and OCR-2 subunits.

Specific accessory proteins are required for some ASH-mediated sensory modalities. For example, the G protein-regulatory kinase GRK-2 is required for sensation of hyperosomolarity, 1-octanol, and quinine, but not anterior touch, suggesting that some mechanosensation may occur independent of GPCRs (Fukuto, Ferkey et al. 2004, de Bono and Maricq 2005, Bargmann 2006). Similarly, animals lacking the cytosolic protein OSM-10 are unresponsive to hyperosmolarity, despite the preservation of aversive responses to nose touch, quinine, and 1-octanol (Hart, Kass et al. 1999, Hilliard, Bergamasco et al. 2004, de Bono and Maricq 2005, Bargmann 2006). Additionally, the novel protein QUI-1, which contains multiple WD-40 repeats, is required for avoidance of quinine, but not high osmolarity (Hilliard, Bergamasco et al. 2004, de Bono and Maricq 2005, Bargmann 2006). There is also evidence for the requirement of accessory proteins in repellent-specific adaptation of behavioral

responses. For instance, animals adapt to repeated nose-touch stimuli and prolonged Cu^{2+} exposure, but not avoidance of high osmolarity or 1-octanol (Hart, Kass et al. 1999, de Bono and Maricq 2005, Hilliard, Apicella et al. 2005, Bargmann 2006). The Gγ-protein GPC-1, one of two Gγ-proteins in *C. elegans*, is required for adaptation to repeated noxious stimulation (Jansen, Thijssen et al. 1999, Jansen, Weinkove et al. 2002, de Bono and Maricq 2005, Hilliard, Apicella et al. 2005, Bargmann 2006).

The amplitude and duration of ASH iCa^{2+} increases evoked by the various sensory stimuli is not uniform, and is dependent on both the type and intensity of the applied stimulus. For example, osmotic shock evokes a greater increase in ASH iCa^{2+} than 10-mM quinine or nose touch (Hilliard, Apicella et al. 2005). Additionally, longer exposure times to Cu^{2+} result in longer lasting iCa^{2+} increases (Hilliard, Apicella et al. 2005). The ASHs express *eat-4* and require glutamatergic signaling to modulate postsynaptic targets (Berger, Hart et al. 1998, Lee, Sawin et al. 1999, de Bono and Maricq 2005, Bargmann 2006, Lindsay, Thiele et al. 2011, Piggott, Liu et al. 2011).

Depolarization of the ASHs evokes glutamate release onto the AVAs (Schafer and Kenyon 1995, Lindsay, Thiele et al. 2011, Piggott, Liu et al. 2011). Anterior touch evokes glutamate release from the ASHs onto GLR-1 and the AMPA-type GLR-2 on the AVAs; mutations in GLR-1 and/or GLR-2 result in defective anterior touch-evoked behavioral responses, as well as diminished postsynaptic currents in the AVAs, whereas high osmolarity avoidance behaviors are unaffected (Hart, Sims et al. 1995, Maricq, Peckol et al. 1995, Mellem, Brockie et al. 2002, de Bono and Maricq 2005, Bargmann 2006, Piggott, Liu et al. 2011). High osmolarity avoidance evokes a larger iCa^{2+} increase in the ASHs than anterior touch, and stimulates aversive behaviors by evoking glutamate

release from the ASHs onto GLR-1, GLR-2, the NMDA-type subunits NMR-1 and NMR-2, and an unidentified GluCl receptor on the AVAs (Brockie, Madsen et al. 2001, Mellem, Brockie et al. 2002, de Bono and Maricq 2005, Bargmann 2006). Furthermore, *nmr-1* mutants are not defective for anterior touch avoidance, supporting the notion that anterior touch does not evoke enough glutamate release from the ASHs to activate perisynaptically localized NMDA-type receptors on the AVAs (Brockie, Mellem et al. 2001, Mellem, Brockie et al. 2002, de Bono and Maricq 2005, Bargmann 2006). These data support that different degrees of ASH activation correspond to differential levels of glutamate release, and thus, differential modulation of postsynaptic targets (Hart, Sims et al. 1995, Maricq, Peckol et al. 1995, Mellem, Brockie et al. 2002, de Bono and Maricq 2005, Bargmann 2006, Lindsay, Thiele et al. 2011).

Peptides processed by the proprotein convertase type 2 ortholog EGL-3 inhibit the ASHs (Kass, Jacob et al. 2001, Mellem, Brockie et al. 2002, de Bono and Maricq 2005). In support of this, *egl-3;glr-1* double-mutants are wild-type for anterior touch- and high osmolarity-evoked aversive responses, and these responses are dependent on EAT-4 and NMR-1 (Kass, Jacob et al. 2001, Mellem, Brockie et al. 2002, de Bono and Maricq 2005). The proposed mechanism for restoration of anterior touch-evoked and high osmolarity-evoked responses in *egl-3;glr-1* double-mutants is that enhanced presynaptic release of glutamate from the ASHs, as a result of a mutation in *egl-3*, is capable of activating perisynaptically localized NMR-1 containing receptors (Kass, Jacob et al. 2001, Mellem, Brockie et al. 2002, de Bono and Maricq 2005). Furthermore, the AVBs, AVDs, and PVCs also express *egl-3* (Kass, Jacob et al. 2001). These data suggest that neuropeptides processed by EGL-3 are released from at least three command

interneurons to downregulate presynaptic release of glutamate from the ASHs (Kass, Jacob et al. 2001, Mellem, Brockie et al. 2002, de Bono and Maricq 2005).

The ASHs stimulate aversive responses not only through activation of the backward command interneurons, but also through activation of a disinhibitory pathway (Piggott, Liu et al. 2011). Although laser ablation of the backward command interneurons decreases backward locomotion, animals still initiate aversive behaviors in response to anterior touch and high osmolarity, as well as spontaneous backward locomotion (Piggott, Liu et al. 2011). However, following laser ablation of the backward command interneurons, in addition to the AIBs, animals exhibit minimal spontaneous, anterior touch-, and high osmolarity-evoked backward locomotion, suggesting that the AIBs stimulate backward locomotion (Piggott, Liu et al. 2011). In support of this, activation and inhibition of the AIBs using light-activated cationic and anionic channels stimulates and inhibits backward locomotion, respectively (Piggott, Liu et al. 2011). Furthermore, ASH activation by anterior touch and high osmolarity increases AIB iCa^{2+} levels, and anterior touch depolarization of the AIBs requires *eat-4* expression in the ASHs and *glr-1* expression in the AIBs (Piggott, Liu et al. 2011). These data suggest that activation of the AIBs stimulates backward locomotion. Additionally, anterior touch and high osmolarity decrease RIM iCa^{2+}, whereas laser ablation of the AIBs abolishes these decreases, suggesting that activation of the AIBs is required for inhibition of the RIMs, thus promoting backward locomotion (Piggott, Liu et al. 2011). In support of this, *eat-4* expression in the AIBs and *avr-14* expression in the RIMs are necessary for anterior touch-evoked inhibitory currents in the RIMs (Piggott, Liu et al. 2011). Furthermore, laser ablating the backward command interneurons in conjunction with the RIMs nearly

abolishes backward locomotion, similar to laser ablation of the backward command interneurons in conjunction with the AIBs (Piggott, Liu et al. 2011). Similarly, activation and inhibition of the RIMs using a light-activated cationic and anionic channel inhibits and stimulates backward locomotion, respectively (Piggott, Liu et al. 2011). Together, these data support a model for a disinhibitory circuit, whereby the ASHs activate the AIBs, which in turn inhibit the RIMs, resulting in stimulation/disinhibition of backward locomotion (Piggott, Liu et al. 2011).

1.7 Multiple monoamines modulate the ASHs and other neurons to alter 1-octanol-evoked avoidance behaviors

The presence of food modulates numerous stimulus-evoked behavioral responses in *C. elegans*. For example, food stimulates aversive responses to a variety of chemorepellants sensed by the ASHs, including Cu^{2+}, high osmolarity, and primaquine, and enhances aversive stimuli-evoked increases of ASH iCa^{2+} (Ezcurra, Tanizawa et al. 2011). Food enhances ASH-mediated aversive responses by mechanically stimulating dopaminergic neurons that sense the presence of bacteria, and incubating animals on NGM plates containing DA (10-mM) mimics the effect of food (Ezcurra, Tanizawa et al. 2011). Additionally, incubating animals on NGM plates containing 5-HT (4-mM) also enhances aversive behaviors similarly to food, and 5-HT is therefore thought to indicate the presence of food (Horvitz, Chalfie et al. 1982, Avery and Horvitz 1990, Segalat, Elkes et al. 1995, Sawin, Ranganathan et al. 2000). In addition to enhancing aversive behaviors, 5-HT (2.5-mM) also enhances anterior touch-evoked ASH iCa^{2+} increases, but has no effect on Cu^{2+}- or high osmolarity-evoked changes in ASH iCa^{2+} (Hilliard,

Apicella et al. 2005). In particular, monoaminergic modulation of avoidance responses to the noxious odorant 1-octanol have been thoroughly investigated.

The ASHs solely sense dilute (30% in ethanol, vol/vol) 1-octanol, whereas the ADLs and AWBs are involved in the sensation of 100% 1-octanol (Chao, Komatsu et al. 2004, Harris, Hapiak et al. 2009, Mills, Wragg et al. 2012). On an NGM plate that contains no food, a forward moving animal exposed to dilute 1-octanol initiates a reversal ~10 seconds after odorant presentation, backs up, and subsequently turns away from the noxious odorant (Chao, Komatsu et al. 2004, Harris, Hapiak et al. 2009, Summers, Layne et al. 2015, Zahratka, Williams et al. 2015). However, if animals are assayed on an NGM plate containing food or 5-HT (4-mM), a forward moving animal initiates a reversal ~5 seconds after odorant presentation, backs up a shorter distance than an animal off food, and subsequently resumes forward locomotion (Chao, Komatsu et al. 2004, Wragg, Hapiak et al. 2007, Harris, Hapiak et al. 2009, Summers, Layne et al. 2015). Modulation of dilute 1-octanol aversive responses by 5-HT requires expression of the 5-HT_6-like GPCR *ser-5* on the ASHs (Harris, Hapiak et al. 2009). Despite lacking chemical synapses onto the ASHs, the NSMs express the 5-HT reuptake transporter *mod-5*, and release 5-HT that activates SER-5 on the ASHs (Harris, Korchnak et al. 2011). In the ASHs, the $G\alpha_q$ subunit EGL-30 functions downstream of SER-5 to modulate aversive responses to dilute 1-octanol (Harris, Hapiak et al. 2009, Harris, Mills et al. 2010, Zahratka, Williams et al. 2015). In addition to $G\alpha_q$, $G\alpha_s$ functions in the ASHs downstream of an as-of-yet unidentified GPCR to also stimulate aversive responses (Harris, Mills et al. 2010). Evidence suggests that 5-HT stimulates aversive responses by activating $G\alpha_s$ signaling to stimulate release of *nlp-3* encoded peptides, leading to

activation of NPR-17 to enhance aversive responses (Harris, Mills et al. 2010).

In addition to the ASHs, 5-HT modulates numerous other neurons to enhance dilute 1-octanol aversive responses. The NSMs release 5-HT that activates the 5-HT_2-like receptor SER-1 on the RIAs to enhance aversive responses to dilute 1-octanol (Harris, Korchnak et al. 2011). The ADFs also reuptake 5-HT using MOD-5, and release 5-HT that activates SER-1 on the RICs, resulting in inhibition of enhanced aversive responses (Harris, Korchnak et al. 2011). Additionally, *mod-1* expression on either the AIYs or AIBs is required for 5-HT enhancement of aversive responses to 1-octanol (Harris, Hapiak et al. 2009). Together, these data demonstrate that 5-HT modulates multiple neurons alter dilute 1-octanol avoidance behaviors.

Incubation of animals on NGM plates containing the monoamine tyramine (TA; 4-mM) inhibits food and 5-HT stimulation of aversive responses to dilute 1-octanol, as well as aversive responses to 100% 1-octanol (Wragg, Hapiak et al. 2007). The GPCR TYRA-3 is required for TA-inhibition of 100% 1-octanol (Wragg, Hapiak et al. 2007). Expression of TYRA-3 appears highest in head and tail neurons, including the dopaminergic ADEs and CEPs (Wragg, Hapiak et al. 2007). Indeed, incubating animals on NGM plates containing DA (4-mM) inhibits 5-HT stimulated aversive responses to dilute 1-octanol (Wragg, Hapiak et al. 2007). Furthermore, DA can both inhibit and enhance ASH-mediated aversive responses by activating the mammalian D2-like GPCR DOP-3 and the human adrenoreceptor alpha 1B (ADRA1B) ortholog GPCR DOP-4, respectively (Ezak and Ferkey 2010, Ezcurra, Tanizawa et al. 2011). However, even in the absence of endogenous dopaminergic signaling, exogenous TA still inhibits 5-HT stimulated aversive responses to dilute 1-octanol, suggesting that TYRA-3 does not

function in the dopaminergic neurons to inhibit aversive responses (Wragg, Hapiak et al. 2007). In fact, the exact site of TYRA-3 function in inhibiting 5-HT stimulated aversive responses to dilute 1-octanol remains unclear (Wragg, Hapiak et al. 2007).

Incubation of animals on NGM plates containing the monoamine octopamine (OA; 4-mM) abolishes food- and 5-HT-dependent enhancement of aversive responses to dilute 1-octanol, and inhibits aversive responses to 100% 1-octanol (Wragg, Hapiak et al. 2007, Mills, Wragg et al. 2012). The ADFs release 5-HT that activates SER-1 on the RICs, evoking release of OA, which in turn activates the α-adrenergic-like GPCR OCTR-1 on the ASHs, thereby abolishing food or 5-HT enhancement of aversive responses to dilute 1-octanol (Wragg, Hapiak et al. 2007, Harris, Mills et al. 2010). The GPCR OCTR-1 stimulates $G\alpha_o$ signaling, resulting in inhibition of $G\alpha_q$ signaling through activation of the regulator of G-protein signaling (RGS) protein EAT-16, thereby antagonizing 5-HT stimulated aversive responses to dilute 1-octanol (Harris, Mills et al. 2010). Conversely, high concentrations of OA activate the α-adrenergic-like GPCR SER-3 on the ASHs, which acts antagonistically to OCTR-1, thereby preserving 5-HT enhancement of aversive responses to dilute 1-octanol (Mills, Wragg et al. 2012).

In addition to the ASHs, other sensory neurons are modulated by OA to alter avoidance to 100% 1-octanol. Low concentrations of OA activate the α-adrenergic-like GPCR SER-6 on the AWBs, ADLs, and ASIs to inhibit aversive responses to 100% 1-octanol (Mills, Wragg et al. 2012). The neuropeptide encoding *nlp-6* (ASIs), *nlp-7* (ADLs and ASIs), *nlp-8* (ADLs), and *nlp-9* (AWBs and ASIs) are also required for low OA concentration inhibition of aversive responses to 100% 1-octanol (Mills, Wragg et al. 2012). The corresponding receptors for the peptides encoded by *nlp-8* and *nlp-9* are

NPR-15 and NPR-18, respectively (Mills, Wragg et al. 2012). Activation of the neuropeptide receptors NPR-15 and NPR-18 on the AWCs and ASER, respectively, inhibits aversive responses to 100% 1-octanol, despite a lack of evidence for either the AWCs or ASER mediating 1-octanol sensation (Mills, Wragg et al. 2012). Animals lacking the AWCs exhibit enhanced aversive responses to dilute 1-octanol off food (Mills, Wragg et al. 2012). This suggests that OA activates SER-6 on the ADLs, evoking release of *nlp-8* encoded peptides onto NPR-15 on the AWCs, thus activating the AWCs and inhibiting aversive responses to 100% 1-octanol (Mills, Wragg et al. 2012). Conversely, signaling from ASER initiates turning behaviors (Suzuki, Thiele et al. 2008, Bretscher, Kodama-Namba et al. 2011). This suggests that OA activates SER-6 on the AWBs, evoking release of *nlp-9* encoded peptides onto NPR-18 on the ASER, thereby inhibiting the ASER and aversive responses to 100% 1-octanol (Mills, Wragg et al. 2012). This demonstrates the ability for sensory neurons not directly involved in 1-octanol sensation to modulate aversive responses to the noxious stimulus, indicating that extensive integration of neural network information is indeed capable of modulating animal behavior (Mills, Wragg et al. 2012, Shingai, Ichijo et al. 2014). Figure 1-3 illustrates how the ASHs sense stimuli (Figure 1-3A) and the complex array of neurons that interact to modulate aversive responses to 1-octanol (Figure 1-3B).

1.8 The AIB interneurons shape 1-octanol-evoked aversive behaviors

A wild-type animal off food that is moving forward initiates a reversal ~10 seconds after presentation of 30% 1-octanol (initial aversive behavior), reverses a long distance,

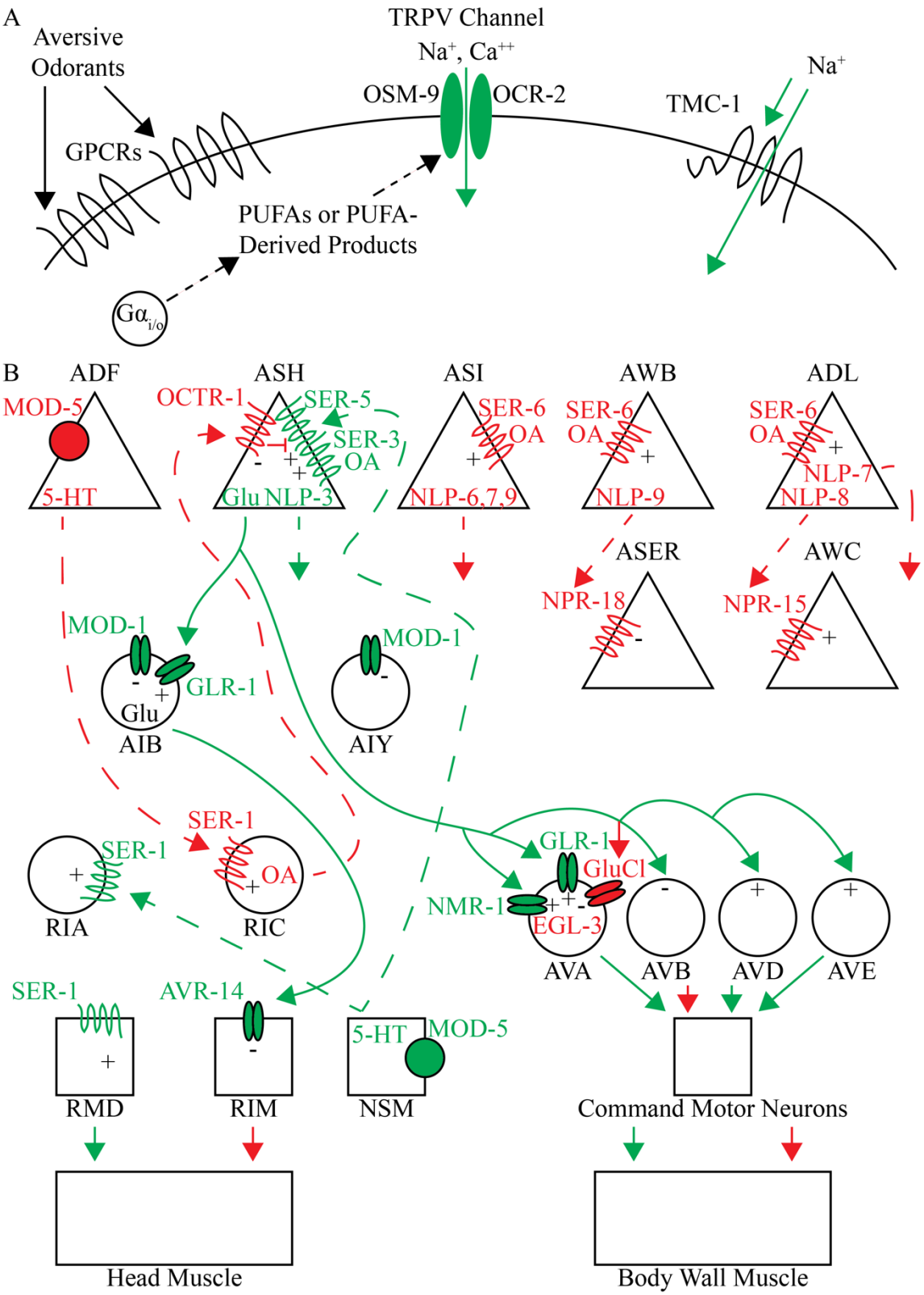
A
Aversive Odorants
GPCRs
TRPV Channel
Na+, Ca++
OSM-9
OCR-2
TMC-1
Na+
PUFAs or PUFA-Derived Products
Gαi/o
B
ADF
MOD-5
5-HT
ASH
OCTR-1
SER-5
SER-3
OA
Glu NLP-3
ASI
SER-6
OA
NLP-6,7,9
AWB
SER-6
OA
NLP-9
ADL
SER-6
OA
NLP-7
NLP-8
ASER
NPR-18
AWC
NPR-15
MOD-1
GLR-1
Glu
AIB
MOD-1
AIY
SER-1
SER-1
OA
RIA
RIC
GLR-1
GluCl
NMR-1
EGL-3
AVA
AVB
AVD
AVE
SER-1
AVR-14
5-HT
MOD-5
RMD
RIM
NSM
Command Motor Neurons
Head Muscle
Body Wall Muscle

Figure 1-3. Classical neurotransmitter, monoaminergic, and peptidergic signaling pathways modulate ASH-mediated aversive responses. A. An odorant binds to a GPCR to activate a $G\alpha_{i/o}$ subunit (i.e. ODR-3, GPA-3). The $G\alpha_{i/o}$ subunit then regulates either PUFA production or degradation to increase PUFA levels, leading to activation of the TRPV channels containing OSM-9 and OCR-2. B. Signaling pathways and components in green stimulate ASH-mediated aversive responses. Signaling pathways and components in red inhibit ASH-mediated aversive responses. Solid and dashed lines indicate synaptic and extrasynaptic signaling pathways, respectively. Additionally, + and - indicates enhancement and inhibition, respectively, of synaptic output in response to input from the signaling pathway and/or receptor activation (effects of glutamate release from the ASHs on AVB, AVD, and AVE synaptic output are hypothesized effects).

and subsequently turns away from the noxious odorant after completing the reversal (collectively, BL and turning away from the odorant are termed postinitiation behaviors; initial and postinitation behaviors are termed aversive behaviors) (Figure 1-4A, B) (Summers, Layne et al. 2015). Conversely, a wild-type animal on food or 5-HT that is moving forward initiates a reversal ~5 seconds after presentation of 30% 1-octanol (enhanced initial aversive behavior), reverses a short distance, and continues moving forward after completing the reversal (collectively, shorter BL and resumed forward locomotion are termed enhanced postinitiation behaviors; enhanced initial and postinitation behaviors are termed enhanced aversive behaviors) (Figure 1-4A, B) (Summers, Layne et al. 2015). Interestingly, animals with ASH-selective *eat-4* overexpression exhibit an enhanced initial aversive behavior to 30% 1-octanol, but postinitiation behaviors are uneffected (Figure 3-2B) (Summers, Layne et al. 2015). These data demonstrate that food, 5-HT, and increased ASH glutamate release enhance the initial aversive behavior to 30% 1-octanol (Summers, Layne et al. 2015). Interestingly, increased ASH glutamate release does not effect postinitiation behaviors to 30% 1-octanol, suggesting that the initiation behavior and postinitiation behaviors are independently modulated (Summers, Layne et al. 2015). Supporting this, food and 5-HT decrease spontaneous turning behaviors, but enhance the initial aversive behavior to 30% 1-octanol (Figure 3-2C) (Summers, Layne et al. 2015).

Like food and 5-HT, AWC-selective *eat-4* RNAi enhances aversive behaviors to 30% 1-octanol off food (Figure 1-5A) (Summers, Layne et al. 2015). However, AWC-selective *eat-4* overexpression does not alter aversive behaviors to 30% 1-octanol on food, but does abolish 5-HT enhancement of aversive behaviors (Figure 1-5B) (Summers,

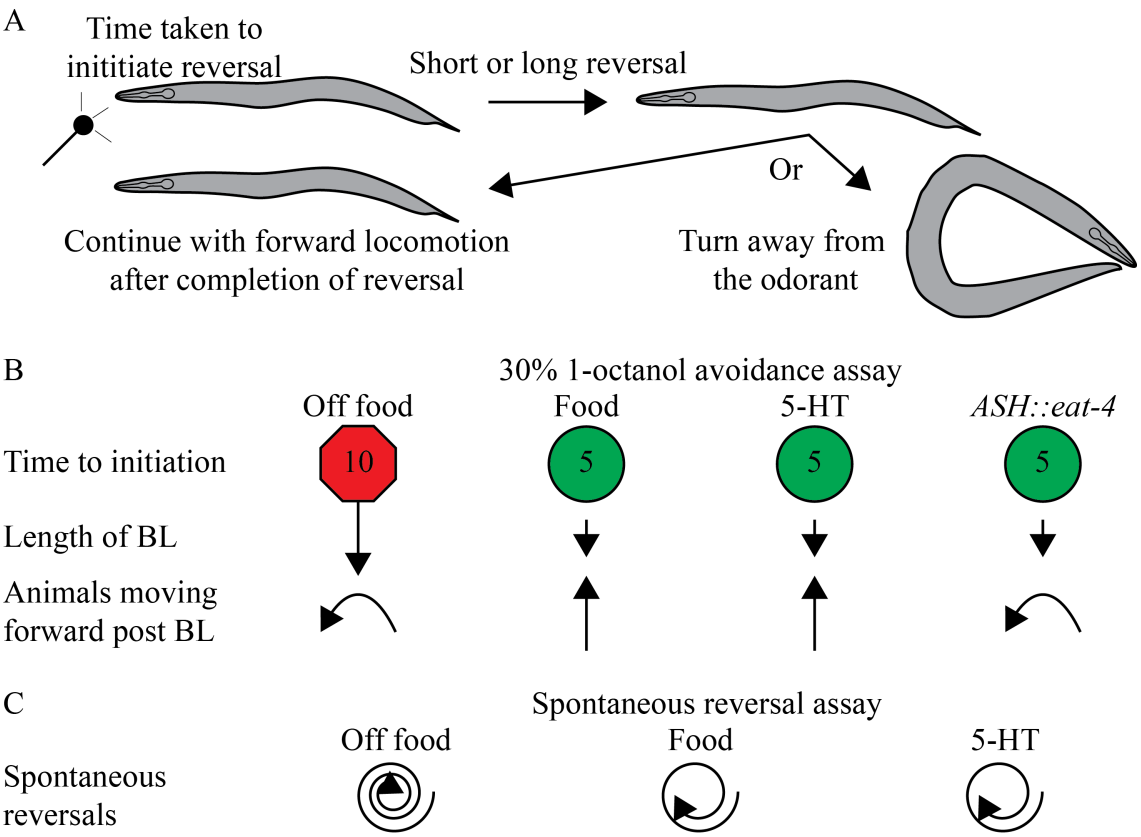

Figure 1-4. Glutamate released by the ASHs in response to 30% 1-octanol presentation initiates a reversal but does not effect postinitiation behaviors. A. Diagram depicting the three behaviors quantified during 1-octanol avoidance. B. Summary of aversive behaviors in response to 30% 1-octanol presentation exhibited by wild-type animals off food, on food, and on 4-mM 5-HT, and transgenic animals off food. The *sra-6* promoter drove *eat-4* cDNA expression in the ASHs of wild-type animals. C. Summary of spontaneous turning behavior exhibited by wild-type animals off food, on food, and on 4-mM 5-HT. For time to initiation, the number inside the red octagon or green circle indicates the average delay in time (seconds) before animals initiated a reversal following 1-octanol presentation. For length of BL (backward locomotion), reversal length was measured by the number of body bends during the

initial reversal. Long arrows indicate a long reversal (~2.5 body bends on average) and short arrows indicate a short reversal (~1.5 body bends on average). For animals moving forward post BL, a curved arrow indicates that the majority of animals performed an ω-turn away from the odorant (~80% of animals assayed on average) after they finished reversing, whereas an arrow pointing forward indicates the majority of animals resumed forward locomotion (~80% of animals assayed on average). For spontaneous locomotion, a spiral that revolves more times indicates that animals on average performed a high number of reversals off food (~6 per minute), while a spiral that terminates more quickly indicates that animals on average performed a low number of reversals off food (~3 per minute).

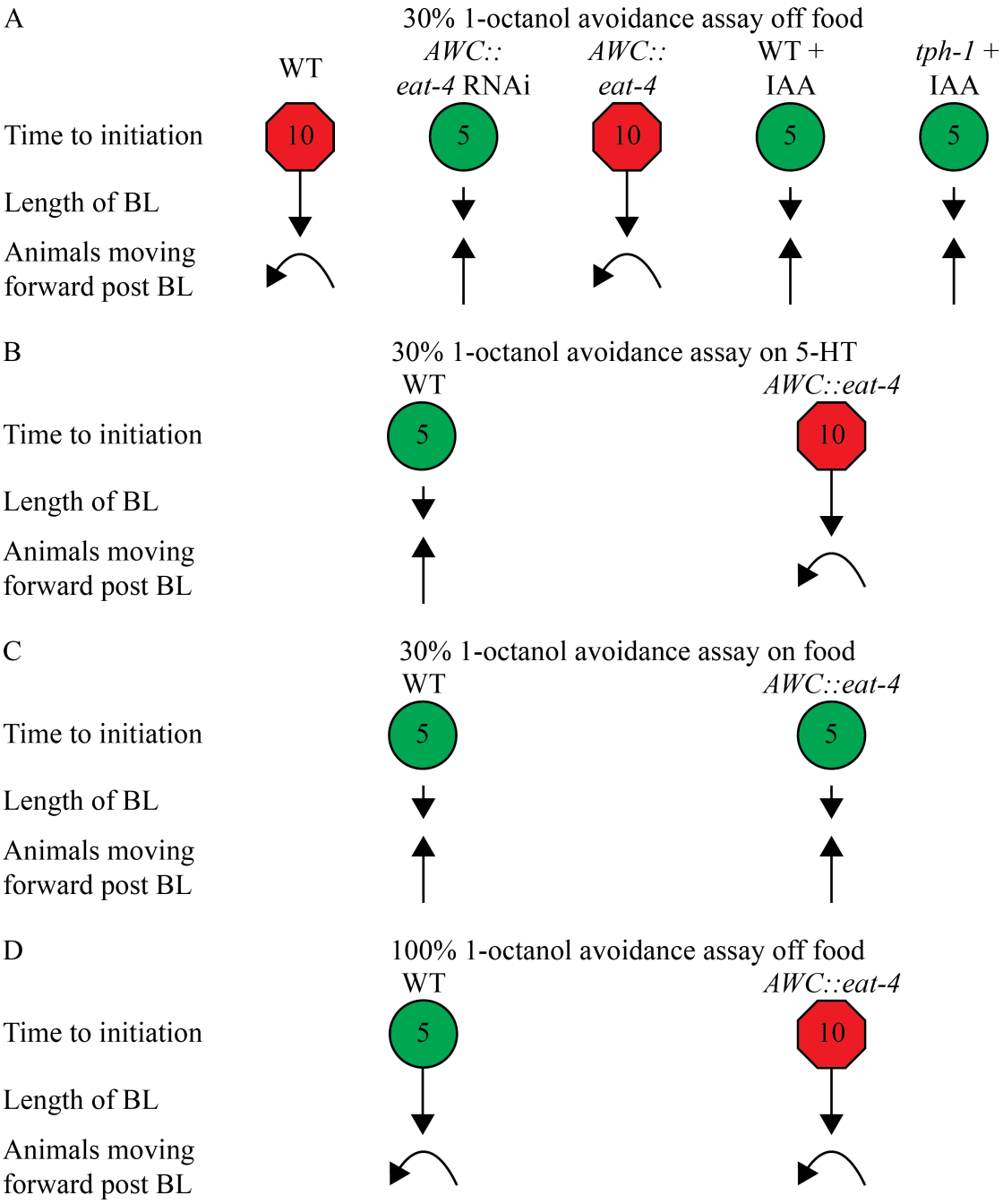

Figure 1-5. Glutamatergic signaling from the AWCs inhibits 5-HT modulation of 30% 1-octanol aversive responses and 100% 1-octanol avoidance behaviors. A. Summary of aversive behaviors in response to 30% 1-octanol presentation exhibited by wild-type and transgenic animals off food, and in response to a dilute IAA/1-octanol

mixture presentation by wild-type and null animals off food. B. Summary of aversive behaviors in response to 30% 1-octanol presentation exhibited by wild-type and transgenic animals on 4-mM 5-HT. C. Summary of aversive behaviors in response to 30% 1-octanol presentation exhibited by wild-type and transgenic animals on food. D. Summary of aversive behaviors to 100% 1-octanol presentation exhibited by wild-type and transgenic animals off food. The *nlp-1* promoter drove *eat-4* cDNA or *eat-4* RNAi expression in the AWCs of wild-type animals in (A), (B), (C), and (D).

Layne et al. 2015). Interestingly, a 40% IAA/30% 1-octanol (dilute IAA/1-octanol) mixture enhances aversive behaviors off food (Figure 1-5A) (Summers, Layne et al. 2015). One possibility for this dichotomy is that food and IAA, but not 5-HT, inhibit AWC activity (Chalasani, Chronis et al. 2007). In support of this, food enhances the initial aversive response of *tph-1* (tryptophan hydroxylase; required for 5-HT synthesis) mutants to 30% 1-octanol (Chao, Komatsu et al. 2004). Similarly, a dilute IAA/1-octanol mixture also enhances the aversive behaviors of *tph-1* mutants to 30% 1-octanol (Figure 1-5A) (Summers, Layne et al. 2015). Together, these data support that tonic AWC glutamatergic signaling inhibits aversive behaviors to 30% 1-octanol (Summers, Layne et al. 2015). Presentation of a concentrated (≥40%) 1-octanol solution enhances the initial aversive behavior, but does not effect postinitiation behaviors, and AWC-selective *eat-4* overexpression inhibits the initial aversive response (Figure 1-5D) (Summers, Layne et al. 2015). These data further support that AWC glutamatergic signaling delays the initial aversive behavior to 1-octanol, but also indicate that concentrated 1-octanol does not enhance the initial aversive behavior by inhibiting the AWCs more than 30% 1-octanol, as postinitiation behaviors are not dependent on 1-octanol concentration (Summers, Layne et al. 2015).

Although saturating 1-octanol has no effect on ASER iCa^{2+}, ASER-specific *eat-4* overexpression enhances aversive behaviors to 30% 1-octanol (Figure 1-6A) (Summers, Layne et al. 2015). Furthermore, ASER-specific *eat-4* RNAi knockdown abolishes 5-HT enhancement of aversive behaviors to 30% 1-octanol (Figure 1-6B) (Summers, Layne et al. 2015). These data demonstrate that tonic ASER glutamate release enhances aversive responses to 30% 1-octanol (Summers, Layne et al. 2015). Supporting these data,

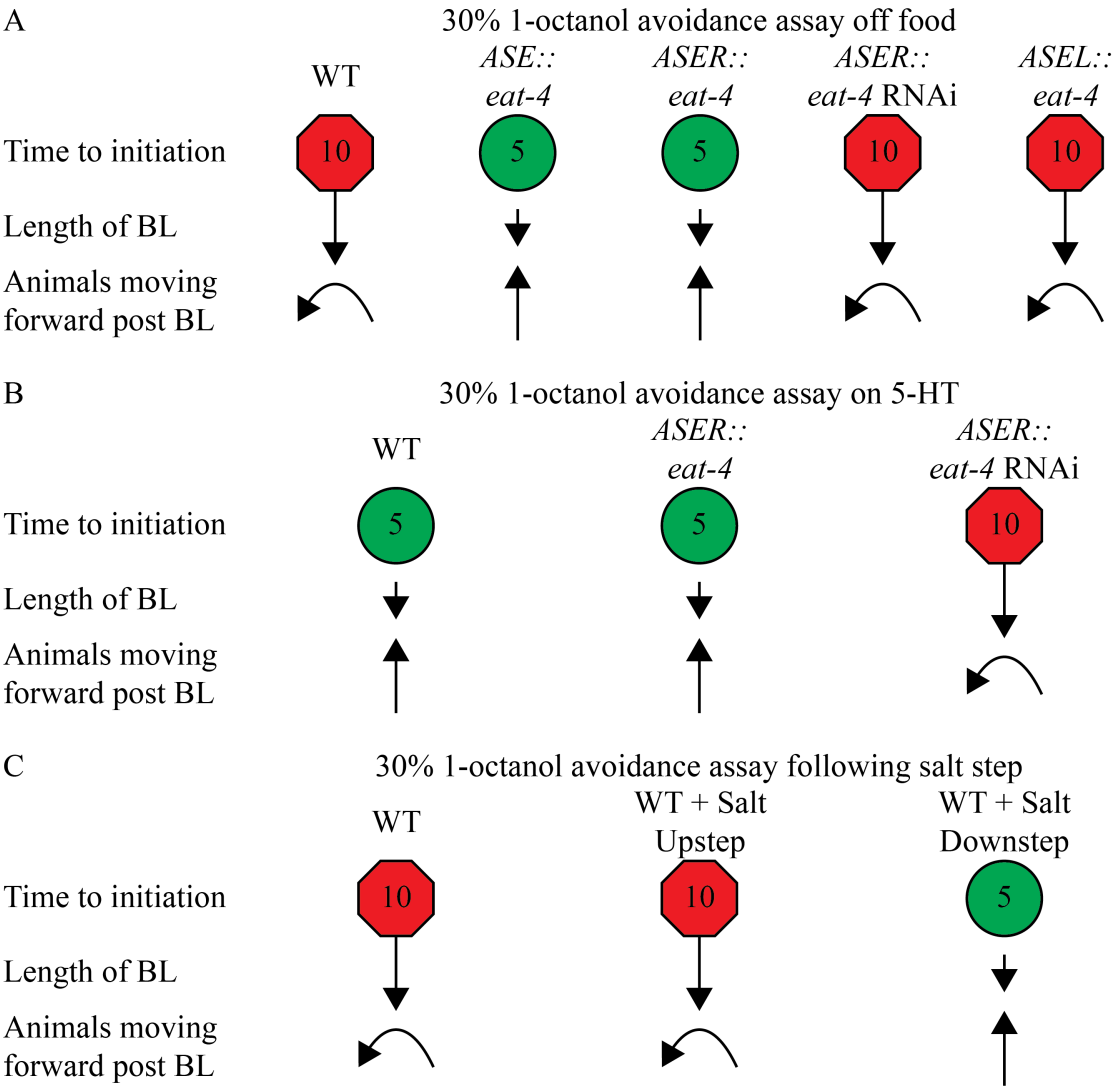

Figure 1-6. Glutamatergic signaling from the ASER stimulates 30% 1-octanol aversive responses off food. A. Summary of aversive behaviors in response to 30% 1-octanol presentation exhibited by wild-type and transgenic animals off food. B. Summary of aversive behaviors to 30% 1-octanol presentation exhibited by wild-type and transgenic animals on 4-mM 5-HT. C. Summary of aversive behaviors to 30% 1-octanol presentation exhibited by wild-type animals off food following no salt step, a salt upstep, or a salt downstep. Salt upstep was performed by incubating animals on an NGM plate (NaCl 50-mM) for 10 minutes and transferring to an NGM plate (NaCl 60-mM) for two

minutes before assaying. Salt downstep was performed by incubating animals on an NGM plate (NaCl 60-mM) for 10 minutes and transferring to an NGM plate (NaCl 50-mM) for two minutes before assaying. The *flp-6* or *gcy-6* promoter drove *eat-4* cDNA expression in the ASEs or ASEL of wild-type animals in (A), respectively. The *gcy-5* promoter drove *eat-4* cDNA or *eat-4* RNAi expression in the ASER of wild-type animals in (A) and (B).

performing a salt downstep immediately prior to 30% 1-octanol presentation enhances aversive behaviors, while performing a salt upstep immediately prior to assaying has no effect (Figure 1-6C) (Summers, Layne et al. 2015). These results demonstrate that ASER activation enhances aversive behaviors to 30% 1-octanol (Summers, Layne et al. 2015). In salt-conditioned animals, exogenous 5-HT abolishes the enhancement of ASER iCa^{2+} increases in response to salt downstep (Oda, Tomioka et al. 2011). Interestingly, enhanced ASER iCa^{2+} increases following salt downstep inversely correlate with ASER synaptic transmission in salt-conditioned animals (Oda, Tomioka et al. 2011). Similarly, ASER-selective *eat-4* RNAi abolishes 5-HT enhancement of aversive behaviors to 30% 1-octanol (Summers, Layne et al. 2015). Together, these data suggest that 5-HT, at least in part, enhances aversive behaviors to 30% 1-octanol by increasing ASER glutamate release (Oda, Tomioka et al. 2011, Summers, Layne et al. 2015).

In order to determine how the AIBs shaped aversive behaviors to 1-octanol, the activity of the AIBs were altered using transgenic manipulation. The AIBs were ablated using AIB-specific expression of the cell death protein encoded by *egl-1* (Conradt and Horvitz 1998, Summers, Layne et al. 2015). Like food and 5-HT, ablation of the AIBs enhances aversive behaviors to 30% 1-octanol (Figure 1-7A) (Summers, Layne et al. 2015). Following the removal of food, animals with ablated AIBs perform fewer spontaneous reversals, reverse a shorter distance, and move forward after completing a reversal (Figure 1-7C) (Summers, Layne et al. 2015). These data suggest that the AIBs delay backward locomotion in response to 30% 1-octanol, stimulate long reversals, and increase turning probability after the reversal is complete (Summers, Layne et al. 2015). Ablating the AIBs may produce numerous developmental defects. Therefore, AIB

signaling was reduced using AIB-specific expression of either the synaptobrevin-specific tetanus toxin (TeTx) or *eat-4* RNAi, or AIB-specific *mod-1* overexpression (Busch, Laurent et al. 2012, Summers, Layne et al. 2015). All three manipulations enhance aversive behaviors to 30% 1-octanol (Figure 1-7A) (Summers, Layne et al. 2015). As expected, none of these manipulations altered 5-HT enhancement of aversive behaviors to 30% 1-octanol (Figure 1-7B) (Summers, Layne et al. 2015). These data support that AIB signaling, specifically glutatmatergic signaling, causes animals to delay reversing following 30% 1-octanol presentation, execute a long reversal, and subsequently turn away from the odorant (Summers, Layne et al. 2015). Furthermore, manipulation with AIB-specific TeTx expression mimicked the effects of AIB ablation on spontaneous turning off food (Figure 1-7C) (Summers, Layne et al. 2015). These data further support that AIB signaling stimulates spontaneous turning behavior and backward locomotion off food (Summers, Layne et al. 2015). Conversely, animals with enhanced AIB excitability as a result of AIB-specific *mod-1* RNAi knockdown or AIB-specific *glr-1* overexpression do not exhibit 5-HT enhancement of aversive behaviors to 30% 1-octanol (Figure 1-7B) (Summers, Layne et al. 2015).

To further rule out the possibility of developmental effects using transgenic techniques that constitutively alter AIB excitability, AIBs were transiently inhibited using AIB-specific HisCl1 expression and incubating animals on HA (Pokala, Liu et al. 2014, Summers, Layne et al. 2015). Inhibition of the AIBs using HisCl produced identical effects to the transgenic techniques used to ablate the AIBs or inhibit AIB signaling in both 30% 1-octanol avoidance and spontaneous reversals off food (Figure 1-8A, B) (Summers, Layne et al. 2015). Interestingly, titrating of the amount of HA in assay plates

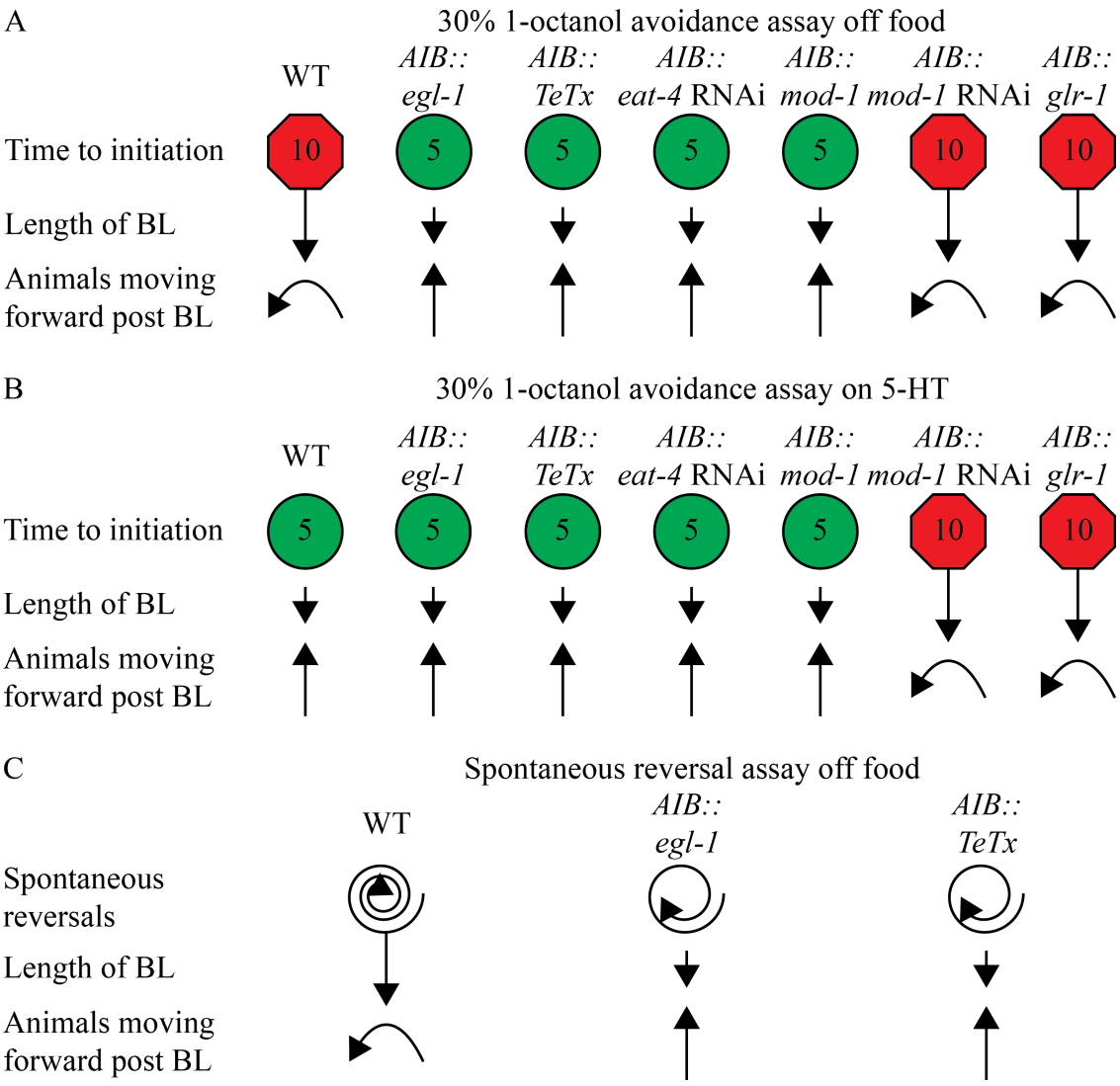

Figure 1-7. The AIBs differentially modulate aversive and spontaneous turning behaviors. A. Summary of aversive behaviors in response to dilute 1-octanol presentation exhibited by wild-type and transgenic animals off food. B. Summary of aversive behaviors in response to dilute 1-octanol presentation exhibited by wild-type and transgenic animals on 4-mM 5-HT. C. Summary of spontaneous turning behaviors exhibited by wild-type and transgenic animals off food. The *npr-9* promoter drove *egl-1* or *mod-1* cDNA, or *eat-4* or *mod-1* RNAi expression in the AIBs of wild type animals in

(A), (B), and (C). The *inx-1* promoter drove TeTx expression in the AIBs of wild-type animals in (A), (B), and (C). The *npr-9* promoter drove expression of *glr-1* cDNA in the AIBs of wild-type animals in (A) and (B).

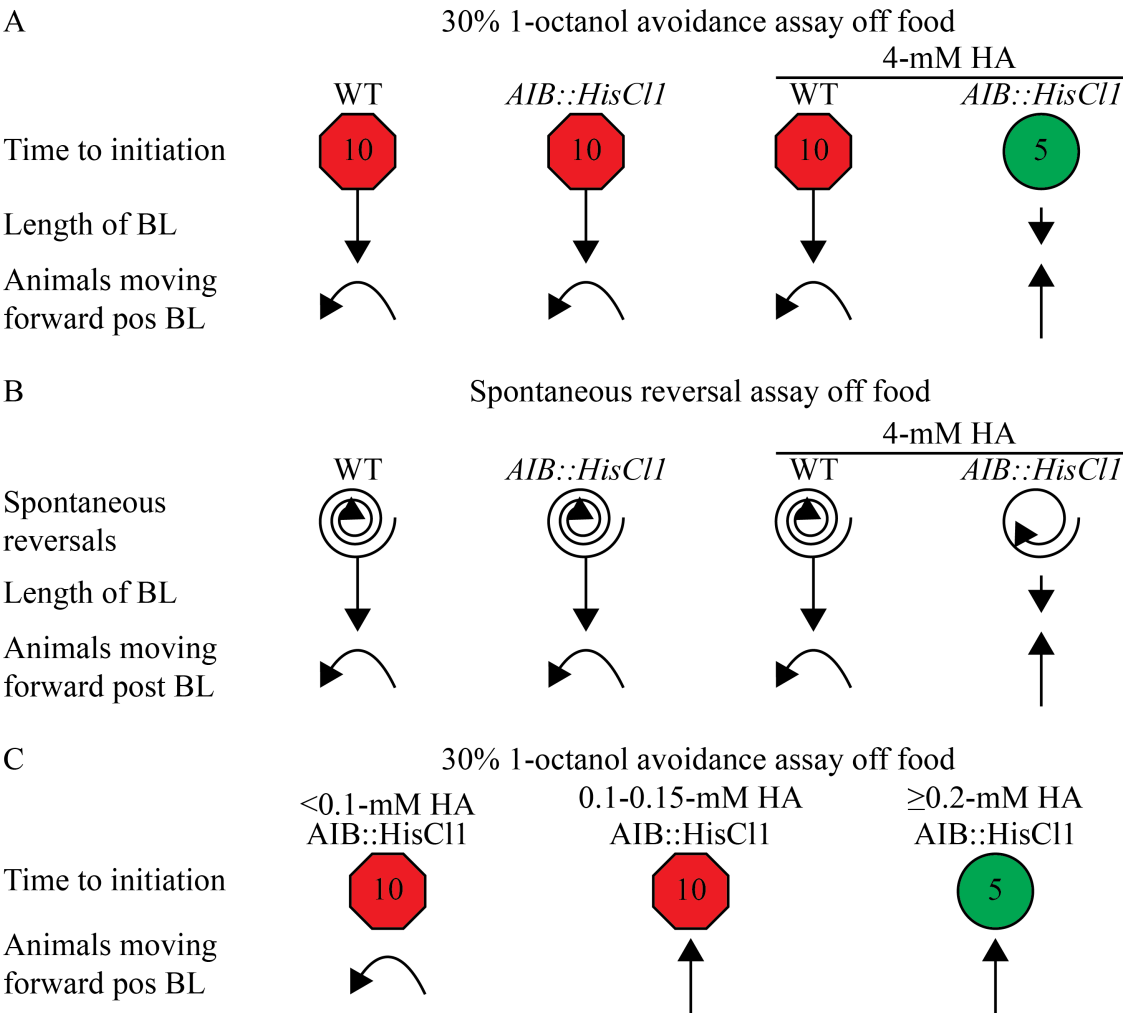

Figure 1-8. Different degrees of AIB inhibition by the heterologously expressed HisCl1 can differentially modulate aversive behaviors. A. Summary of aversive behaviors in response to dilute 1-octanol presentation exhibited by wild-type and transgenic animals off food or on 4-mM HA. B. Summary of spontaneous turning behaviors exhibited by wild-type and transgenic animals off food or on 4-mM HA. C. Summary of aversive behaviors in response to dilute 1-octanol presentation exhibited by transgenic animals on <0.1-mM HA, 0.1-.15-mM HA, or ≥0.2-mM HA. The *inx-1* promoter drove expression of HisCl1 in the AIBs of wild-type animals in (A), (B), and (C).

yielded a concentration range (0.1-0.15-mM) that caused animals to initiate a reversal 10 seconds after dilute 1-octanol presentation, but subsequently resume forward locomotion; HA concentrations lower or higher mimicked behavioral responses off food and on food/5-HT, respectively (Figure 1-8C) (Summers, Layne et al. 2015). These data demonstrate that aspects of the AIBs effects on dilute 1-octanol avoidance can be differentially modulated, depending on AIB activity state (Summers, Layne et al. 2015).

The AWC sensory neurons signal onto the AIBs through GLR-1 (Chalasani, Chronis et al. 2007). As previously discussed, animals with AWC-specific *eat-4* RNAi knockdown have enhanced aversive responses to 30% 1-octanol (Summers, Layne et al. 2015). Therefore, *glr-1* mutants were examined to see if they exhibit similar aversive behaviors (Summers, Layne et al. 2015). In contrast to animals with AWC *eat-4* RNAi knockdown, *glr-1* mutants off food behave like wild type animals in response to 30% 1-octanol (Figure 1-9A) (Summers, Layne et al. 2015). This was not entirely unexpected, as the ASHs signal onto GLR-1 in the AVAs, an integral component of the backward locomotory circuit (Mellem, Brockie et al. 2002). However, *glr-1* mutants with AVA-specific *glr-1* rescue exhibit enhanced aversive behaviors to 30% 1-octanol off food (Figure 1-9A) (Summers, Layne et al. 2015). Additionally, AIB-specific *glr-1* RNAi knockdown also enhances aversive behaviors to 30% 1-octanol off food (Figure 1-9A) (Summers, Layne et al. 2015). Furthermore, animals with both AWC-specific *eat-4* overexpression and AIB-specific *glr-1* RNAi knockdown display 5-HT enhancement of aversive behaviors to 30% 1-octanol off food, as well as enhanced aversive behaviors to 100% 1-octanol off food (Figure 1-9B, C) (Summers, Layne et al. 2015). Together, these data demonstrate that glutamate release from the AWCs onto GLR-1 in the AIBs inhibits

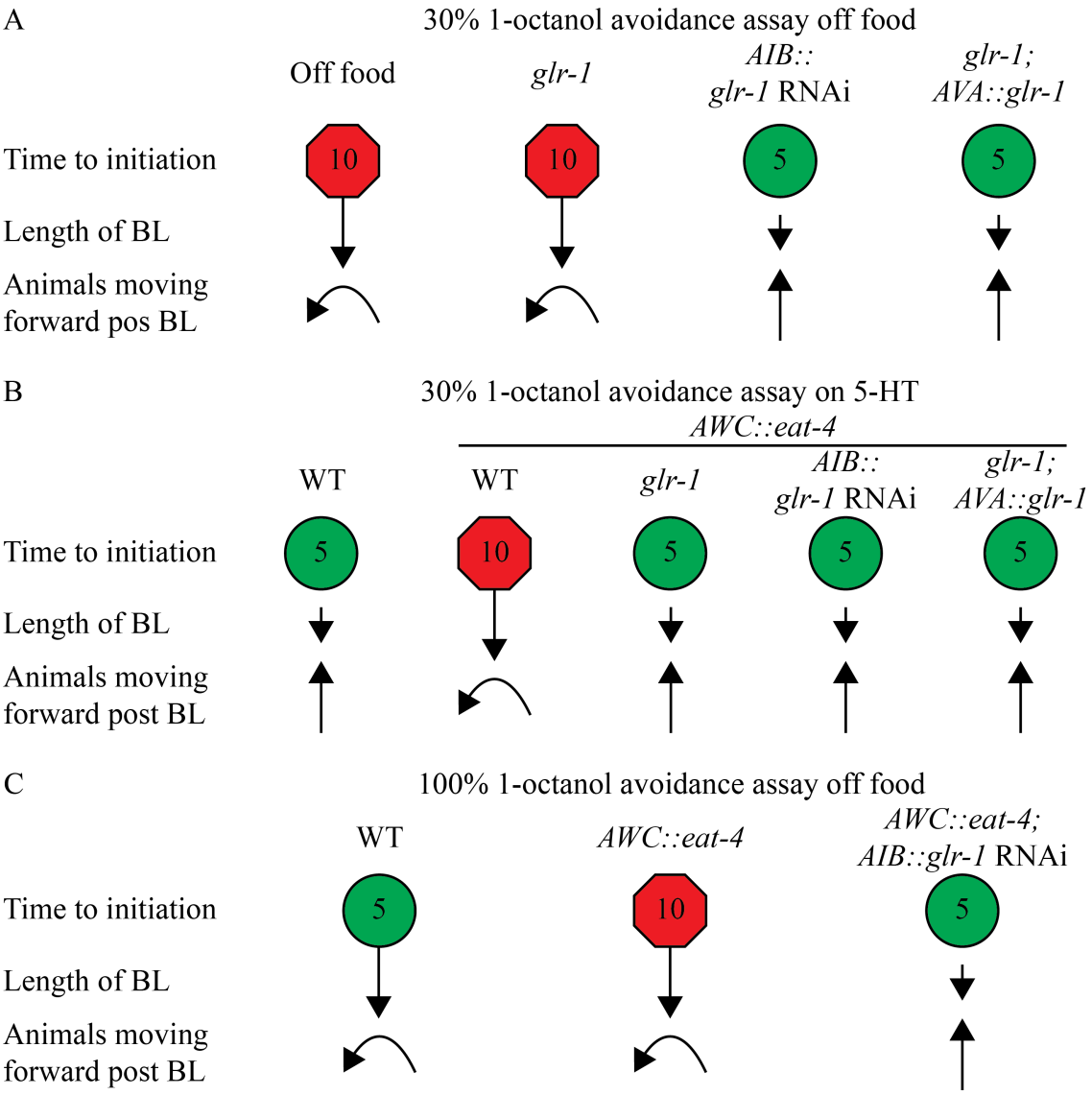

Figure 1-9. The AWCs modulate 1-octanol aversive responses by releasing glutamate onto GLR-1 on the AIBs. A. Summary of aversive behaviors in response to 30% 1-octanol presentation exhibited by wild-type, null, transgenic, and transgenic null animals off food. B. Summary of aversive behaviors in response to 30% 1-octanol presentation exhibited by wild-type, null, transgenic, and transgenic null animals on 4-mM 5-HT. C. Summary of aversive behaviors in response to 100% 1-octanol presentation exhibited by wild-type and transgenic animals off food. The *npr-9* promoter

drove expression of *glr-1* RNAi in the AIBs of wild-type and transgenic animals in (A), (B), and (C). The *nmr-1* promoter drove *glr-1* expression in the AVAs of null and transgenic null animals in (A) and (B). The *nlp-1* promoter drove *eat-4* expression in the AWCs of wild-type, null, transgenic, and transgenic null animals in (B) and (C).

data demonstrate that glutamate release from the AWCs onto GLR-1 in the AIBs inhibits the initiation of reversals in response to 1-octanol, stimulates long reversals, and promotes turning away from the odorant (Summers, Layne et al. 2015).

In contrast to AWC-specific *eat-4* overexpression, ASER-specific *eat-4* overexpression enhances aversive behaviors to 30% 1-octanol off food (Summers, Layne et al. 2015). Additionally, the AWCs signal onto GLR-1 in the AIBs, and glutamate evokes an inhibitory current in the AIBs by activating the AVR-14 (Chalasani, Chronis et al. 2007, Piggott, Liu et al. 2011, Summers, Layne et al. 2015). Therefore, it was predicted that the ASER to AIB synapses would be mediated by glutamate release onto AVR-14. Avoidance responses to 30% 1-octanol off food are not altered in *avr-14* mutants (Figure 1-10A) (Summers, Layne et al. 2015). In contrast, 5-HT does not enhance aversive behaviors to 30% 1-octanol in *avr-14* mutants or animals with AIB-specific *avr-14* RNAi knockdown (Figure 1-10B) (Summers, Layne et al. 2015). Furthermore, ASE-specific *eat-4* overexpression does not enhance aversive behaviors to 30% 1-octanol off food in *avr-14* mutants or animals with AIB-specific *avr-14* RNAi knockdown (Figure 1-10A). Additionally, although salt downstep followed by 30% 1-octanol exposure enhances aversive behaviors to 30% 1-octanol off food, salt downstep does not enhance aversive responses in *avr-14* mutants or animals with AIB-specific *avr-14* RNAi knockdown (Figure 1-10C) (Summers, Layne et al. 2015). Together, these data demonstrate that the ASER inhibits the AIBs by releasing glutamate onto AVR-14 (Summers, Layne et al. 2015). This result was somewhat surprising, as previous evidence indicates that ASER activation increases AIB iCa^{2+} (Oda, Tomioka et al. 2011). However, salt downsteps prior to 30% 1-octanol aversive assays were performed by

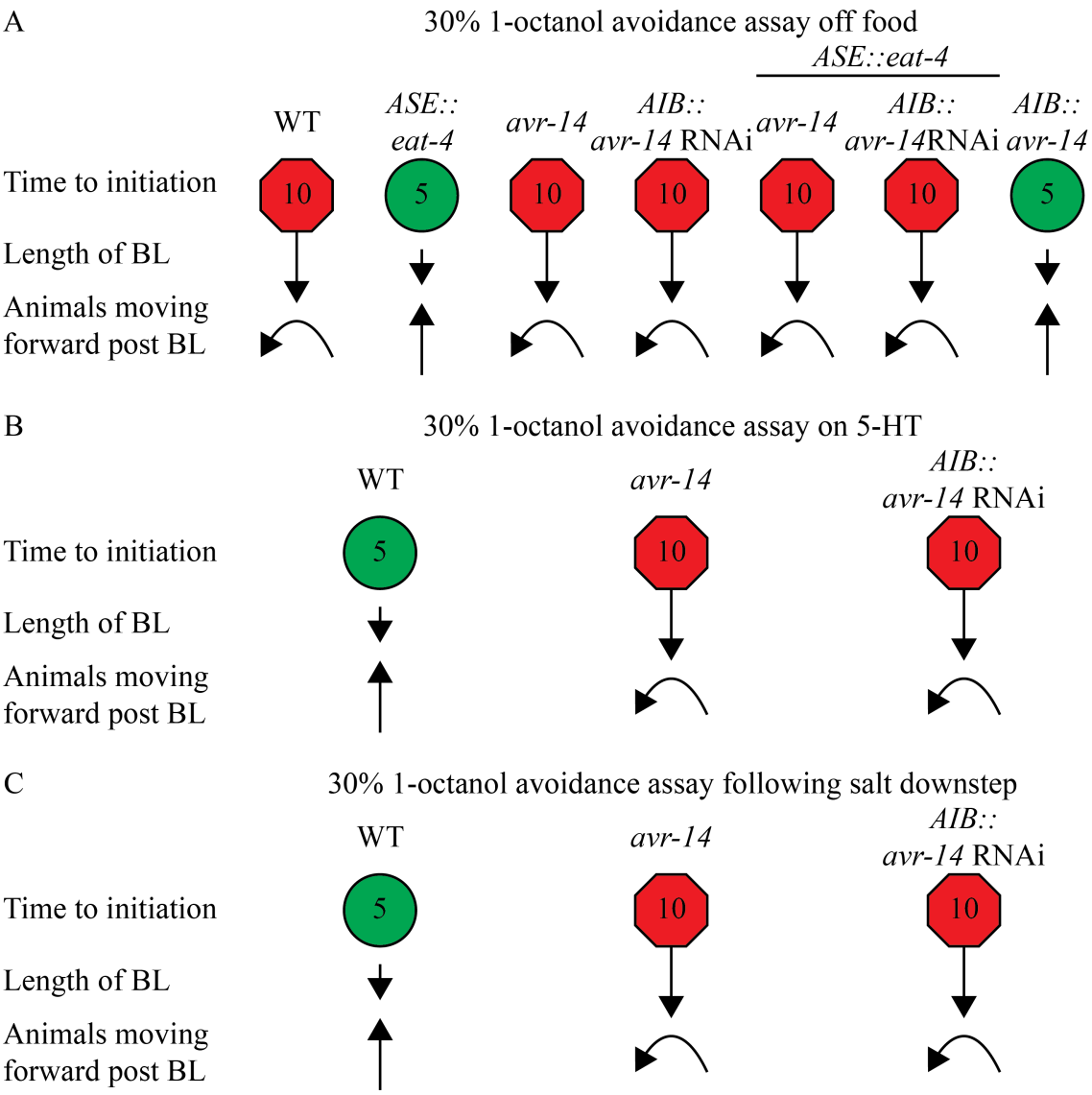

Figure 1-10. The ASER modulates 30% 1-octanol aversive responses by releasing glutamate onto AVR-14 on the AIBs. A. Summary of aversive behaviors in response to dilute 1-octanol presentation exhibited by wild-type, null, transgenic, and transgenic null animals off food. B. Summary of aversive behaviors in response to dilute 1-octanol presentation exhibited by wild-type, null, and transgenic animals on 5-HT. C. Summary of aversive behaviors in response to dilute 1-octanol presentation exhibited by wild-type, null, and transgenic animals off food following a salt downstep. The *gcy-5* promoter

drove *eat-4* cDNA expression in the ASER of wild-type, null, and transgenic animals in (A). The *inx-1* promoter drove *avr-14* RNAi or cDNA expression in the AIBs of wild-type and transgenic animals in (A), (B), and (C).

transferring animals to an NGM (NaCl 60-mM) plate for 10 minutes, then to an NGM (NaCl 50-mM) plate for two minutes, after which animals were presented with 30% 1-octanol (Summers, Layne et al. 2015). Previous investigations found that washing a food free 20-mM NaCl solution across an animals amphid for 10 minutes prior to performing a salt downstep to a NaCl free solution abolished AIB iCa^{2+} increases (Oda, Tomioka et al. 2011). Therefore, the salt downstep prior to assaying avoidance behaviors to 30% 1-octanol and the assay whereby animals were conditioned to associate NaCl with the absence of food were comparable. As a result, animals may have associated NGM plates (NaCl 60-mM) with the absence of food, and salt downstep to NGM plates (NaCl 50-mM) may have not evoked AIB iCa^{2+} increases, as supported by behavioral data indicating that ASER signals onto AVR-14 on the AIBs. Additionally, recent work demonstrates that AIB iCa^{2+} correlates with motor output, with peaks in iCa^{2+} occurring after completion of a reversal as forward locomotion resumes, rather than modulation by upstream sensory inputs (Luo, Wen et al. 2014). Thus, calcium-imaging experiments may not accurately reflect the effect of ASER synaptic inputs on AIB activity.

1.9 Project focus

In my investigation, I describe how three pairs of sensory neurons (ASHs, AIBs, AWCs) modulate the activity of the AIBs, thereby leading to changes in locomotion, one of which was previously not implicated in 1-octanol sensation (AWCs). Furthermore, excitatory and inhibitory glutamatergic signaling pathways, and an inhibitory cholinergic pathway are involved in modulation of the AIBs. Additionally, an L-Type VGCC enhances AIBs activity. Presentation of dilute 1-octanol off food stimulated animals to

reverse ~10 seconds after presentation, perform an Ω-turn, and subsequently move away from the odorant source. Conversely, presentation of dilute 1-octanol on food and 5-HT stimulated animals to reverse ~5 seconds after presentation and subsequently resume forward locomotion after completing backward locomotion. Additionally, despite the ASER not responding directly to 1-octanol, animals exposed to a salt downstep followed by dilute 1-octanol stimulus behaved similarly to animals on food and 5-HT. Together, these results demonstrate that extensive integration of sensory inputs by the AIBs produces differential behavioral responses to a noxious odorant.

Chapter 2

Materials and Methods

2.1 Worms strains and maintenance

Worm strains were cultured and handled using standard techniques (Brenner 1974). The Bristol N2 strain was used as wild-type. The strains used were: FY858 *fvIs1 [Pnpr-9::RFP]; kyEx4018 [Pinx-1::GCaMP3]*, FY860 *fvIs1 [Pnpr-9::RFP]; kyEx3253 [Pinx-1::GCaMP3]*, FY928 *grIs18 [Psra-6::GCaMP3]; fvEx [Pgpa-4::RFP]*, FY976 *fvIs1 [Pnpr-9::RFP]; vuEx [Pacc-1::GFP, Pnpr-9::RFP, rol-6]*, FY977 *fvIs1 [Pnpr-9::RFP]; vuEx [Plgc-47::GFP, Pnpr-9::RFP, rol-6]*, FY978 *fvIs1 [Pnpr-9::RFP]; vuEx [Pacc-3::GFP, Pnpr-9::RFP, rol-6]*, FY979 *fvIs1 [Pnpr-9::RFP]; vuEx [Plgc-49::GFP, Pnpr-9::RFP, rol-6]*, FY980 *fvIs1 [Pnpr-9::RFP]; vuEx [Plgc-46::GFP, Pnpr-9::RFP, rol-6]*, FY981 *fvIs1 [Pnpr-9::RFP]; vuEx [Pacc-2::GFP, Pnpr-9::RFP, rol-6]*, FY982 *unc-31(e928) IV; fvIs1 [Pnpr-9::RFP]; kyEx4018 [Pinx-1::GCaMP3]*, FY983 *und-13(e51) I; fvIs1 [Pnpr-9::RFP] kyEx4018 [Pinx-1::GCaMP3]*, FY984 *avr-14(ad1302) I; fvIs1 [Pnpr-9::RFP] kyEx4018 [Pinx-1::GCaMP3]*, FY985 *egl-3(n150) V; fvIs1 [Pnpr-9::RFP]; kyEx4018 [Pinx-1::GCaMP3]*, FY987 *eat-4(ky5) III; fvIs1 [Pnpr-9::RFP]; kyEx4018 [Pinx-1::GCaMP3]*, FY988 *avr-14(ad1302) I; glr-1(n2461) III; fvIs1 [Pnpr-9::RFP]; kyEx4018 [Pinx-1::GCaMP3]*, FY989 *acc-1(tm3268) IV; fvIs1 [Pnpr-9::RFP];*

kyEx4018 [Pinx-1::GCaMP3], FY991 *cha-1(y226) IV; fvIs1 [Pnpr-9::RFP]; kyEx4018 [Pinx-1::GCaMP3]*, IV15 *unc-13(e51) I; kyEx2595 [str- 2::GCaMP2.2b, unc-122::GFP]*, IV23 *unc-31(e928) IV; kyEx2595 [str- 2::GCaMP2.2b, unc-122::GFP]*, IV28 *ueEx10 [gcy-5::GCaMP3, unc-122::GFP]*, IV61 *ueEx8 [ins-1::GCaMP3, unc-122::GFP]*, and IV388 *ueEx7 [gcy-7::GCaMP3, unc-122::GFP]*. The mutant strains FY858 and FY976-FY991 were constructed using standard genetic techniques. The IV worm strains were a generous gift from Dr. Sreekanth Chalasani, the worm strains used to make FY976-FY981 were a generous gift from Dr. Joe Dent, and the worm strain used to make FY858 was a generous gift from Dr. Cornelia Bargmann. All other worm strains were obtained from the Caenorhabditis Genetics Center (University of Minnesota, Minneapolis, MN) or National BioResource Project of Japan (Tokyo Women's Medical University, Shinjuku-ku, Tokyo, Japan).

2.2 Molecular biology and transgenesis

The *inx-1* (0.3 kb; AIB), *npr-9* (1.8 kb; AIB), *sro-1* (2.0 kb; ADLs), *sra-6* (3.3 kb; ASHs, ASIs, PVQs, SPDs/Ms), *flp-6* (2.0 kb; ASEs, AFDs, ASGs, PVT, I1), *gcy-5* (3.2 kb; ASER), *gcy-6* (0.5 kb; ASEL), *str-2* (3.7 kb, AWC), and *nlp-1* (2.5 kb; AWCs, ASIs, BDUs, HSN, PHBs, four head neurons) promoters, respectively, were used for neuron selective expression. Experiments using the *inx-1* promoter were confirmed using the *npr-9* promoter, and similar results were observed. Promoter expression was confirmed by GFP expression and confocal microscopy.

For neuron selective RNAi, transgenes were constructed using standard molecular techniques (Esposito, Di Schiavi et al. 2007). A neuron selective promoter was fused to

unique exon rich regions of the target gene. The unique exon rich sequence was amplified with Phusion DNA Polymerase (New England BioLabs, Ipswich, MA), a forward primer, and a reverse primer (template A). Neuron selective promoters were amplified using Phusion DNA Polymerase, a forward primer, and a reverse primer with a 5' overhang that was complementary to either the sense (template B) or antisense (template C) exon rich forward primer. Template A and template B were fused using Phusion DNA polymerase to create a sense construct (product D). Template A and template C were fused using Phusion DNA polymerase to create a sense construct (product E). PCR products were pooled from at least three separate PCR reactions and co-injected with a selectable marker (*cc::RFP*, *myo-3::GFP*, or *Psra-6::RFP*) with Salmon sperm carrier DNA into the gonads of *C. elegans* wild-type or null-mutants using standard microinjection techniques (Kramer, French et al. 1990, Mello, Kramer et al. 1991).

For rescue/overexpression, transgenes were constructed using standard overlap PCR fusion techniques (Hobert 2002). A neuron selective promoter was fused to either a cDNA or a genomic region corresponding to the entire coding sequence. The cDNA or genomic region was amplified with Phusion DNA Polymerase, a forward primer, and a reverse primer (template A). Neuron selective promoters were amplified using Phusion DNA Polymerase, a forward primer, and a reverse primer with a 5' overhang that was complementary to the cDNA or genomic region forward primer (template B). Template A and B were fused using Phusion DNA polymerase to create the neuron selective cDNA or genomic construct (product C). PCR products were pooled from at least three separate PCR reactions and co-injected with a selectable marker (*cc::RFP* or *myo-3::GFP*) with

Salmon sperm carrier DNA into the gonads of *C. elegans* wild-type or null-mutants using standard microinjection techniques (Kramer, French et al. 1990, Mello, Kramer et al. 1991).

2.3 Calcium Imaging

To characterize the effects of glutamate on AIB iCa^{2+}, hermaphrodite animals were glued to Sylgard (Dow Corning)-coated coverslips using WormGlu cyanoacrylate glue (GluStitch) while immersed in an electrophysiology external solution (Ephys solution) containing the following (in mM): NaCl 150, KCl 5, $CaCl_2$ 5, $MgCl_2$ 1, glucose 10, and HEPES 15, pH 7.30, 330 mOsm. The coverslip was then placed in a laminar flow chamber (RC26G, Warner Instruments) mounted on an Axioskop 2 FS Plus upright compound microscope (40 Achroplan water-immersion objective, GFP filter set #38) and perfused with Ephys solution. Animals were dissected open longitudinally using a polished electrode (TW150-3, World Precision Instruments, Sarasota, FL) mounted on the headstage of a micromanipulator (Sutter MP285, Sutter Instruments, Novato, CA), and glutamate dissolved in Ephys solution (500-mM) was applied using a multibarrel fast perfusion system (Warner Instruments SF77B, barrel width 300 μm) that was controlled by pCLAMP10 acquisition software (Molecular Devices). To perform GCaMP3 recordings, the microscope was fitted with an Orca ER CCD camera and programmable shutter (Uniblitz; Vincent Associates). MetaVue 7.6.5 (MDS ANALytical Technologies) was used to capture fluorescence images. A rectangular region of interest was used to record from AIB cell bodies and neurites. Samples were acquired at 20 Hz (50 ms exposure time) with 4x binning. Fluorescent images were analyzed using Jmalyze

software (Rex Kerr).

To image the effects of 1-octanol, salt steps, and Ephys solution on iCa^{2+}, hermaphrodite animals were glued to Sylgard-coated coverslips while immersed in a solution with an ionic composition identical to that of NGM plates (NGM solution), which contained the following (in mM): NaCl 50, KPO_4 5, $MgSO_4$ 1, and $CaCl_2$ 1. The coverslip was then placed in a laminar flow chamber under the microscope and perfused with NGM solution. For odorant application, 1-octanol was diluted in NGM solution (saturating 2.3-µM, dilute 0.69-µM) and applied using a multibarrel fast perfusion system The slope of recovery was calculated for individual traces. For salt steps, the multibarrel fast perfusion system was used to step between NGM solution (NaCl 50-mM) and a high salt NGM solution (NaCl 60-mM). For Ephys solution application, the multibarrel fast perfusion system was used to step between NGM solution and Ephys solution. To capture GCaMP3 recordings, the microscope was fitted with a camera and programmable shutter. MetaVue 7.6.5 was used to capture fluorescence images. A rectangular region of interest was used to record from cell bodies and neurites. Samples were acquired at 10 Hz (100 ms exposure time) with 4x binning. Fluorescent images were analyzed using Jmalyze software. To examine the effects of 5-HT on 1-octanol responses, animals were first incubated on a food free plate containing 5-HT (4-mM) for 30-60 minutes prior to being glued to Sylgard-coated coverslips.

2.4 Electrophysiology

For whole-cell patch clamp electrophysiology, animals were glued to Sylgard-coated coverslips while immersed in Ephys solution. The coverslip was then placed in a

laminar flow chamber mounted under the microscope and perfused with Ephys solution. Dissections were performed using a polished electrode mounted on the headstage of a micromanipulator. Animals either had an AIB cell body exposed with a small incision in the cuticle using standard protocols (Goodman et al., 1998; Piggott et al., 2011), or were further dissected open longitudinally on the contralateral side to expose the entirety of the AIB interneurons to the drug-containing solution. Switching between glutamate dissolved in Ephys solution (500-mM), acetylcholine dissolved in Ephys solution (500-mM), and Ephys solution was performed using a multibarrel fast perfusion system that was controlled by pCLAMP10 acquisition software. Whole-cell patch clamp electrophysiology recordings were performed as described previously (Goodman et al., 1998) using an Axon Axopatch 2B amplifier and Axon Digidata 1440 digitizer (Molecular Devices). Voltage-clamp recordings were filtered using a Butterworth (8-pole) low-pass filter with a 3 dB cutoff of 100 Hz.

2.5 Statistical analysis

To analyze the effects of glutamate on AIB iCa^{2+}, Jmalyze output files were analyzed in Microsoft Excel. The maximal change in fluorescence relative to baseline, max $\Delta F_t/F_0$, was found during glutamate exposure, $0<t\leq30$, using

$$\Delta F_t/F_0=((F_t-F_0)/F_0)*100$$

, where F_t is the fluorescence value at time t and F_0 is the fluorescence value immediately before glutamate exposure. The max $\Delta F_t/F_0$ was calculated on $0<t\leq30$ for individual traces, and were statistically analyzed in GraphPad Prism (GraphPad, La Jolla, CA) using an unpaired two-tailed Student's *t* test with Welch's correction. Graphs of the data were

made in GraphPad Prism. For simplicity, values are reported as $\Delta F/F_0$.

To analyze the effects of 1-octanol on iCa^{2+}, Jmalyze output files were analyzed in Microsoft Excel. If 1-octanol evoked a net decrease in the trace averaged iCa^{2+}, the time t_{max} occurs when $\Delta F_t/F_0$ is greatest after the trace averaged decrease, max $\Delta F_t/F_0$ was calculated on $0<t\leq t_{max}$, and max $\Delta F_t/F_0$ occurs at t_{abs}. Conversely, if 1-octanol evoked a net increase in the trace averaged iCa^{2+}, the value t_{min} occurs when $\Delta F_t/F_0$ is least after the trace averaged increase, max $\Delta F_t/F_0$ was calculated on $0<t\leq t_{min}$, and max $\Delta F_t/F_0$ occurs at t_{abs}. The $\Delta F_{tabs}/F_0$ was calculated for individual traces and were statistically analyzed in GraphPad Prism using an unpaired two-tailed Student's *t* test with Welch's correction. Graphs of the data were made in GraphPad Prism. For simplicity, values are reported as $\Delta F/F_0$.

To calculate the slope of recovery of AIB iCa^{2+} following 1-octanol exposure, $t_1=t_{abs}$, and $t_2=t_{max}$, since 1-octanol evokes a trace averaged decrease in AIB iCa^{2+}. The slope of recovery was calculated for individual traces using

$$\text{Slope of Recovery}=[(\Delta F_{t2}/F_0)-(\Delta F_{t1}/F_0)]/(t_2-t_1)$$

. The slopes of recovery were statistically analyzed in GraphPad Prism using an unpaired two-tailed Student's *t* test with Welch's correction. Graphs of the data were made in GraphPad Prism.

Glutamate- and acetylcholine-evoked current amplitudes in the same AIB were measured using the pCLAMP10 acquisition software. Since glutamate-evoked currents were absent in the AIBs of minimally dissected *avr-14* mutants and fully dissected *avr-14;glr-1* double mutants, AIB glutamate-evoked current amplitudes were statistically analyzed in GraphPad Prism using an unpaired two-tailed Student's *t* test with Welch's

correction. However, since acetylcholine-evoked currents were still present in minimally dissected *acc-1* mutants, the ratios of the acetylcholine-evoked current amplitude to the glutamate-evoked current amplitude in the same AIB were statistically analyzed in GraphPad Prism using an unpaired two-tailed Student's *t* test with Welch's correction. Graphs of the data were made in GraphPad Prism.

2.6 Other materials

All materials other than those specified elsewhere in Chapter 2 were obtained from Fisher Scientific (Pittsburgh, PA) or Sigma-Aldrich (St. Louis, MO) unless otherwise specified.

Chapter 3

Results

3.1 The ASHs, AWCs, and ASER shape aversive behaviors to the noxious odorant 1-octanol

In a 1-octanol aversive assay, the ASHs are solely responsible for sensing dilute concentrations of the noxious odorant (Chao, Komatsu et al. 2004). Similarly, saturating 1-octanol presentation evokes iCa^{2+} increases in the ASHs, while animals treated with 5-HT exhibit reduced iCa^{2+} increases (Zahratka, Williams et al. 2015). In contrast, the ASHs, ADLs, and AWBs mediate aversive behaviors to 100% 1-octanol (Chao, Komatsu et al. 2004). Interestingly, saturating 1-octanol presentation has no effect on ADL or AWB iCa^{2+} (Mills, Wragg et al. 2012). One possibility is that the AWBs and ADLs do not directly sense 1-octanol, but tonic signaling from the AWBs and ADLs modulates downstream inputs that shape aversive behaviors. In support of this, modulation of the AWCs or ASER activity can alter aversive behavior to 100% 1-octanol (Mills, Wragg et al. 2012). Therefore, we first sought to determine whether tonic signaling from the AWCs and/or ASER shape 1-octanol aversive behaviors, or if the odorant directly modulates the AWCs and/or ASER activity.

Previous studies that reported 1-octanol evokes ASH iCa^{2+} increases were

performed using saturating odorant diluted in Ephys solution, which contains ion concentrations greater than NGM behavioral assay plates (Zahratka, Williams et al. 2015). Therefore, we wanted to confirm that saturating 1-octanol diluted in NGM solution elicits ASH iCa^{2+} increases. As anticipated, saturating 1-octanol diluted in NGM solution evokes ASH iCa^{2+} increases (Figure 3-1A, B). Interestingly, saturating 1-octanol presentation decreases AWC iCa^{2+} and removal allows iCa^{2+} levels to return back near baseline (Figure 3-1A, B). To determine if 1-octanol directly modulates AWC iCa^{2+}, we examined the effects of odorant presentation on AWC activity in *unc-13* and *unc-31* (calcium-dependent activator protein for secretion/CADPS ortholog; required for DCVs release) mutants, as well as animals with ASH-selective *eat-4* RNAi knockdown. Although *unc-13* and *unc-31* mutants have reduced and enhanced saturating 1-octanol inhibition of AWC iCa^{2+}, respectively, the AWCs still respond to odorant presentation (Figure 3-1C, D). These data demonstrate that the AWCs are directly modulated by 1-octanol. Furthermore, these results demonstrate that the AWCs are extensively modulated by feedback that is dependent on SVs and DCVs. Conversely, neither saturating 1-octanol presentation or removal effect ASER iCa^{2+}, and all decreases observed were likely due to fluorophore bleaching (Figure 3-1A, B). Together, these data demonstrate that saturating 1-octanol presentation activates and inhibits the ASHs and AWCs, respectively, but has no effect on the ASER.

3.2 The AIB interneurons are activated and inhibited by GLR-1 and AVR-14, respectively, to modulate dilute 1-octanol aversive responses

Isoamyl alcohol removal evokes a glutamate- and GLR-1-dependent increase in

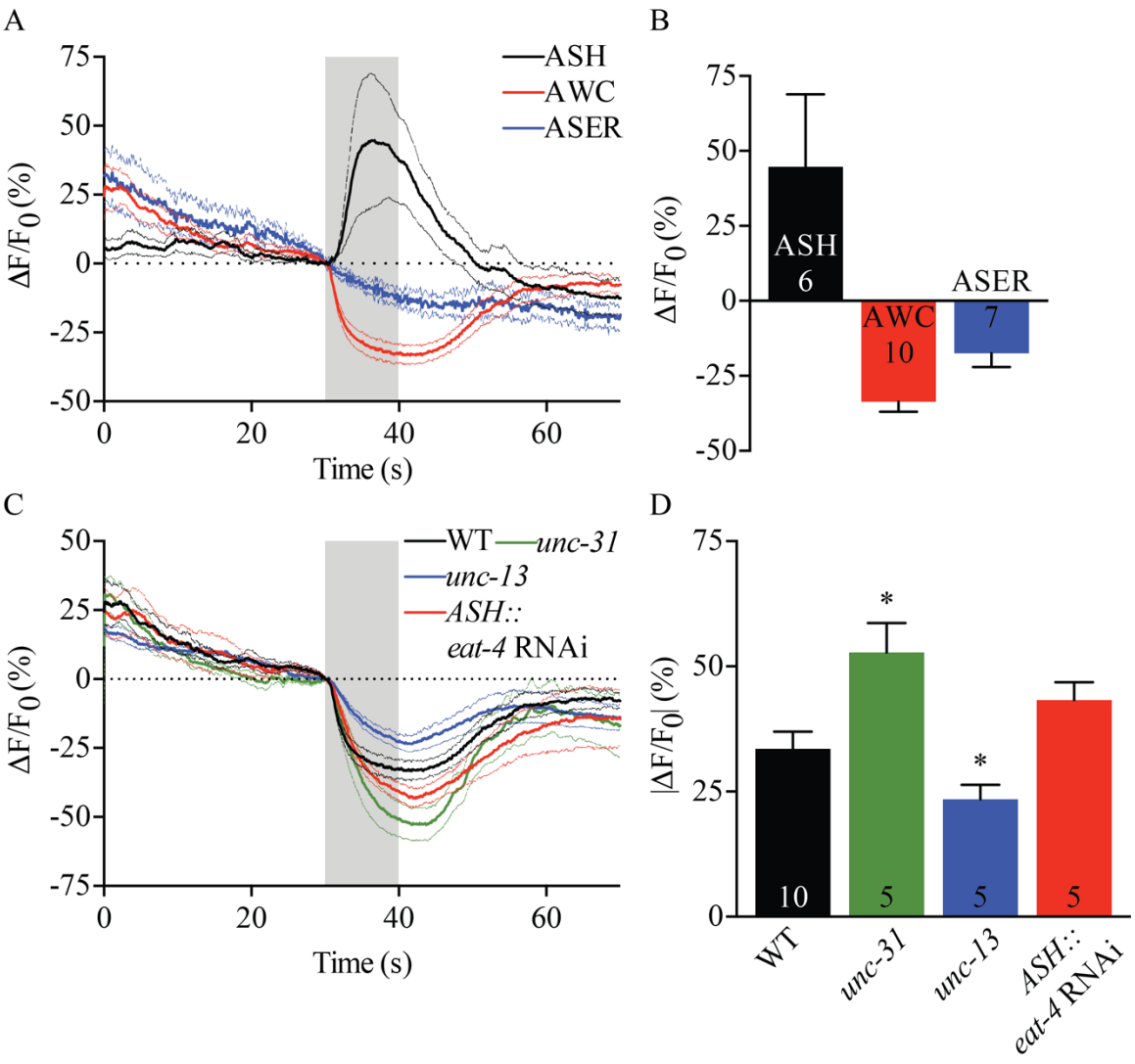

Figure 3-1. Presentation of 1-octanol increases, decreases, and does not effect ASH, AWC, and ASER iCa^{2+}, respectively. A. Trace averages of 1-octanol-evoked iCa^{2+} transients in the ASHs, AWCs, or ASER of wild-type animals. B. Comparison of maximum 1-octanol-evoked iCa^{2+} changes from (A). Data are presented as mean ± SEM. Numbers within bars indicate *n*. C. Trace averages of 1-octanol-evoked iCa^{2+} transients in the AWCs of wild-type, null, or transgenic animals. The *sra-6* promoter drove *eat-4* RNAi expression in the ASHs of wild-type animals. D. Comparison of the absolute value of maximum 1-octanol-evoked iCa^{2+} changes, which were all decreases, from (C).

Data are presented as mean ± SEM and were analyzed by two-tailed Student's *t* test with Welch's correction. *$p<0.05$, significantly different from wild-type animals under identical conditions. Numbers within bars indicate *n*.

AIB iCa^{2+} (Chalasani, Chronis et al. 2007, Piggott, Liu et al. 2011). Similarly, nose-touch evokes a glutamate- and GLR-1-dependent cationic current in the AIBs (Piggott, Liu et al. 2011). However, previous work has not demonstrated that direct glutamate application to the AIBs either increases AIB iCa^{2+}, or elicits a cationic current. Therefore, we sought to determine the effects of direct glutamate application on the AIBs.

Whole-cell patch clamp electrophysiology allows for the quantification of either changes in membrane (current clamp) or evoked currents at a specified membrane potential (voltage clamp) in response to ligand application. Voltage-clamp is especially useful for determining the ionic composition of evoked currents, because the ionic concentration of the intracellular solution is determined by the electrode solution. Therefore, knowledge of the intracellular and extracellular ionic concentrations makes it possible to determine the reversal potential for anions (e.g. Cl^-) and cations (i.e. K^+, Na^+, Ca^{++}), with each having a unique reversal potential (membrane potential at which the net current is 0 pA). The combination of our internal and external electrophysiology solutions result in a reversal potential near -30 mV for Cl^- and +15 mV for cations (Pirri, McPherson et al. 2009). Interestingly, glutamate evokes an inward current at -60 mV, no net current at -30 mV, and an outward current at +15 mV in the AIBs (Figure 3-2A, B, C, G). These results demonstrate that the AIBs express a GluCl, but provides no evidence for the previously reported GLR-1 receptor (Chalasani, Chronis et al. 2007, Piggott, Liu et al. 2011). This is consistent with previous work performed in our lab, which found that glutamate-evoked currents in the AIBs are present in *glr-1* mutants (Bamber Unpublished). The glutamate-gated Cl^- channel subunits in *C. elegans* are encoded by

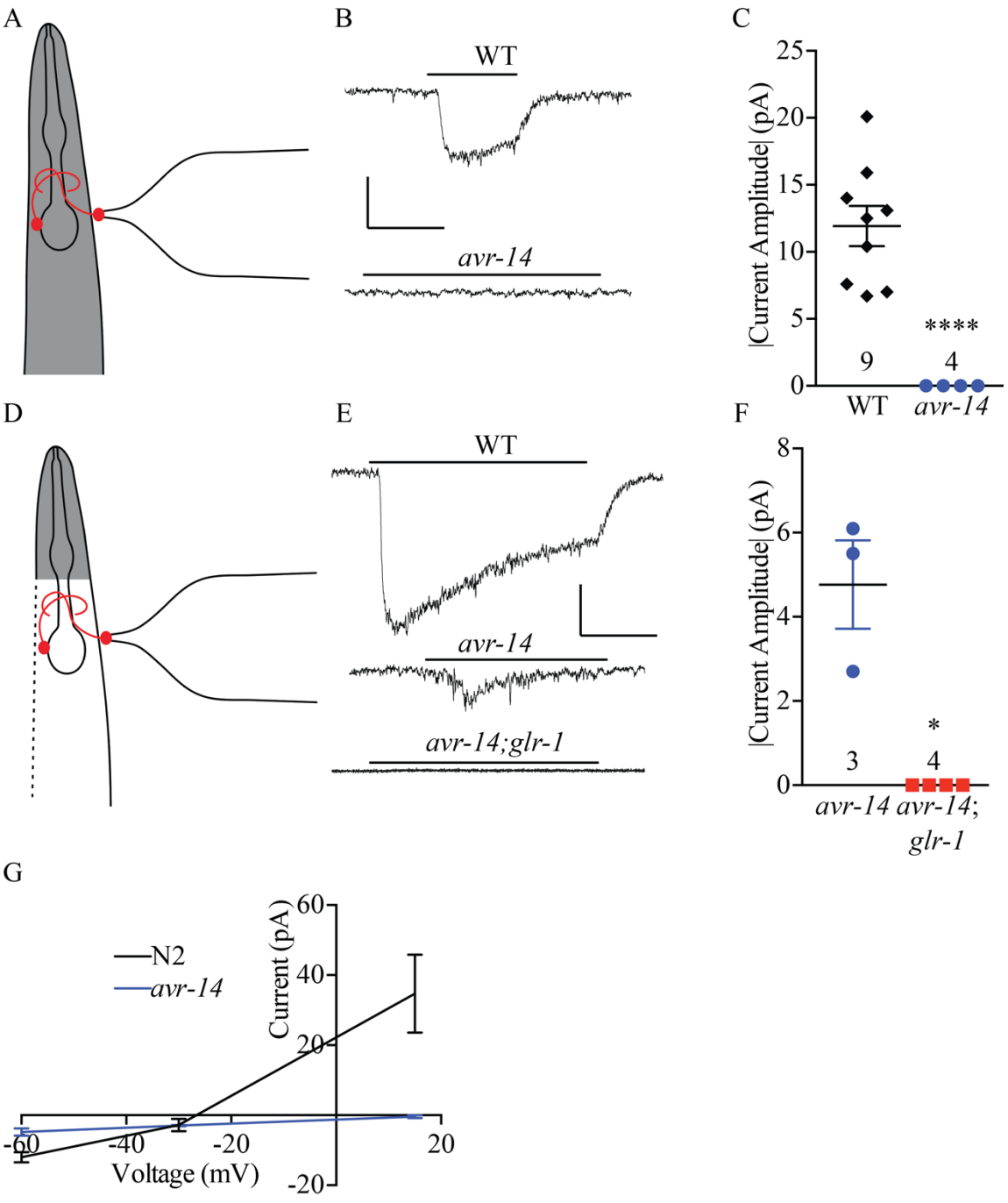

Figure 3-2. Exogenous glutamate application evokes currents in the AIBs. A. Diagram depicting partially dissected electrophysiology preparation. B. Representative traces of glutamate-evoked currents in the AIBs of wild-type and null animals obtained using the partially dissected electrophysiology preparation (A). Vertical scale bar, 10 pA;

horizontal scale bar, 1 s. C. Comparison of glutamate-evoked currents in the AIBs of wild-type and null animals obtained using the partially dissected electrophysiology preparation (A). Data are presented as mean ± SEM and were analyzed by two-tailed Student's *t* test with Welch's correction. ****$p<0.0001$, significantly different from wild-type animals under identical conditions. Numbers above genotype indicate *n*. D. Diagram depicting fully dissected electrophysiology preparation. E. Representative traces of glutamate-evoked currents in the AIBs of wild-type, null, and double null animals obtained using the fully dissected electrophysiology preparation (D). Vertical scale bar, 10 pA; horizontal scale bar, 1 s. F. Comparison of glutamate-evoked currents in the AIBs of null and double null animals obtained using the full dissected electrophysiology preparation (D). Data are presented as mean ± SEM and were analyzed by two-tailed Student's *t* test with Welch's correction. *$p<0.05$, significantly different from wild-type animals under identical conditions. Numbers above genotype indicate *n*. G. Current-voltage relationship for glutamate-evoked currents in the AIBs of nine wild-type (A) and three null (D) animals.

avr-14, *avr-15*, *glc-1*, *glc-2*, *glc-3*, and *glc-4* (Cully, Vassilatis et al. 1994, Dent, Davis et al. 1997, Laughton, Lunt et al. 1997, Vassilatis, Arena et al. 1997, Dent, Smith et al. 2000, Brockie, Mellem et al. 2001, Horoszok, Raymond et al. 2001, Brockie and Maricq 2003, Cook, Aptel et al. 2006). Furthermore, glutamate-evoked Cl^- currents are absent in *avr-14* mutants (Figure 3-2B, C). These data indicate that the GluCl receptor subunit AVR-14 mediates glutamate-evoked Cl^- currents in the AIBs. Since only an AIB cell is exposed using the minimally invasive dissection preparation, the glutamate-containing solution may not have access to the synaptic regions along the length of the AIB neurite (Figure 3-2A). If so, this implies that the observed AVR-14-mediated currents in minimally dissected animals are due to extrasynaptic AVR-14 receptors. Furthermore, this also presents a plausible explanation for the absence of glutamate-evoked cationic currents. To test this possibility, the AIB process of *avr-14* mutants was fully exposed to the glutamate-containing solution by adding an additional dissection step, whereby animals were dissected open on the side contralateral to where the AIB cell body was exposed (Figure 3-2D). With this configuration, glutamate evokes a cationic current in the AIBs of *avr-14* mutants that is absent in *avr-14;glr-1* double-mutants (Figure 3-2E, F, G). This both confirms and provides direct evidence for GLR-1-mediated currents in the AIBs. Furthermore, the AVR-14-mediated inhibitory currents are much larger than the GLR-1-mediated excitatory currents, implying that low levels of glutamate release onto the AIBs may depolarize the entire neuron, whereas high levels of glutamate release may activate extrasynaptic inhibitory currents to inhibit neuronal activity. Indeed, similar effects regarding low and high levels of glutamate release are observed in the AVA command motor neurons (Mellem, Brockie et al. 2002).

In order to confirm our electrophysiology results, we examined the effects of glutamate application on AIB iCa^{2+}. Glutamate application to the AIBs in wild-type animals decreases AIB iCa^{2+} (Figure 3-3A, B). Conversely, glutamate application to the AIBs in *avr-14* mutant animals increases iCa^{2+}, and these increases are absent in *avr-14;glr-1* double-mutants (Figure 3-3A, B). Together, these data demonstrate that glutamate is both capable of activating and inactivating the AIBs. Furthermore, these results support that inhibitory glutamatergic signaling more prevalently regulates AIB activity, as exogenous glutamate application only increases AIB iCa^{2+} in *avr-14* mutants. It has been proposed that at least some portion of the locomotory circuitry functions as a bimodal switch, and evidence supports that the AIBs maintain reverberant excitation of neurons responsible for backward locomotion (Chao, Komatsu et al. 2004, Harris, Hapiak et al. 2009, Harris, Mills et al. 2010, Gordus, Pokala et al. 2015). Despite evidence indicating that continuous glutamatergic GLR-1 stimulation mediates prolonged elevations of AIB iCa^{2+}, it seems unlikely that this is the sole mechanism, as GLR-1 currents desensitize during prolonged glutamate application (Chalasani, Chronis et al. 2007). Since EGL-19 expresses in multiple unidentified *C. elegans* neurons, we wanted to test whether EGL-19 plays any role in AIB modulating iCa^{2+}, as activation of EGL-19 and intermittent signaling through GLR-1 may jointly function to keep the AIBs in an active state (Lee, Lobel et al. 1997, Busch, Laurent et al. 2012). Indeed, *avr-14* mutants treated with the selective L-type VGCC blocker nemadipine-A display a significant reduction in glutamate-evoked AIB iCa^{2+} increases (Figure 3-3C, D). These data demonstrate that EGL-19 predominantly contributes to glutamate-evoked increases of AIB iCa^{2+}. Furthermore, these data support the notion that GLR-1 serves as an initial

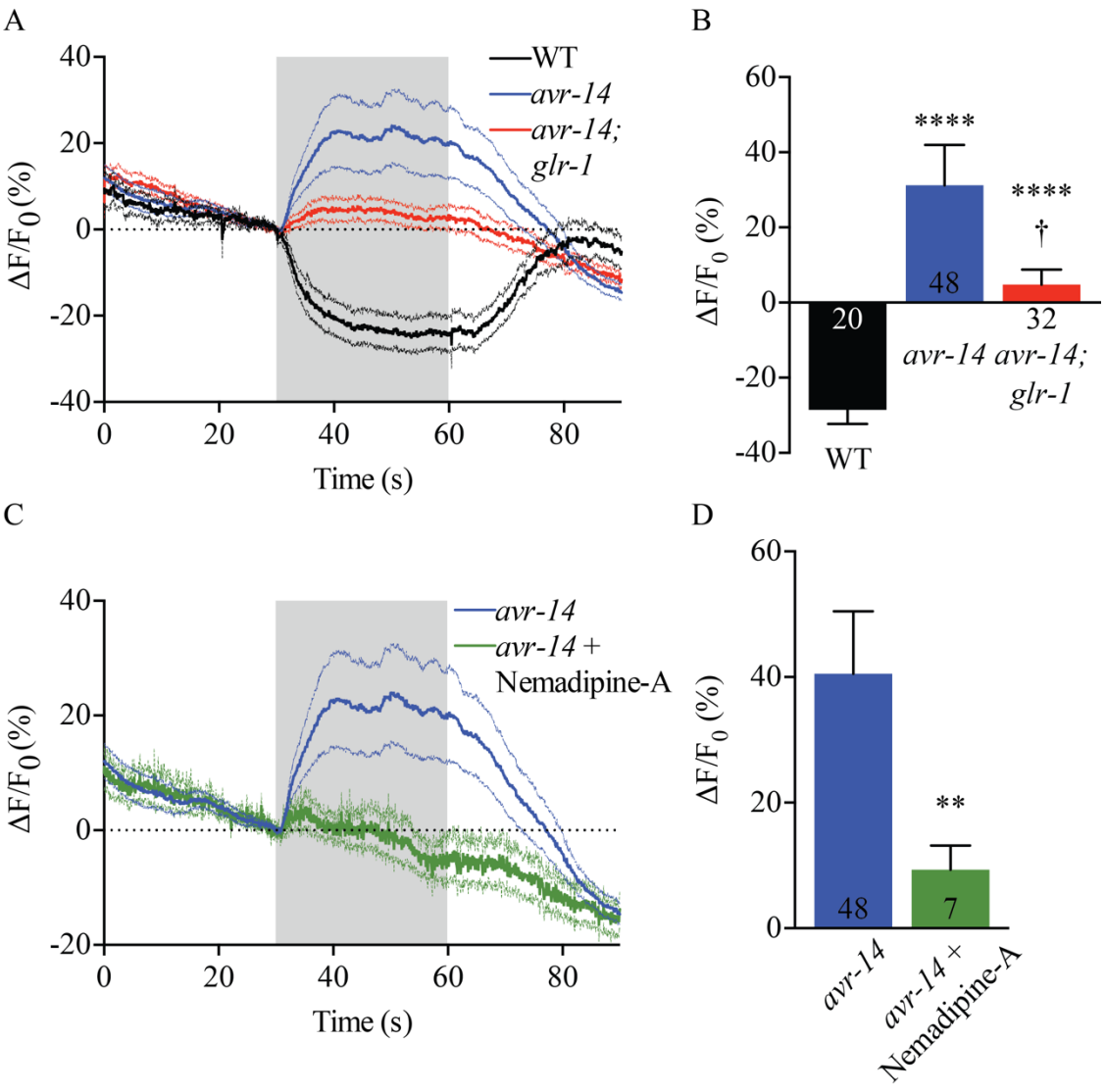

Figure 3-3. Exogenous glutamate application modulates AIB iCa^{2+}. A. Trace averages of glutamate-evoked AIB iCa^{2+} transients in the AIBs of wild-type, null, and double null animals obtained using fully dissected animals. B. Comparison of maximum AIB iCa^{2+} changes during glutamate application from (A). Data are presented as mean ± SEM and were analyzed by two-tailed Student's *t* test with Welch's correction. ****p<0.0001, significantly different from wild-type animals under identical conditions. †<0.05, significantly different from *avr-14* animals under identical conditions. Numbers

within/beneath bars indicate *n*. C. Trace averages of glutamate-evoked AIB iCa^{2+} transients in the AIBs of null animals in the presence or absence of 5-μM nemadipine-A obtained using fully dissected animals. D. Comparison of maximum AIB iCa^{2+} increases during glutamate application from (C). Data are presented as mean ± SEM and were analyzed by two-tailed Student's *t* test with Welch's correction. **P<0.01, significantly different from null animals in the absence of 5-μM nemadipine-A. Numbers within bars indicate *n*.

depolarization stimulus that directly mediates a small amount of AIB Ca^{2+} influx, and that EGL-19 responds to the depolarization stimulus by activating and amplifying Ca^{2+} influx.

3.3 The odorant 1-octanol activates and inhibits the AIAs and AIBs, respectively

A variety of stimuli alter the activity of the AIBs. For instance, presentation of ligands sensed by the AWCs such as butanone and IAA decrease AIB iCa^{2+}, whereas removal increases AIB iCa^{2+} (Chalasani, Chronis et al. 2007). Additionally, salt downstep increases AIB iCa^{2+}, whereas salt upstep decreases AIB iCa^{2+} (Oda, Tomioka et al. 2011). Finally, noxious stimuli sensed by the ASHs, such as osmotic shock and nose touch, increase AIB iCa^{2+} (Piggott, Liu et al. 2011). Therefore, we wanted to examine the effect of 1-octanol on AIB iCa^{2+}.

Presentation of saturating 1-octanol diluted in NGM solution evokes a sharp decrease in AIB iCa^{2+} (Figure 3-4A, B). Conversely, saturating 1-octanol diluted in Ephys solution decreases AIB iCa^{2+} on a significantly slower time scale (Supplementary Figure A-1A, B). Furthermore, presentation of Ephys solution to animals immersed in NGM solution is sufficient to activate the ASHs (Supplementary Figure A-1C, D). Therefore, neural network activity may be altered by the Ephys solution, resulting in differential modulation of AIB iCa^{2+} in response to saturating 1-octanol presentation. For instance, a salt upstep greater than 20-mM activates the AIA interneurons, and activation of the AIA interneurons can stimulate release of neuropeptides that provide inhibitory feedback onto sensory neurons (Chalasani, Kato et al. 2010, Leinwand and Chalasani 2013). Therefore, we used saturating 1-octanol diluted in NGM solution for all

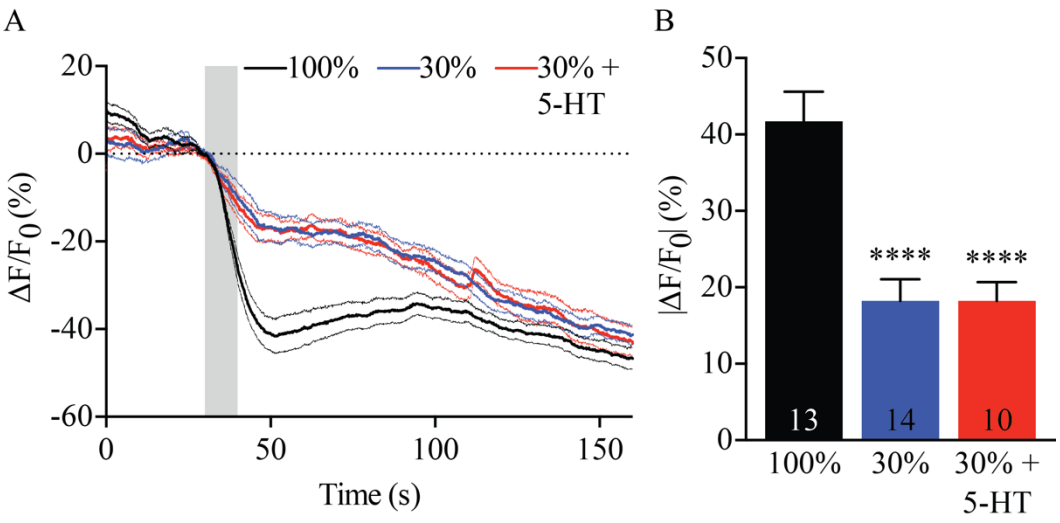

Figure 3-4. Presentation of 1-octanol inhibits the AIBs. A. Trace averages of saturating and dilute 1-octanol-evoked iCa^{2+} transients in the AIBs of wild-type animals, and trace average of dilute 1-octanol-evoked iCa^{2+} transients in the AIBs of wild-type animals incubated on 4-mM 5-HT. B. Comparison of the absolute value of maximum 1-octanol-evoked iCa^{2+} changes, which were all decreases, from (A). Data are presented as mean ± SEM and were analyzed by two-tailed Student's *t* test with Welch's correction. *p<0.05, significantly different from 100% 1-octanol exposed animals under identical conditions. Numbers within bars indicate *n*. Animals treated with 5-HT are not significantly different from untreated animals exposed to 30% 1-octanol under identical conditions.

subsequent experiments.

Dilute 1-octanol decreases AIB iCa^{2+} significantly less than saturating 1-octanol (Figure 3-4A, B). Interestingly, 5-HT does not affect dilute 1-octanol-evoked AIB iCa^{2+} decreases (Figure 3-4A, B). This is surprising because *mod-1* expression in the AIBs is required for 5-HT enhancement of aversive behaviors to 30% 1-octanol (Harris, Hapiak et al. 2009). One possible explanation is that 5-HT modulates AIB iCa^{2+} near synapses in microdomains that are unable to be resolved with our calcium-imaging configuration. Another possibility is the previously described disconnect between sensory inputs directly modulating AIB iCa^{2+}, as AIB iCa^{2+} closely correlates with locomotion (Luo, Wen et al. 2014). Furthermore, saturating 1-octanol-evoked AIB iCa^{2+} decreases in *egl-3* mutants are not significantly different from wild-type animals (Supplementary Figure A-2A, B). This is not entirely surprising, as *egl-3* is only required for 5-HT enhancement of aversive behaviors to 30% 1-octanol (Harris, Mills et al. 2010). However, as previously mentioned, 5-HT does not effect dilute 1-octanol-evoked AIB iCa^{2+} decreases. From our electrophysiology and calcium-imaging experiments, we identified glutamate-evoked inhibitory currents in the AIBs, as well as glutamate-evoked decreases of AIB iCa^{2+}, both of which are dependent on *avr-14* expression in the AIBs. Furthermore, 5-HT-enhancement of aversive behaviors to 30% 1-octanol are dependent on *avr-14* expression in the AIBs. Therefore, we examined the effect of saturating 1-octanol on AIB iCa^{2+} in *avr-14* mutants.

Saturating 1-octanol-evoked decreases of AIB iCa^{2+} are significantly reduced in *avr-14* mutants, and significant effects are lost in *avr-14;glr-1* double-mutants, although maximal decreases are comparable to *avr-14* mutants (Figure 3-5A, B). These data

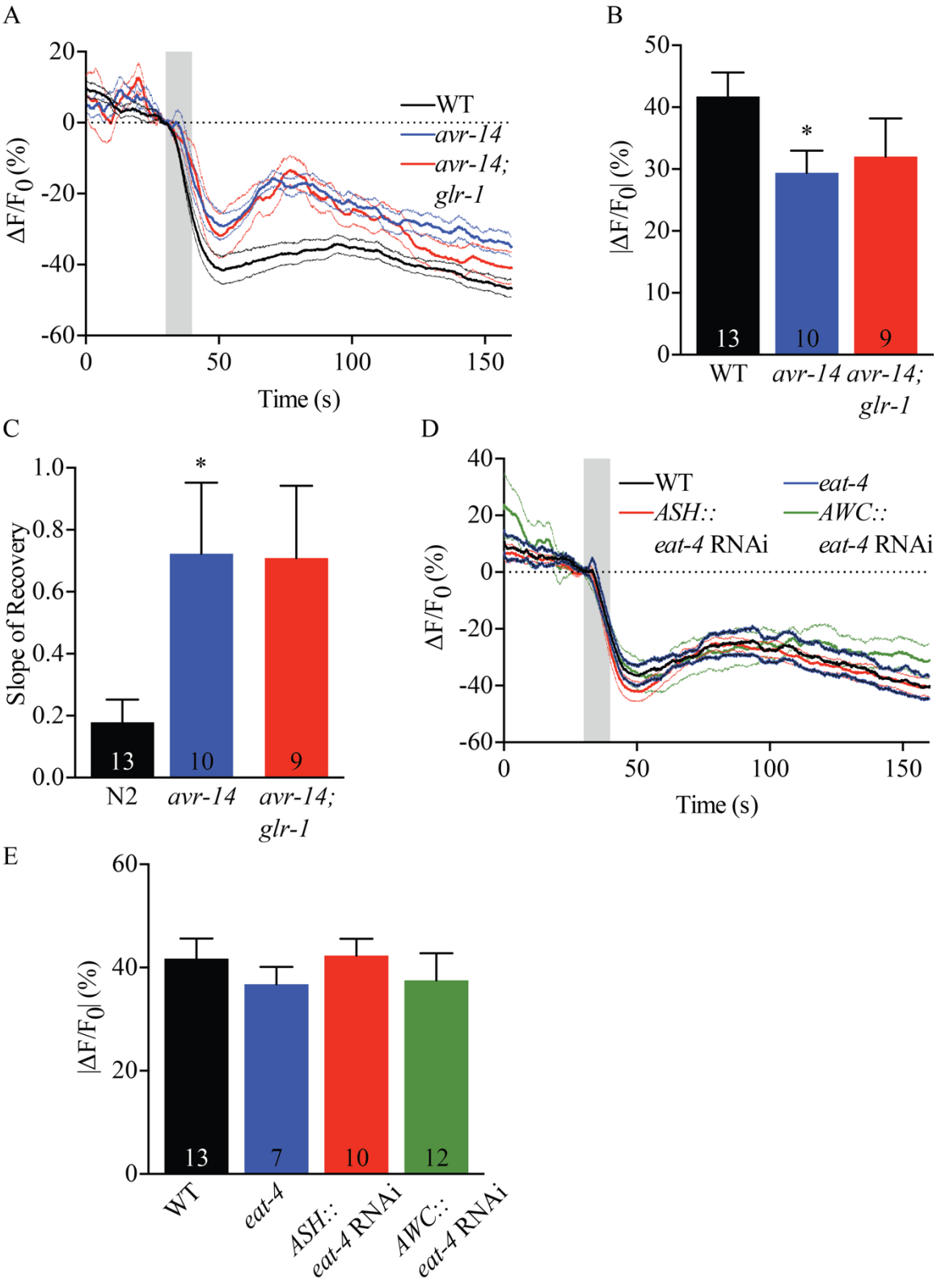

Figure 3-5. The GluCl AVR-14 contributes to 1-octanol inhibition of AIB iCa^{2+}. A.

Trace averages of 100% 1-octanol-evoked iCa^{2+} transients in the AIBs of wild-type and null animals. B. Comparison of the absolute value of maximum 1-octanol-evoked iCa^{2+} changes, which were all decreases, from (A). Data are presented as mean ± SEM and were analyzed by two-tailed Student's *t* test with Welch's correction. *$p<0.05$, significantly different from wild-type animals under identical conditions. Numbers within bars indicate *n*. C. Comparison of the rate of recovery of AIB iCa^{2+} to baseline levels between wild-type and null animals from (A). Data are presented as mean ± SEM and were analyzed by two-tailed Student's *t* test with Welch's correction. *$p<0.05$, significantly different from wild-type animals under identical conditions. Numbers within bars indicate *n*. D. Trace averages of 100% 1-octanol-evoked iCa^{2+} transients in the AIBs of wild-type, null, and transgenic animals. E. Comparison of the absolute value of maximum 1-octanol-evoked iCa^{2+} changes, which were all decreases, from (D). There is not a significant difference from wild-type animals under identical conditions. Data are presented as mean ± SEM and were analyzed by two-tailed Student's *t* test with Welch's correction. Numbers within bars indicate *n*. The *sra-6* promoter drove *eat-4* RNAi expression in the ASHs of wild-type animals. The *nlp-1* promoter drove *eat-4* RNAi expression in the AWCs of wild-type animals.

indicate that 1-octanol-evoked inhibition of AIB iCa^{2+} is partially dependent on AVR-14. This is consistent with results obtained using 1-octanol avoidance behavioral assays, as 1-octanol aversive behaviors and modulation of these behaviors are dependent on *mod-1*, *glr-1*, and *avr-14* expression in the AIBs (Harris, Hapiak et al. 2009, Summers, Layne et al. 2015). Since the GLR-1 receptor increases AIB iCa^{2+}, *avr-14* mutants may have enhanced AIB excitability due to imbalanced excitatory and inhibitory glutamatergic signaling, and are therefore less susceptible to 1-octanol inhibition of AIB iCa^{2+}. However, as *avr-14;glr-1* double-mutants are comparable to *avr-14* mutants, another possibility is that the AIBs are intrinsically excitable, possibly as a result of a low-threshold VGCC. In support of this, the AIBs are commonly at a relatively depolarized membrane potential of -20 mV in current-clamp while providing a 0 pA clamping current. Indeed, neurons in recurrent circuits in the brain maintain depolarized membrane potentials at -30 mV, near their threshold of firing, thereby allowing continued activity in the absence of sensory input (Haider, Duque et al. 2006). In addition to reduced saturating 1-octanol inhibition of AIB iCa^{2+}, AIB iCa^{2+} recovers to peak values more quickly in *avr-14* mutants following saturating 1-octanol removal, and as is the case with maximal AIB iCa^{2+} decreases, *avr-14;glr-1* double-mutants are comparable to *avr-14* mutants in their recovery rate (Figure 3-5C). In addition to recovering to peak values more quickly, it appears as though GCaMP3 fluorescence recovery may be to new baseline GCaMP3 fluorescence levels, as GCaMP3 bleaching seems to result in a linear decrease in fluorescence before odorant application. Indeed, this also seems to be the case for wild-type animals, as well as all other genotypes examined. Surprisingly, saturating 1-octanol-evoked AIB iCa^{2+} decreases are not altered in *eat-4* mutants, animals

with AWC-specific *eat-4* RNAi knockdown, or animals with ASH-specific *eat-4* RNAi knockdown (Figure 3-5D, E). However, in addition to *eat-4*, there are three other putative vesicular glutamate transporters expressed in the nervous system, including *vglu-2*, *vglu-3*, and *slc-17.2* (Sulston, Du et al. 1992, Lee, Sawin et al. 1999, McKay, Johnsen et al. 2003). Therefore, glutamatergic signaling may not be abolished in *eat-4* mutants.

3.4 The AIB interneurons express the AChCl subunits *acc-1* and *lgc-49*

The AIA interneurons direct over a third of their synaptic outputs onto the AIBs and, in contrast to the AIBs, promote forward locomotion (White, Southgate et al. 1986, Wakabayashi, Kitagawa et al. 2004, Gray, Hill et al. 2005). Tonic glutamate release from the AWCs onto GLC-3 on the AIAs inhibits the AIAs, and the AWCs are inhibited by saturating 1-octanol presentation (Chalasani, Kato et al. 2010). Therefore, we predicted that saturating 1-octanol presentation may increase AIA iCa^{2+}. Indeed, saturating 1-octanol presentation increases AIA iCa^{2+}, but has little effect on AIA cell body iCa^{2+} (Figure 3-13A, B). These data demonstrate that 1-octanol presentation activates the AIAs.

The AIA interneurons are predicted to release acetylcholine (Altun-Gultekin, Andachi et al. 2001). Similarly, both the AIAs and AIYs are inhibited by tonic AWC glutamate release onto GLC-3 (Chalasani, Chronis et al. 2007, Chalasani, Kato et al. 2010). Disinhibition of the AIYs stimulates acetylcholine release onto an AChCl channel containing the ACC-2 subunit on the AIZs (Li, Liu et al. 2014). The AChCl channel subunits are encoded by *acc-1*, *acc-2*, *acc-3*, *acc-4*, *lgc-46*, *lgc-47*, *lgc-48*, and *lgc-49*, and ACC-1, ACC-2, ACC-3, and LGC-49 can form a functional homomeric channel

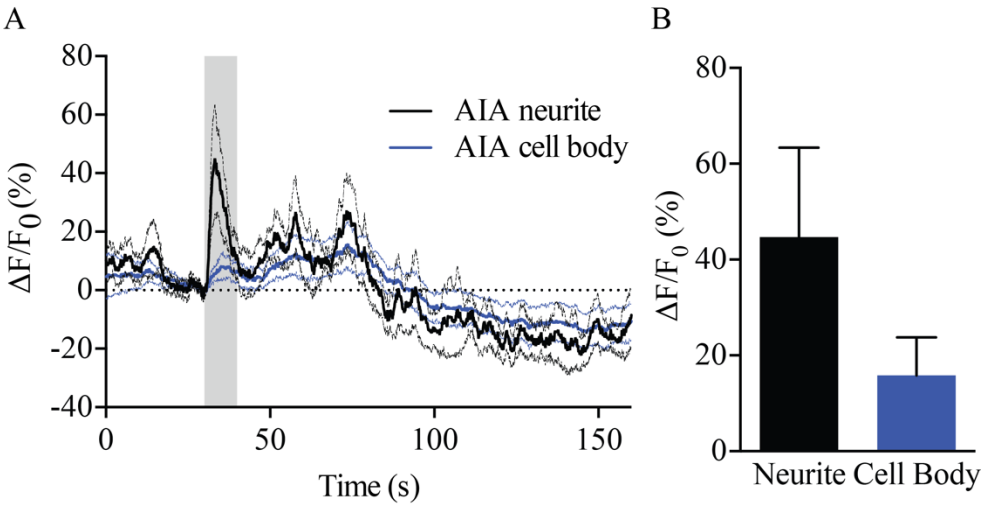

Figure 3-6. The AIAs are activated by 1-octanol presentation. A. Trace averages of 100% 1-octanol-evoked iCa^{2+} transients in the AIAs of wild-type. B. Maximum 1-octanol-evoked iCa^{2+} changes from (A). Data are presented as mean ± SEM.

(Putrenko, Zakikhani et al. 2005). Therefore, we predicted that the AIAs may inhibit the AIBs using a similar pathway.

There is no published evidence indicating that the AIBs are either modulated by acetylcholine or express an acetylcholine gated ion channel. Therefore, we first examined whether acetylcholine evokes a current in the AIBs. Interestingly, acetylcholine evokes an inward current at -60 mV, no net current at -30 mV, and an outward current at +15 mV (Figure 3-7C, F). These data demonstrate that acetylcholine inhibits the AIBs by activating an AChCl channel. Analysis of *acc-1*, *acc-2*, *acc-3*, *lgc-46*, *lgc-47*, and *lgc-49* promoters fused to GFP, generously provided to us by Dr. Joe Dent, indicate that the AIBs express the AChCl channel subunits *acc-1* and *lgc-49* (Figure 3-7A, B). Furthermore, the ratio of ratio of acetylcholine-evoked currents to glutamate-evoked currents is significantly reduced in *acc-1* mutants, while glutamate-evoked currents are not significantly different (Figure 3-7D, E). Together, these data demonstrate that ACC-1 and, potentially, LGC-49 mediate inhibitory acetylcholine-evoked currents in the AIBs.

Since *avr-14* mutants only exhibit a partial reduction in saturating 1-octanol-evoked AIB iCa^{2+} and the AIAs are activated upon 1-octanol presentation, the AIAs may be the primary inhibitory input that inhibit AIB iCa^{2+} during saturating 1-octanol presentation. To test this, we examined temperature-sensitive mutants for the synthetic enzyme choline acetyltransferase encoded by *cha-1* (Rand and Russell 1984). The temperature-sensitive allele allows animals to develop normally at a low temperature, so that developmental defects are minimal or absent, and subsequent heat-shock prior to experimentation confers the mutant phenotype (Zhao and Nonet 2000). Surprisingly,

heat-shocked *cha-1* mutants do not exhibit altered saturating 1-octanol-evoked decreases of AIB iCa^{2+} (Figure 3-8A, B). Animals were heat-shocked for four hours prior to imaging responses, as this time period was sufficient to produce locomotory phenotypes identical to other *cha-1* mutant alleles. However, it may be that locomotory phenotypes arise due to depletion of acetylcholine levels at neuromuscular junctions, while concentrations in other neurons are unaffected, due to intermittent use. Therefore, the AIAs may have still had adequate levels of acetylcholine to inhibit the AIBs. In contrast, animals with AIA-specific *cha-1* RNAi knockdown exhibit reduced saturating 1-octanol inhibition of AIB iCa^{2+} (Figure 3-8A, B). These data support that the AIAs inhibit the AIBs by releasing acetylcholine onto an AChCl channel containing the ACC-1 subunit. Furthermore, since both *avr-14* mutants and animals with AIA-specific *cha-1* RNAi knockdown exhibit partial reduction of saturating 1-octanol-evoked AIB inhibition, acetylcholine and glutamate may both inhibit the AIBs during 1-octanol presentation to precisely modulate AIB activity, thereby allowing for specific aversive behaviors. This idea is further supported by the finding that a narrow range of HA concentration can cause animals to reverse in ~10 seconds in response to dilute 1-octanol, but continue forward after completing their reversal (Summers, Layne et al. 2015).

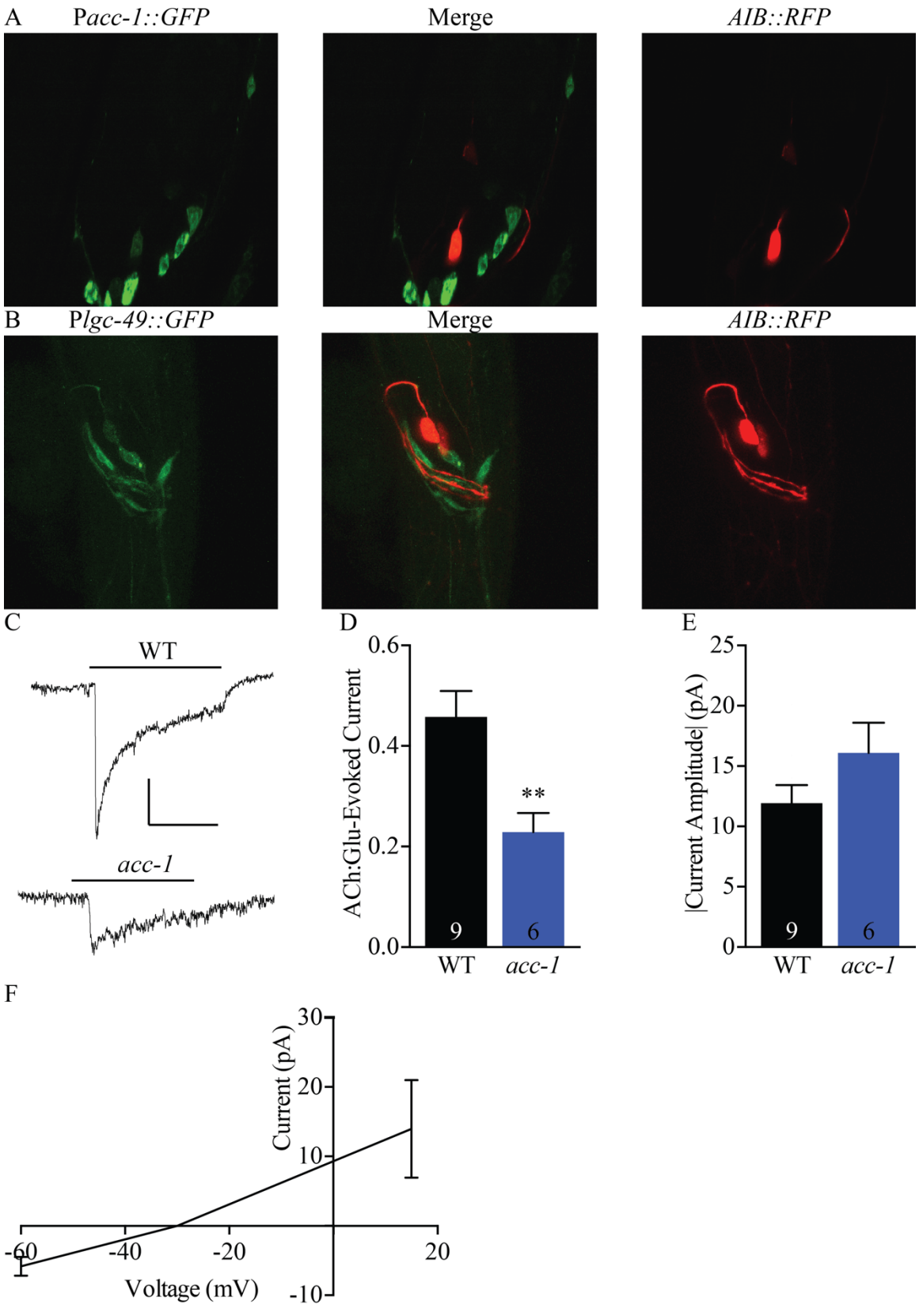
A
Pacc-1::GFP
Merge
AIB::RFP
B
Plgc-49::GFP
Merge
AIB::RFP
C
WT
acc-1
D
ACh:Glu-Evoked Current
0.6
0.4
0.2
0.0
**
9
6
WT
acc-1
E
|Current Amplitude| (pA)
25
20
15
10
5
0
9
6
WT
acc-1
F
Current (pA)
30
20
10
-10
-60
-40
-20
20
Voltage (mV)

Figure 3-7. Currents in the AIBs evoked by acetylcholine application. A. Confocal image of P*acc-1::GFP* (left), *AIB::RFP* (right), and an overlay of the two channels (middle). B. Confocal image of P*lgc-49::GFP* (left), *AIB::RFP* (right), and an overlay of the two channels (middle). C. Representative traces of acetylcholine-evoked currents in the AIBs of wild-type and null animals obtained using the partially dissected electrophysiology preparation (Figure 8A). Vertical scale bar, 5 pA; horizontal scale bar, 1 s. D. Comparison of acetylcholine-evoked currents in the AIBs of wild-type and null animals obtained using the partially dissected electrophysiology preparation (Figure 8A). Data are presented as mean ± SEM and were analyzed by two-tailed Student's *t* test with Welch's correction. **$p<0.01$, significantly different from wild-type animals under identical conditions. Numbers within bars indicate *n*. E. Comparison of glutamate-evoked currents in the AIBs of wild-type and null animals obtained using the partially dissected electrophysiology preparation (Figure 8A). Data are presented as mean ± SEM and were analyzed by two-tailed Student's *t* test with Welch's correction. There is not a significant difference from wild-type animals under identical conditions. Numbers within bars indicate *n*. F. Current-voltage relationship for acetylcholine-evoked currents in the AIBs of nine wild-type animals. The promoter *npr-9* drove expression of RFP in the AIBs of transgenic animals in (A) and (B).

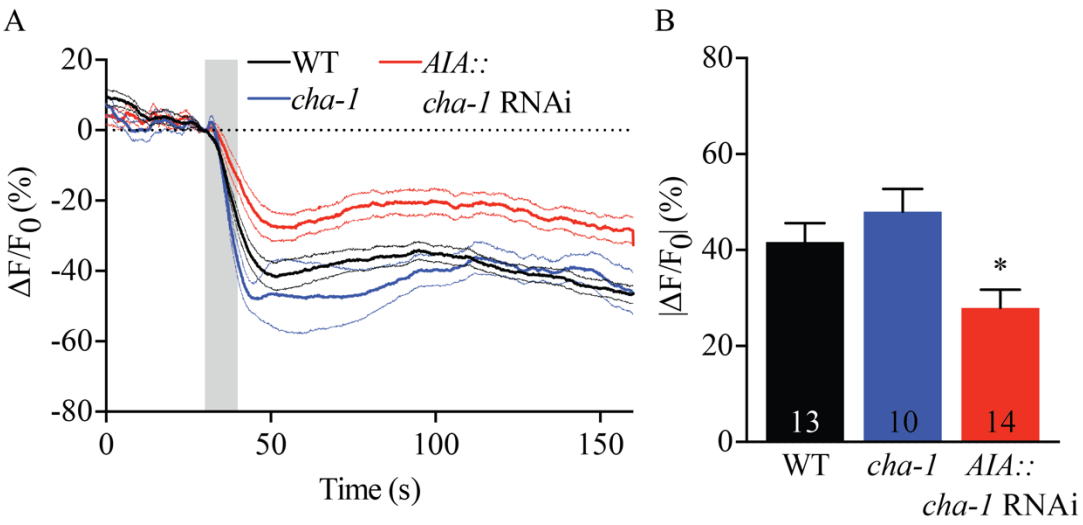

Figure 3-8. Acetylcholine released from the AIAs contributes to 1-octanol inhibition of AIB iCa^{2+}. A. Trace averages of 100% 1-octanol-evoked iCa^{2+} transients in the AIBs of wild-type, null, and transgenic animals. B. Comparison of the absolute value of maximum 1-octanol-evoked iCa^{2+} changes, which were all decreases, from (A). Data are presented as mean ± SEM and were analyzed by two-tailed Student's *t* test with Welch's correction. *$p<0.05$, significantly different from wild-type animals under identical conditions. Numbers within bars indicate *n*.

Chapter 4

Discussion

A balance of excitatory and inhibitory signaling is crucial for recurrent networks of neurons in the brain to remain in an excited state near their threshold of activation in the absence of sensory input (Haider, Duque et al. 2006). Additionally, extensive integration of a variety of sensory inputs that encode information regarding the intrinsic and extrinsic environment effects cognitive function and behavior, with numerous disorders such as autism, depression, and schizophrenia associated with altered multisensory integration (Iarocci and McDonald 2006, Javitt 2009, Farb, Anderson et al. 2012). *C. elegans* is a useful tool for understanding sensorimotor integration, due to its well-defined nervous system, quantifiable behaviors, and the availability of powerful genetic techniques to alter gene expression in a cell-specific manner. In this investigation, we have identified inhibitory and excitatory glutamatergic pathways and an inhibitory cholinergic pathway that modulate the activity of two AIB interneurons to alter animal behavior.

The noxious odorant 1-octanol activates and inhibits a mosaic of glutamatergic and peptidergic sensory neurons that, in conjunction with tonically active 1-octanol insensitive sensory neurons, modulate neural network activity to shape context-dependent aversive behaviors. Many 1-octanol sensitive and insensitive neurons modulate the

activity state of the layer 1 AIB interneurons. The AIB interneurons are inhibited by acetylcholine and glutamate through an ACC-1 containing and AVR-14 receptor, respectively, as well as activated by glutamate through a GLR-1 receptor. Different levels of AIB activity modulate certain aspects of 1-octanol aversive responses, with intermediate levels of activation delaying initial aversive responses to the odorant but allowing for forward locomotion after backing up, and high levels of activation inhibiting initial aversive responses, stimulating the length of reversal, and promoting subsequent turning away from the odorant. Low concentrations of 1-octanol do not strongly effect AIB activity, while high concentrations of odorant elicit long-lasting inhibition of AIB activity, even after odorant withdrawal. Conversely, 1-octanol presentation results in rapid activation of the cholinergic AIA interneurons, a presynaptic partner of the AIBs that is innervated by many of the same sensory neurons, exhibits reciprocal responses to many, if not all sensory stimuli, and has opposing effects animal behavior. However, how AIB activity correlates with stimulus presentation remains uncertain, with some positing that sensory input has little direct effect on AIB activity, and that motor feedback predominantly modulates the activation state of the AIBs (Luo, Wen et al. 2014). Indeed, recent work suggests that the AIBs are not reliably modulated by many sensory stimuli, and that responses are dependent on the activity of the neural network as a whole at the time of stimulus presentation (Gordus, Pokala et al. 2015). Furthermore, it is unclear whether AIB activation serves to initiate reversals or simply promote recurrent activation of neurons more directly responsible for stimulating backward locomotion (Gordus, Pokala et al. 2015). Together, current knowledge of the signaling pathways that regulate AIB activity and the uncertainty of how sensory stimuli ultimately correlate with changes

in AIB activation state, despite the "simplicity" of the nervous system, continue to make *C. elegans* an attractive model for understanding sensory integration.

4.1 Pathological conditions in the nervous system result from altered processing of sensory inputs

In the present investigation, we identified two inhibitory pathways and an excitatory pathway that modulate the activity of the AIBs. The AIBs receive input from numerous sensory sneurons, which mediate chemoattraction (ASEs, ASGs, ASIs, AWCs, ASKs), chemorepulsion (ADLs, ASHs, AWBs), mechanosensation (FLPs), and O_2/CO_2-sensation (BAGs) (Ward, Thomson et al. 1975, Ware, Clark et al. 1975, Perkins, Hedgecock et al. 1986, White, Southgate et al. 1986, Inglis, Ou et al. 2007, Bretscher, Busch et al. 2008, Hallem and Sternberg 2008, Zimmer, Gray et al. 2009, Skora and Zimmer 2013). The AIBs are also gap-junctioned with neurons that mediate thermosensation (AFDs) (Ward, Thomson et al. 1975, Ware, Clark et al. 1975, Perkins, Hedgecock et al. 1986, White, Southgate et al. 1986). The chemoattractant sensing AWCs, which were previously not implicated in 1-octanol sensation, are inhibited by odorant presentation, while the ASHs are activated by odorant presentation. The noxious odorant 1-octanol elicits a reproducible behavioral response, as well reliable inhibition of AIB iCa^{2+}. This consistent inhibition of AIB seems to be unique for 1-octanol, as recent evidence indicates that AIB iCa^{2+} responses are highly variable from trial to trial, and are highly dependent on neural network activity at the time of presentation (Gordus, Pokala et al. 2015). However, this is also consistent with spatial and temporal rules of multisensory integration, which states that stimuli that are spatially and temporally

coincident elicit the strongest response (King and Palmer 1985, Meredith and Stein 1986, Meredith, Nemitz et al. 1987).

Deficits in spatial and temporal integration are an underlying cause of numerous pathophysiologic conditions in humans. For example, people with autism are defective in their ability to integrate multisensory information. When speaking to someone, a comprehensive contextual understanding is dependent on the ability to integrate both auditory and visual cues, such as facial expressions, and integration of these sensory modalities is defective in autistic individuals (Stevenson, Siemann et al. 2014). In the case of 1-octanol, the AWCs and ASHs both contain cilia in the amphid, and as is evident from the time course of iCa^{2+} changes in the ASHs and AWCs, simultaneously respond to the odorant, resulting in a stronger effect on postsynaptic inputs. Therefore, animals exhibit more consistent behavior in response to a stimulus if the stimulus is perceived by more than one modality-specific pathway, in this case, the AWCs, ASHs, and potentially other sensory neurons (e.g. ADLs, AWBs). Furthermore, stimuli sensed by more than one modality-specific pathway may effect the activity of postsynaptic inputs in a more consistent manner, independent of the current neural network state. However, whether the response in AIB iCa^{2+} is a result of direct synaptic input from the ASHs and/or AWCs, or from feedback from another neuron postsynaptic to the AWCs and/or ASHs (i.e. AIAs) remains unclear. Similarly, presentation of a dilute IAA/1-octanol mixture, or dilute 1-octanol soon after a salt step also altered avoidance behaviors.

In children with ADHD, there is significantly more activity in sensory and sensory-related cortices while conscious but not performing a task than in children without ADHD (Tian, Jiang et al. 2008). In children with ADHD characterized by tactile

defensiveness, somatosensation is unimpaired, whereas central processing of somatosensory inputs is impaired (Parush, Sohmer et al. 2007). Similarly, overexpressing the excitatory subunit GLR-1 in the AIBs abolishes 5-HT modulation of aversive responses to dilute 1-octanol. Enhancing synaptic output from the AWCs is also sufficient to abolish 5-HT modulation to dilute 1-octanol. Conversely, enhancing synaptic output from the ASER, which that inhibits the AIBs, or strengthening the ASER to AIB synapse by overexpressing AVR-14 in the AIBs produces the opposite effect, causing animals to exhibit enhanced behaviors to dilute 1-octanol off food. Thus, artificially enhancing signaling in a sensory pathway directly modulated by 1-octanol, as well as a sensory pathway insensitive to 1-octanol is capable of modulating behavior.

4.2 Possibilities of neurotransmitter switching contributing to 5-HT modulation of 1-octanol avoidance

The ability of 5-HT to modulate aversive responses is still largely understood, and requires the function of various 5-HT GPCRs and MOD-1 at many different levels of the nervous system to facilitate its effect, in addition to glutamate release from multiple sensory neurons, and AVR-14 in the AIBs (Harris, Hapiak et al. 2009, Summers, Layne et al. 2015). Recent work demonstrates that hypoxic conditions induce expression of *tph-1* in the ASG sensory neurons due to inhibiting basal levels of degradation of the bHLH-PAS domain-containing transcription factor HIF-1, as well as enhance *tph-1* expression in the ADFs and NSMs (Pocock and Hobert 2010). Induction of *tph-1* expression results in enhanced gustatory perception, whereby, in the absence of the primary gustatory sensory neurons the ASEs, animals display enhanced responses to an NaCl gradient

(Pocock and Hobert 2010). Furthermore, in *tph-1* mutant animals, exogenous 5-HT is sufficient to confer hypoxia-enhanced sensory perception (Pocock and Hobert 2010). Together, these results support that *C. elegans* is capable of neurotransmitter switching, as well as open up new possibilities to explore for 1-octanol modulation of aversive responses, and sensory perception in general.

Neurotransmitter switching can occur *in vitro* in cell culture. Neonatal rat superior cervical ganglion neurons cultured in the presence of non-neuronal cells or medium conditioned by these cells induced cholinergic versus noradrenergic differentiation, thereby determining whether neurons make inhibitory cholinergic, excitatory noradrenergic, or dual-function synapses (Mains and Patterson 1973, Mains and Patterson 1973, Mains and Patterson 1973, O'Lague, Obata et al. 1974, Patterson and Chun 1974, Furshpan, MacLeish et al. 1976, Spitzer 2015). Similarly, ectopic expression of VGLUT in GABAergic hippocampal neurons is sufficient to induce glutamate release at synapses (Takamori, Rhee et al. 2000). In addition to altering cholinergic versus noradrenergic differentiation, levels of tyrosine hydroxylase (TH) are significantly higher in neurons that are cholinergically differentiated (Higgins, Iacovitti et al. 1981, Iacovitti, Joh et al. 1981, Spitzer 2015). The leukemia inhibitory factor (LIF) in medium conditioned by non-neuronal cells induces cholinergic differentiation, suppresses noradrenergic differentiation, increases vasoactive intestinal peptide (VIP), substance P, and somatostatin levels, and decreases neuropeptide Y (NPY) and TH (Fukada 1985, Yamamori, Fukada et al. 1989, Nawa and Patterson 1990, Freidin and Kessler 1991, Nawa, Nakanishi et al. 1991, Mulderry 1994, Spitzer 2015). Ciliary neurotrophic factor (CNTF) and brain-derived neurotrophic factor (BDNF) induce the same changes as LIF,

with BDNF achieving switching within 15 minutes (Saadat, Sendtner et al. 1989, Rao, Landis et al. 1990, Yang, Slonimsky et al. 2002, Spitzer 2015). Furthermore, Ca^{2+} influx due to depolarization can block cholinergic differentiation in conditioned medium induced by LIF, although peptide expression levels are not uniformly altered, but has no effect on CNTF-induced cholinergic differentiation (Walicke, Campenot et al. 1977, Kessler, Adler et al. 1981, Walicke and Patterson 1981, Rao, Tyrrell et al. 1992, Spitzer 2015). These observations may have functional correlates in the *C. elegans* nervous system. For instance, peptidergic feedback and insulin-like signaling cascades modulate iCa^{2+} responses in sensory neurons (i.e. *ins-1* encodes peptides inhibit AWC iCa^{2+} and 5-HT can inhibit salt conditioning potentiated ASER iCa^{2+} increases that inversely correlate with neurotransmitter release) (Chalasani, Kato et al. 2010, Oda, Tomioka et al. 2011). Furthermore, despite not initiating aversive responses to 1-octanol, odorant presentation still inhibits AIB iCa^{2+} in *eat-4* mutants, possibly due to mosaic changes in neurotransmitter expression that don't elicit wild-type behavioral responses, but are sufficient to mediate 1-octanol modulation of AIB iCa^{2+}. Furthermore, feedback that modulates sensory neuron iCa^{2+}, at least in some instances, is dependent on *eat-4* (Chalasani, Kato et al. 2010).

Neurotransmitter switching can also occur during development *in vitro*. Embryonic *Xenopus* striated muscle cells express glutamate, GABA, glycine, and acetylcholine receptors, but acetylcholine receptor expression is most prominent as development progresses (Borodinsky and Spitzer 2007). However, artificially suppressing or enhancing presynaptic motor neuron activity induces AMPA and NMDA receptor or GABA and glycine receptor expression, respectively (Borodinsky and Spitzer 2007).

Furthermore, corresponding increases in GABA or glutamate expression in presynaptic nerve terminals also occur (Borodinsky and Spitzer 2007). Indeed, cotransmission of acetylcholine and glutamate occurs at adult vertebrate neuromuscular junctions (Brunelli, Spano et al. 2005). Together, this supports that neurons signal to muscle cells using diffusable factors, potentially including but not limited to the neurotransmitters themselves, and postsynaptic receptors are stabilized by activation, while those not utilized are either inactivated or removed (Borodinsky and Spitzer 2007). This raises the possibility that developmental compensation occurs in *eat-4* mutants that doesn't preserve behavioral phenotypes in response to certain stimuli (e.g. 1-octanol) due to a variant pattern of presynaptic/postsynaptic neurotransmitter/receptor combinations, but may be sufficient to exhibit wild-type modulation of individual postsynaptic targets (e.g. AIBs). Furthermore, it allows a new avenue of investigation regarding how potentiation or inhibition of an individual signaling pathway from an individual presynaptic/postsynaptic pair may possibly alter parallel signaling pathways.

Mature neurons in the fully developed nervous system undergo neurotransmitter switching. For example, perturbing olfactory input does not alter glutamic acid decarboxylase (GAD) or GABA expression, but reduces TH expression, demonstrating specificity of transmitter specification (Kosaka, Kosaka et al. 1987, Baker, Towle et al. 1988, Stone, Grillo et al. 1991, Baker, Morel et al. 1993, Spitzer 2015). Furthermore, postmortem examination of the prefrontal cortex reveals that GAD transcript and protein levels are reduced, despite the absence of neuronal degradation (Akbarian, Huntsman et al. 1995, Spitzer 2015). Additionally, following lesion of dopaminergic neurons using MPTP, there is an increase in the number of interneurons expressing the dopamine

transporter (DAT) and GAD, despite a lack of neurogenesis, suggesting that dopaminergic neurons were derived from GABAergic neurons (Tande, Hoglinger et al. 2006, Borodinsky and Spitzer 2007). Similarly, neurons in rat paraventricular and periventricular nuclei had increases and decreases in dopaminergic and somatostatin (SST) expressing neurons, respectively, following exposure to a short-day photoperiod. Exposure to a long-day photoperiod had the opposite effect, and the effects of both long- and short-day photoperiods were reversible; neurons express both neurotransmitters following exposure to a balanced day-night period (Dulcis, Jamshidi et al. 2013, Spitzer 2015). Levels of D2 dopamine receptors correlated with changes in neurotransmitter expression, while SST receptor expression was not effected (Dulcis, Jamshidi et al. 2013, Spitzer 2015). Furthermore, changes in neurotransmitter and, in the case of dopamine, receptor expression levels elicited behavioral changes, characterized by increased anxiety following a long-photoperiod, and alleviation of these effects following a short-photoperiod (Dulcis, Jamshidi et al. 2013, Spitzer 2015). Together, these data support that neurotransmitter switching can occur in the fully developed nervous system to modulate behavior.

Neuronal plasticity of neurotransmitter expression and corresponding receptor expression on postsynaptic inputs presents an interesting avenue to continue our current line of inquiry. Furthermore, it provides possible explanations for the dichotomy between 1-octanol-evoked decreases in AIB iCa^{2+} and the lack of odorant avoidance behaviors exhibited by *eat-4* mutants. For example, it is unknown whether all neurons in the nervous system demonstrate the same level of plasticity for neurotransmitter switching. Therefore, one possibility is that the input into AIBs that is primarily or

absolutely responsible for 1-octanol-evoked inhibition of AIB iCa^{2+} is able to compensate for the loss of *eat-4* expression, either by upregulating or inducing expression of another vesicular glutamate transporter, or by switching to another neurotransmitter entirely (e.g. acetylcholine). However, it may not be the case that compensatory effects for the loss of *eat-4* result in the same balance of expression necessary to preserve wild-type behavior in response to 1-octanol presentation, resulting in the loss of aversive responses.

4.3 Physiologic implications of AIB iCa^{2+} changes

Many conclusions drawn in *C. elegans* neurobiology, and neurobiology in general, rely on iCa^{2+} indicators as a readout of neuronal activity. However, recent work demonstrates that although iCa^{2+} increases may be a reliable readout of depolarization, the magnitude of iCa^{2+} increase may not correspond to either the magnitude of depolarization or subsequent neurotransmitter release. For instance, as has been discussed, salt conditioning of ASER and ASEL results in increases and decreases in iCa^{2+} increases following salt downstep and upstep, respectively, relative to naive animals (Oda, Tomioka et al. 2011). However, despite enhanced iCa^{2+} increases in the ASER of salt-conditioned animals following salt downstep, synaptic release was decreased, while synaptic release was not altered in the ASEL of salt-conditioned animals following salt upstep, despite inhibition of iCa^{2+} increases (Oda, Tomioka et al. 2011). Interestingly, salt-conditioned modulation of ASER iCa^{2+} and synaptic release are dependent on insulin-like signaling, whereas ASEL responses are not (Oda, Tomioka et al. 2011). Similarly, 1-octanol presentation to naive animals both evokes large iCa^{2+} increases and depolarizes the ASHs (Zahratka, Williams et al. 2015).

Presentation of 1-octanol to 5-HT treated animals evokes reduced 1-octanol iCa^{2+} increases, but a larger depolarization in the ASHs (Zahratka, Williams et al. 2015). In 5-HT treated animals, iCa^{2+} increases are reduced due to inactivation of the EGL-19 (Zahratka, Williams et al. 2015). In mammals, the L-type VGCCs are activated at depolarized membrane potentials (≥-10 mV) (Snutch, Peloquin et al. 2000). In addition to mediating Ca^{2+} currents, the C-terminus fragment of L-type VGCC can translocate into the nucleus to positively and negatively regulate transcription (Gomez-Ospina, Tsuruta et al. 2006, Schroder, Byse et al. 2009). This begs the question of what function EGL-19 serves in modulating neuronal activity in naive animals, and how 5-HT inhibition of EGL-19 facilitates a change in neuronal output. It does not seem that EGL-19 potentiates depolarization, as EGL-19 inhibition allows for a larger depolarization (Goodman, Hall et al. 1998).

Similar to the ASHs of naive animals in response to 1-octanol presentation, other *C. elegans* neurons, including the ASEs, AWCs, AQRs, PQRs, URXs, AIBs and AIZs, also exhibit iCa^{2+} increases throughout the entirety of the neuron (Busch, Laurent et al. 2012, Li, Liu et al. 2014). Like the ASHs, the iCa^{2+} increases in the AIBs, AQRs, PQRs, and URXs are primarily due to EGL-19. Furthermore, EGL-19 in the AQRs, PQRs, and URXs helps maintain persistent activity (Bretscher, Busch et al. 2008). Therefore, these data suggest that EGL-19 may function in the AIBs to maintain persistent activity in the absence of stimulation to promote long-lasting increases in turning probability. Additionally, recent evidence supports that motor feedback plays a role in modulating the activity state of the AIBs (Luo, Wen et al. 2014). In contrast, the AIAs and AIYs predominantly exhibit iCa^{2+} changes in neurites (Li, Liu et al. 2014). Increases in AIA

neurite iCa^{2+} rise and decay quickly, with moderate persistent activity lasting ~50 seconds following 1-octanol exposure. Although not directly indicative of any significant meaning, this provides some implication that VGCC expression on cell bodies may serve an auxiliary function. Collectively, these observations demonstrate that much remains to be understood regarding the meaning of iCa^{2+} increases, especially in neuronal cell bodies, and further investigation is warranted.

4.4 Conclusions

In the present study, we have identified three signaling pathways that modulate the AIBs: (1) an excitatory glutamatergic pathway that activates the AMPA-type GLR-1 on the AIBs,, (2) an inhibitory glutamatergic pathway that activates the GluCl AVR-14 on the AIBs, and (3) an inhibitory cholinergic pathway that activates an AChCl containing ACC-1 on the AIBs. Presentation of saturating 1-octanol inhibits the AIBs, and is partially dependent on AVR-14, as well as acetylcholine release from the AIAs. Animals in which the AIBs are actively signaling take longer to initiate an aversive response following 1-octanol presentation, back up farther, and subsequently turn away from the odorant. Conversely, animals with depressed AIBs synaptic output initiate an aversive response more quickly following 1-octanol presentation, decrease the distance they reverse, and continue moving forward after completing their reversal. Interestingly, a moderate amount AIBs synaptic output can differentially modulate aspects of 1-octanol aversive behaviors, causing animals to delay initiating an aversive response to 1-octanol, but continue forward after backward locomotion is complete. Finally, 1-octanol inhibits the AWCs, and the AWCs modulate aversive behaviors by tonically releasing glutamate

onto GLR-1 on the AIBs. Conversely, 1-octanol does not modulate ASER activity, but tonic glutamate release from the ASER onto AVR-14 on the AIBs modulates 1-octanol avoidance behaviors. Figure 4-1 illustrates signaling pathways identified in the present study and/or defined by previous work that the AWCs, ASHs, and ASER use to modulate the activity of the AIAs and AIBs.

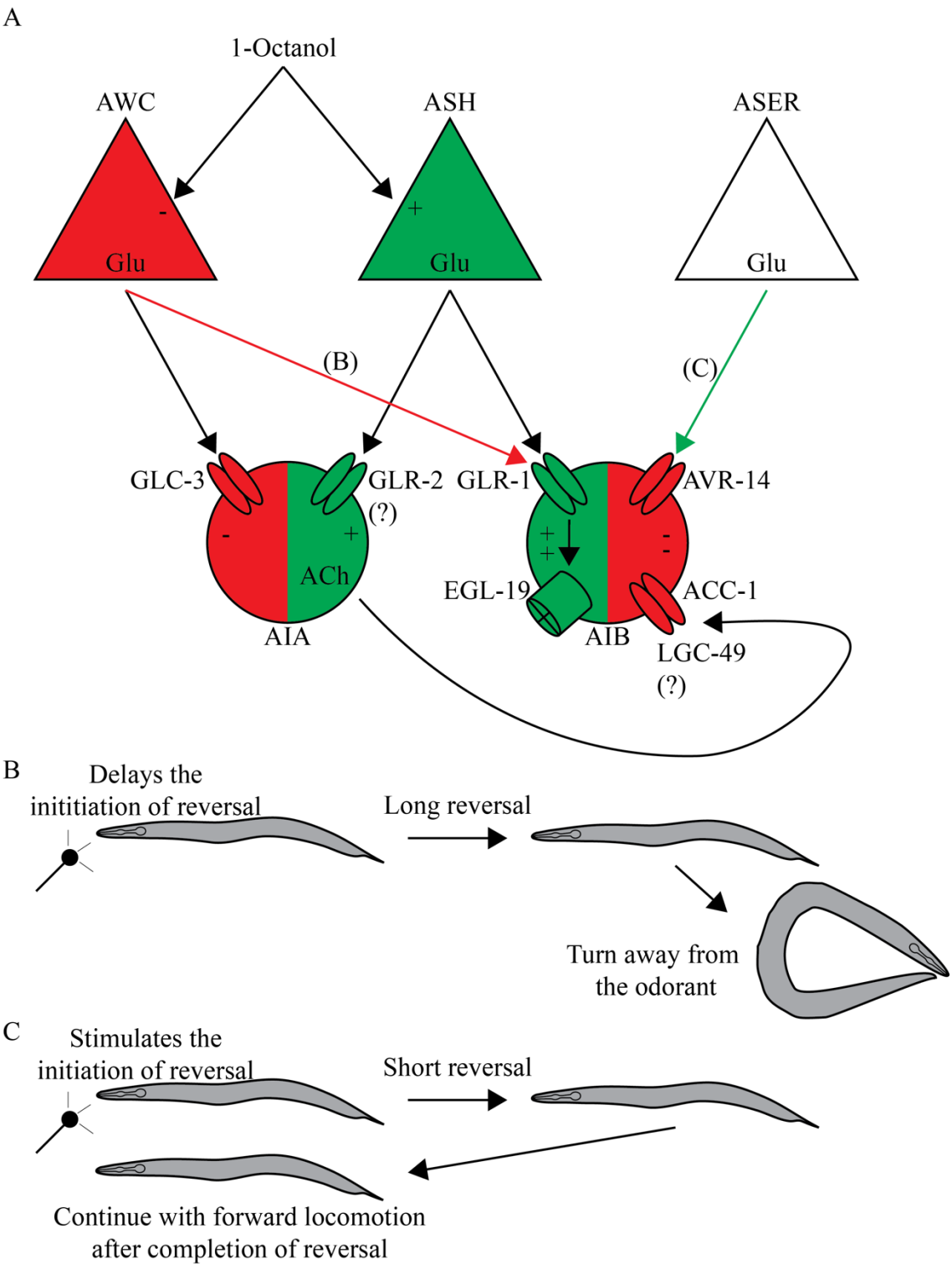

Figure 4-1. Signaling pathways from the AWCs, ASHs, and ASER that modulate the AIAs and AIBs. A. The odorant 1-octanol inhibits, stimulates, and has no effect on

the AWCs, ASHs, and ASER, respectively. The AWCs tonically inhibit the AIAs by releasing glutamate onto GLC-3, as well as activate the AIBs with tonic and evoked glutamate release onto GLR-1. The ASHs activate the AIAs and AIBs by releasing glutamate onto GLR-2 and GLR-1, respectively (Choi, Taylor, et al. 2015). Signaling onto GLR-1 on the AIBs activates EGL-19 on the AIBs. The ASER tonically inhibits the AIBs by releasing glutamate onto AVR-14. The AIAs inhibit the AIBs by releasing glutamate onto an AChCl channel or channels containing the ACC-1 and/or, potentially, LGC-49 subunits. B. Tonic glutamate release from the AWCs onto GLR-1 on the AIBs delays the initial aversive response to 1-octanol, stimulates a long reversal, and promotes turning away from the odorant after completing the initial reversal. This pathway is illustrated by the red arrow in (A). C. Tonic glutamate release from the ASER onto AVR-14 on the AIBs delays the initial aversive response to 1-octanol, stimulates a long reversal, and promotes turning away from the odorant after completing the initial reversal. This pathway is illustrated by the green arrow in (A).

References

Akbarian, S., M. M. Huntsman, J. J. Kim, A. Tafazzoli, S. G. Potkin, W. E. Bunney, Jr. and E. G. Jones (1995). "GABAA receptor subunit gene expression in human prefrontal cortex: comparison of schizophrenics and controls." Cereb Cortex 5(6): 550-560.

Altun, Z. F. and D. H. Hall (2011). Nervous system, general description.

Altun-Gultekin, Z., Y. Andachi, E. L. Tsalik, D. Pilgrim, Y. Kohara and O. Hobert (2001). "A regulatory cascade of three homeobox genes, *ceh-10*, *ttx-3* and *ceh-23*, controls cell fate specification of a defined interneuron class in *C. elegans*." Development 128(11): 1951-1969.

Aoki, R., T. Yagami, H. Sasakura, K. Ogura, Y. Kajihara, M. Ibi, T. Miyamae, F. Nakamura, T. Asakura, Y. Kanai, Y. Misu, Y. Iino, M. Ezcurra, W. R. Schafer, I. Mori and Y. Goshima (2011). "A seven-transmembrane receptor that mediates avoidance response to dihydrocaffeic acid, a water-soluble repellent in *Caenorhabditis elegans*." J Neurosci 31(46): 16603-16610.

Avery, L. and H. R. Horvitz (1990). "Effects of starvation and neuroactive drugs on feeding in *Caenorhabditis elegans*." J Exp Zool 253(3): 263-270.

Azevedo, F. A., L. R. Carvalho, L. T. Grinberg, J. M. Farfel, R. E. Ferretti, R. E. Leite, W. Jacob Filho, R. Lent and S. Herculano-Houzel (2009). "Equal numbers of neuronal and nonneuronal cells make the human brain an isometrically scaled-up primate brain." J Comp Neurol 513(5): 532-541.

Baker, H., K. Morel, D. M. Stone and J. A. Maruniak (1993). "Adult naris closure profoundly reduces tyrosine hydroxylase expression in mouse olfactory bulb." Brain Res 614(1-2): 109-116.

Baker, H., A. C. Towle and F. L. Margolis (1988). "Differential afferent regulation of dopaminergic and GABAergic neurons in the mouse main olfactory bulb." Brain Res 450(1-2): 69-80.

Baldridge, W. H., D. I. Vaney and R. Weiler (1998). "The modulation of intercellular coupling in the retina." Semin Cell Dev Biol 9(3): 311-318.

Bamber, B. (Unpublished).

Bargmann, C. I. (1998). "Neurobiology of the *Caenorhabditis elegans* genome." Science 282(5396): 2028-2033.

Bargmann, C. I. (2006). "Chemosensation in *C. elegans*." WormBook: 1-29.

Bargmann, C. I., E. Hartwieg and H. R. Horvitz (1993). "Odorant-selective genes and neurons mediate olfaction in *C. elegans*." Cell 74(3): 515-527.

Bargmann, C. I. and H. R. Horvitz (1991). "Chemosensory neurons with overlapping

functions direct chemotaxis to multiple chemicals in *C. elegans*." Neuron 7(5): 729-742.

Bargmann, C. I. and J. M. Kaplan (1998). "Signal transduction in the *Caenorhabditis elegans* nervous system." Annu Rev Neurosci 21: 279-308.

Bargmann, C. I., J. H. Thomas and H. R. Horvitz (1990). "Chemosensory cell function in the behavior and development of *Caenorhabditis elegans*." Cold Spring Harb Symp Quant Biol 55: 529-538.

Bell, W. J. (1991). Searching Behavior: The Behavioral Ecology of Finding Resources. New York, Chapman and Hall.

Bergamasco, C. and P. Bazzicalupo (2006). "Chemical sensitivity in *Caenorhabditis elegans*." Cell Mol Life Sci 63(13): 1510-1522.

Berger, A. J., A. C. Hart and J. M. Kaplan (1998). "G alphas-induced neurodegeneration in *Caenorhabditis elegans*." J Neurosci 18(8): 2871-2880.

Birnby, D. A., E. M. Link, J. J. Vowels, H. Tian, P. L. Colacurcio and J. H. Thomas (2000). "A transmembrane guanylyl cyclase (DAF-11) and Hsp90 (DAF-21) regulate a common set of chemosensory behaviors in *Caenorhabditis elegans*." Genetics 155(1): 85-104.

Borodinsky, L. N. and N. C. Spitzer (2007). "Activity-dependent neurotransmitter-receptor matching at the neuromuscular junction." Proc Natl Acad Sci U S A 104(1): 335-340.

Brenner, S. (1974). "The genetics of *Caenorhabditis elegans*." Genetics 77(1): 71-94.

Bretscher, A. J., K. E. Busch and M. de Bono (2008). "A carbon dioxide avoidance behavior is integrated with responses to ambient oxygen and food in *Caenorhabditis elegans*." Proc Natl Acad Sci U S A 105(23): 8044-8049.

Bretscher, A. J., E. Kodama-Namba, K. E. Busch, R. J. Murphy, Z. Soltesz, P. Laurent and M. de Bono (2011). "Temperature, oxygen, and salt-sensing neurons in *C. elegans* are carbon dioxide sensors that control avoidance behavior." Neuron 69(6): 1099-1113.

Brockie, P. J., D. M. Madsen, Y. Zheng, J. Mellem and A. V. Maricq (2001). "Differential expression of glutamate receptor subunits in the nervous system of *Caenorhabditis elegans* and their regulation by the homeodomain protein UNC-42." J Neurosci 21(5): 1510-1522.

Brockie, P. J. and A. V. Maricq (2003). "Ionotropic glutamate receptors in *Caenorhabditis elegans*." Neurosignals 12(3): 108-125.

Brockie, P. J., J. E. Mellem, T. Hills, D. M. Madsen and A. V. Maricq (2001). "The *C. elegans* glutamate receptor subunit NMR-1 is required for slow NMDA-activated currents that regulate reversal frequency during locomotion." Neuron 31(4): 617-630.

Brunelli, G., P. Spano, S. Barlati, B. Guarneri, A. Barbon, R. Bresciani and M. Pizzi (2005). "Glutamatergic reinnervation through peripheral nerve graft dictates

assembly of glutamatergic synapses at rat skeletal muscle." Proc Natl Acad Sci U S A 102(24): 8752-8757.

Busch, K. E., P. Laurent, Z. Soltesz, R. J. Murphy, O. Faivre, B. Hedwig, M. Thomas, H. L. Smith and M. de Bono (2012). "Tonic signaling from O(2) sensors sets neural circuit activity and behavioral state." Nat Neurosci 15(4): 581-591.

Chalasani, S. H., N. Chronis, M. Tsunozaki, J. M. Gray, D. Ramot, M. B. Goodman and C. I. Bargmann (2007). "Dissecting a circuit for olfactory behaviour in *Caenorhabditis elegans*." Nature 450(7166): 63-70.

Chalasani, S. H., S. Kato, D. R. Albrecht, T. Nakagawa, L. F. Abbott and C. I. Bargmann (2010). "Neuropeptide feedback modifies odor-evoked dynamics in *Caenorhabditis elegans* olfactory neurons." Nat Neurosci 13(5): 615-621.

Chalfie, M., J. E. Sulston, J. G. White, E. Southgate, J. N. Thomson and S. Brenner (1985). "The neural circuit for touch sensitivity in *Caenorhabditis elegans*." J Neurosci 5(4): 956-964.

Chao, M. Y., H. Komatsu, H. S. Fukuto, H. M. Dionne and A. C. Hart (2004). "Feeding status and serotonin rapidly and reversibly modulate a *Caenorhabditis elegans* chemosensory circuit." Proc Natl Acad Sci U S A 101(43): 15512-15517.

Chatzigeorgiou, M., S. Bang, S. W. Hwang and W. R. Schafer (2013). "*tmc-1* encodes a sodium-sensitive channel required for salt chemosensation in *C. elegans*." Nature 494(7435): 95-99.

Chatzigeorgiou, M., S. Yoo, J. D. Watson, W. H. Lee, W. C. Spencer, K. S. Kindt, S. W. Hwang, D. M. Miller, 3rd, M. Treinin, M. Driscoll and W. R. Schafer (2010). "Specific roles for DEG/ENaC and TRP channels in touch and thermosensation in *C. elegans* nociceptors." Nat Neurosci 13(7): 861-868.

Chiang, A. S., C. Y. Lin, C. C. Chuang, H. M. Chang, C. H. Hsieh, C. W. Yeh, C. T. Shih, J. J. Wu, G. T. Wang, Y. C. Chen, C. C. Wu, G. Y. Chen, Y. T. Ching, P. C. Lee, C. Y. Lin, H. H. Lin, C. C. Wu, H. W. Hsu, Y. A. Huang, J. Y. Chen, H. J. Chiang, C. F. Lu, R. F. Ni, C. Y. Yeh and J. K. Hwang (2011). "Three-dimensional reconstruction of brain-wide wiring networks in *Drosophila* at single-cell resolution." Curr Biol 21(1): 1-11.

Choi, S., K. P. Taylor, M. Chatzigeorgiou, Z. Hu, W. R. Schafer and J. M. Kaplan (2015). "Sensory Neurons Arouse *C. elegans* Locomotion via Both Glutamate and Neuropeptide Release." PLoS Genet 11(7): e1005359.

Coburn, C. M. and C. I. Bargmann (1996). "A putative cyclic nucleotide-gated channel is required for sensory development and function in *C. elegans*." Neuron 17(4): 695-706.

Colbert, H. A., T. L. Smith and C. I. Bargmann (1997). "OSM-9, a novel protein with structural similarity to channels, is required for olfaction, mechanosensation, and olfactory adaptation in *Caenorhabditis elegans*." J Neurosci 17(21): 8259-8269.

Conradt, B. and H. R. Horvitz (1998). "The *C. elegans* protein EGL-1 is required for programmed cell death and interacts with the Bcl-2-like protein CED-9." Cell

93(4): 519-529.

Cook, A., N. Aptel, V. Portillo, E. Siney, R. Sihota, L. Holden-Dye and A. Wolstenholme (2006). "*Caenorhabditis elegans* ivermectin receptors regulate locomotor behaviour and are functional orthologues of *Haemonchus contortus* receptors." Mol Biochem Parasitol 147(1): 118-125.

Croll, N. A. (2009). "Components and patterns in the behaviour of the nematode *Caenorhabditis elegans*." Journal of Zoology 176(2): 159-176.

Cully, D. F., D. K. Vassilatis, K. K. Liu, P. S. Paress, L. H. Van der Ploeg, J. M. Schaeffer and J. P. Arena (1994). "Cloning of an avermectin-sensitive glutamate-gated chloride channel from *Caenorhabditis elegans*." Nature 371(6499): 707-711.

Culotti, J. G. and R. L. Russell (1978). "Osmotic avoidance defective mutants of the nematode *Caenorhabditis elegans*." Genetics 90(2): 243-256.

de Bono, M. and A. V. Maricq (2005). "Neuronal substrates of complex behaviors in *C. elegans*." Annu Rev Neurosci 28: 451-501.

Dent, J. A., M. W. Davis and L. Avery (1997). "*avr-15* encodes a chloride channel subunit that mediates inhibitory glutamatergic neurotransmission and ivermectin sensitivity in *Caenorhabditis elegans*." EMBO J 16(19): 5867-5879.

Dent, J. A., M. M. Smith, D. K. Vassilatis and L. Avery (2000). "The genetics of ivermectin resistance in *Caenorhabditis elegans*." Proc Natl Acad Sci U S A

97(6): 2674-2679.

Dorman, J. B., B. Albinder, T. Shroyer and C. Kenyon (1995). "The *age-1* and *daf-2* genes function in a common pathway to control the lifespan of *Caenorhabditis elegans*." Genetics 141(4): 1399-1406.

Dulcis, D., P. Jamshidi, S. Leutgeb and N. C. Spitzer (2013). "Neurotransmitter switching in the adult brain regulates behavior." Science 340(6131): 449-453.

Esposito, G., E. Di Schiavi, C. Bergamasco and P. Bazzicalupo (2007). "Efficient and cell specific knock-down of gene function in targeted *C. elegans* neurons." Gene 395(1-2): 170-176.

Ezak, M. J. and D. M. Ferkey (2010). "The *C. elegans* D2-like dopamine receptor DOP-3 decreases behavioral sensitivity to the olfactory stimulus 1-octanol." PLoS One 5(3): e9487.

Ezcurra, M., Y. Tanizawa, P. Swoboda and W. R. Schafer (2011). "Food sensitizes *C. elegans* avoidance behaviours through acute dopamine signalling." EMBO J 30(6): 1110-1122.

Farb, N. A., A. K. Anderson and Z. V. Segal (2012). "The mindful brain and emotion regulation in mood disorders." Can J Psychiatry 57(2): 70-77.

Freidin, M. and J. A. Kessler (1991). "Cytokine regulation of substance P expression in sympathetic neurons." Proc Natl Acad Sci U S A 88(8): 3200-3203.

Fu, Y. and K. W. Yau (2007). "Phototransduction in mouse rods and cones." Pflugers Arch 454(5): 805-819.

Fukada, K. (1985). "Purification and partial characterization of a cholinergic neuronal differentiation factor." Proc Natl Acad Sci U S A 82(24): 8795-8799.

Fukuto, H. S., D. M. Ferkey, A. J. Apicella, H. Lans, T. Sharmeen, W. Chen, R. J. Lefkowitz, G. Jansen, W. R. Schafer and A. C. Hart (2004). "G protein-coupled receptor kinase function is essential for chemosensation in *C. elegans*." Neuron 42(4): 581-593.

Furshpan, E. J., P. R. MacLeish, P. H. O'Lague and D. D. Potter (1976). "Chemical transmission between rat sympathetic neurons and cardiac myocytes developing in microcultures: evidence for cholinergic, adrenergic, and dual-function neurons." Proc Natl Acad Sci U S A 73(11): 4225-4229.

Ghanizadeh, A. (2011). "Sensory processing problems in children with ADHD, a systematic review." Psychiatry Investig 8(2): 89-94.

Gomez-Ospina, N., F. Tsuruta, O. Barreto-Chang, L. Hu and R. Dolmetsch (2006). "The C terminus of the L-type voltage-gated calcium channel Ca(V)1.2 encodes a transcription factor." Cell 127(3): 591-606.

Goodman, M. B., D. H. Hall, L. Avery and S. R. Lockery (1998). "Active currents regulate sensitivity and dynamic range in *C. elegans* neurons." Neuron 20(4): 763-772.

Gordus, A., N. Pokala, S. Levy, S. W. Flavell and C. I. Bargmann (2015). "Feedback from network states generates variability in a probabilistic olfactory circuit." Cell 161(2): 215-227.

Gray, J. M., J. J. Hill and C. I. Bargmann (2005). "A circuit for navigation in *Caenorhabditis elegans*." Proc Natl Acad Sci U S A 102(9): 3184-3191.

Haider, B., A. Duque, A. R. Hasenstaub and D. A. McCormick (2006). "Neocortical network activity in vivo is generated through a dynamic balance of excitation and inhibition." J Neurosci 26(17): 4535-4545.

Hallem, E. A. and P. W. Sternberg (2008). "Acute carbon dioxide avoidance in *Caenorhabditis elegans*." Proc Natl Acad Sci U S A 105(23): 8038-8043.

Harris, G., A. Korchnak, P. Summers, V. Hapiak, W. J. Law, A. M. Stein, P. Komuniecki and R. Komuniecki (2011). "Dissecting the serotonergic food signal stimulating sensory-mediated aversive behavior in *C. elegans*." PLoS One 6(7): e21897.

Harris, G., H. Mills, R. Wragg, V. Hapiak, M. Castelletto, A. Korchnak and R. W. Komuniecki (2010). "The monoaminergic modulation of sensory-mediated aversive responses in *Caenorhabditis elegans* requires glutamatergic/peptidergic cotransmission." J Neurosci 30(23): 7889-7899.

Harris, G. P., V. M. Hapiak, R. T. Wragg, S. B. Miller, L. J. Hughes, R. J. Hobson, R. Steven, B. Bamber and R. W. Komuniecki (2009). "Three distinct amine receptors operating at different levels within the locomotory circuit are each

essential for the serotonergic modulation of chemosensation in *Caenorhabditis elegans*." J Neurosci 29(5): 1446-1456.

Hart, A. C., J. Kass, J. E. Shapiro and J. M. Kaplan (1999). "Distinct signaling pathways mediate touch and osmosensory responses in a polymodal sensory neuron." J Neurosci 19(6): 1952-1958.

Hart, A. C., S. Sims and J. M. Kaplan (1995). "Synaptic code for sensory modalities revealed by *C. elegans* GLR-1 glutamate receptor." Nature 378(6552): 82-85.

Hidaka, K., N. Ashizawa, H. Endoh, M. Watanabe and S. Fukumoto (1995). "Fine structure of the cilia in the pancreatic duct of WBN/Kob rat." Int J Pancreatol 18(3): 207-213.

Higgins, D., L. Iacovitti, T. H. Joh and H. Burton (1981). "The immunocytochemical localization of tyrosine hydroxylase within rat sympathetic neurons that release acetylcholine in culture." J Neurosci 1(2): 126-131.

Hilliard, M. A., A. J. Apicella, R. Kerr, H. Suzuki, P. Bazzicalupo and W. R. Schafer (2005). "In vivo imaging of *C. elegans* ASH neurons: cellular response and adaptation to chemical repellents." EMBO J 24(1): 63-72.

Hilliard, M. A., C. I. Bargmann and P. Bazzicalupo (2002). "*C. elegans* responds to chemical repellents by integrating sensory inputs from the head and the tail." Curr Biol 12(9): 730-734.

Hilliard, M. A., C. Bergamasco, S. Arbucci, R. H. Plasterk and P. Bazzicalupo (2004).

"Worms taste bitter: ASH neurons, QUI-1, GPA-3 and ODR-3 mediate quinine avoidance in *Caenorhabditis elegans*." EMBO J 23(5): 1101-1111.

Hills, T., P. J. Brockie and A. V. Maricq (2004). "Dopamine and glutamate control area-restricted search behavior in *Caenorhabditis elegans*." J Neurosci 24(5): 1217-1225.

Hobert, O. (2002). "PCR fusion-based approach to create reporter gene constructs for expression analysis in transgenic *C. elegans*." Biotechniques 32(4): 728-730.

Hooper, S. L. and M. Moulins (1989). "Switching of a neuron from one network to another by sensory-induced changes in membrane properties." Science 244(4912): 1587-1589.

Horoszok, L., V. Raymond, D. B. Sattelle and A. J. Wolstenholme (2001). "GLC-3: a novel fipronil and BIDN-sensitive, but picrotoxinin-insensitive, L-glutamate-gated chloride channel subunit from *Caenorhabditis elegans*." Br J Pharmacol 132(6): 1247-1254.

Horvitz, H. R., M. Chalfie, C. Trent, J. E. Sulston and P. D. Evans (1982). "Serotonin and octopamine in the nematode *Caenorhabditis elegans*." Science 216(4549): 1012-1014.

Iacovitti, L., T. H. Joh, D. H. Park and R. P. Bunge (1981). "Dual expression of neurotransmitter synthesis in cultured autonomic neurons." J Neurosci 1(7): 685-690.

Iarocci, G. and J. McDonald (2006). "Sensory integration and the perceptual experience of persons with autism." J Autism Dev Disord 36(1): 77-90.

Ignell, R., C. M. Root, R. T. Birse, J. W. Wang, D. R. Nassel and A. M. Winther (2009). "Presynaptic peptidergic modulation of olfactory receptor neurons in *Drosophila*." Proc Natl Acad Sci U S A 106(31): 13070-13075.

Inglis, P. N., G. Ou, M. R. Leroux and J. M. Scholey (2007). "The sensory cilia of *Caenorhabditis elegans*." WormBook: 1-22.

Jansen, G., K. L. Thijssen, P. Werner, M. van der Horst, E. Hazendonk and R. H. Plasterk (1999). "The complete family of genes encoding G proteins of *Caenorhabditis elegans*." Nat Genet 21(4): 414-419.

Jansen, G., D. Weinkove and R. H. Plasterk (2002). "The G-protein gamma subunit *gpc-1* of the nematode C.elegans is involved in taste adaptation." EMBO J 21(5): 986-994.

Javitt, D. C. (2009). "Sensory processing in schizophrenia: neither simple nor intact." Schizophr Bull 35(6): 1059-1064.

Jin, Y. (2002). "Synaptogenesis: insights from worm and fly." Curr Opin Neurobiol 12(1): 71-79.

Jospin, M., V. Jacquemond, M. C. Mariol, L. Segalat and B. Allard (2002). "The L-type

voltage-dependent Ca2+ channel EGL-19 controls body wall muscle function in *Caenorhabditis elegans*." J Cell Biol 159(2): 337-348.

Kahn-Kirby, A. H. and C. I. Bargmann (2006). "TRP channels in *C. elegans*." Annu Rev Physiol 68: 719-736.

Kahn-Kirby, A. H., J. L. Dantzker, A. J. Apicella, W. R. Schafer, J. Browse, C. I. Bargmann and J. L. Watts (2004). "Specific polyunsaturated fatty acids drive TRPV-dependent sensory signaling in vivo." Cell 119(6): 889-900.

Kantrowitz, J. T. and D. C. Javitt (2010). "Thinking glutamatergically: changing concepts of schizophrenia based upon changing neurochemical models." Clin Schizophr Relat Psychoses 4(3): 189-200.

Kaplan, J. M. and H. R. Horvitz (1993). "A dual mechanosensory and chemosensory neuron in *Caenorhabditis elegans*." Proc Natl Acad Sci U S A 90(6): 2227-2231.

Kass, J., T. C. Jacob, P. Kim and J. M. Kaplan (2001). "The EGL-3 proprotein convertase regulates mechanosensory responses of *Caenorhabditis elegans*." J Neurosci 21(23): 9265-9272.

Kerr, R., V. Lev-Ram, G. Baird, P. Vincent, R. Y. Tsien and W. R. Schafer (2000). "Optical imaging of calcium transients in neurons and pharyngeal muscle of *C. elegans*." Neuron 26(3): 583-594.

Kessler, J. A., J. E. Adler, M. C. Bohn and I. B. Black (1981). "Substance P in principal sympathetic neurons: regulation by impulse activity." Science 214(4518): 335-

336.

King, A. J. and A. R. Palmer (1985). "Integration of visual and auditory information in bimodal neurones in the guinea-pig superior colliculus." Exp Brain Res 60(3): 492-500.

Kodama, E., A. Kuhara, A. Mohri-Shiomi, K. D. Kimura, M. Okumura, M. Tomioka, Y. Iino and I. Mori (2006). "Insulin-like signaling and the neural circuit for integrative behavior in *C. elegans*." Genes Dev 20(21): 2955-2960.

Komatsu, H., Y. H. Jin, N. L'Etoile, I. Mori, C. I. Bargmann, N. Akaike and Y. Ohshima (1999). "Functional reconstitution of a heteromeric cyclic nucleotide-gated channel of *Caenorhabditis elegans* in cultured cells." Brain Res 821(1): 160-168.

Komatsu, H., I. Mori, J. S. Rhee, N. Akaike and Y. Ohshima (1996). "Mutations in a cyclic nucleotide-gated channel lead to abnormal thermosensation and chemosensation in *C. elegans*." Neuron 17(4): 707-718.

Kosaka, T., K. Kosaka, K. Hama, J. Y. Wu and I. Nagatsu (1987). "Differential effect of functional olfactory deprivation on the GABAergic and catecholaminergic traits in the rat main olfactory bulb." Brain Res 413(1): 197-203.

Kramer, J. M., R. P. French, E. C. Park and J. J. Johnson (1990). "The *Caenorhabditis elegans* rol-6 gene, which interacts with the sqt-1 collagen gene to determine organismal morphology, encodes a collagen." Mol Cell Biol 10(5): 2081-2089.

Kuhara, A., M. Okumura, T. Kimata, Y. Tanizawa, R. Takano, K. D. Kimura, H. Inada,

K. Matsumoto and I. Mori (2008). "Temperature sensing by an olfactory neuron in a circuit controlling behavior of *C. elegans*." Science 320(5877): 803-807.

L'Etoile, N. D. and C. I. Bargmann (2000). "Olfaction and odor discrimination are mediated by the *C. elegans* guanylyl cyclase ODR-1." Neuron 25(3): 575-586.

Lans, H., S. Rademakers and G. Jansen (2004). "A network of stimulatory and inhibitory Galpha-subunits regulates olfaction in *Caenorhabditis elegans*." Genetics 167(4): 1677-1687.

Laughton, D. L., G. G. Lunt and A. J. Wolstenholme (1997). "Alternative splicing of a *Caenorhabditis elegans* gene produces two novel inhibitory amino acid receptor subunits with identical ligand binding domains but different ion channels." Gene 201(1-2): 119-125.

Lee, R. Y., L. Lobel, M. Hengartner, H. R. Horvitz and L. Avery (1997). "Mutations in the alpha1 subunit of an L-type voltage-activated Ca2+ channel cause myotonia in *Caenorhabditis elegans*." EMBO J 16(20): 6066-6076.

Lee, R. Y., E. R. Sawin, M. Chalfie, H. R. Horvitz and L. Avery (1999). "EAT-4, a homolog of a mammalian sodium-dependent inorganic phosphate cotransporter, is necessary for glutamatergic neurotransmission in *Caenorhabditis elegans*." J Neurosci 19(1): 159-167.

Leinwand, S. G. and S. H. Chalasani (2013). "Neuropeptide signaling remodels chemosensory circuit composition in *Caenorhabditis elegans*." Nat Neurosci

16(10): 1461-1467.

Li, W., L. Kang, B. J. Piggott, Z. Feng and X. Z. Xu (2011). "The neural circuits and sensory channels mediating harsh touch sensation in *Caenorhabditis elegans*." Nat Commun 2: 315.

Li, Z., J. Liu, M. Zheng and X. Z. Xu (2014). "Encoding of both analog- and digital-like behavioral outputs by one *C. elegans* interneuron." Cell 159(4): 751-765.

Liedtke, W., D. M. Tobin, C. I. Bargmann and J. M. Friedman (2003). "Mammalian TRPV4 (VR-OAC) directs behavioral responses to osmotic and mechanical stimuli in *Caenorhabditis elegans*." Proc Natl Acad Sci U S A 100 Suppl 2: 14531-14536.

Lindsay, T. H., T. R. Thiele and S. R. Lockery (2011). "Optogenetic analysis of synaptic transmission in the central nervous system of the nematode *Caenorhabditis elegans*." Nat Commun 2: 306.

Liu, J., A. Ward, J. Gao, Y. Dong, N. Nishio, H. Inada, L. Kang, Y. Yu, D. Ma, T. Xu, I. Mori, Z. Xie and X. Z. Xu (2010). "*C. elegans* phototransduction requires a G protein-dependent cGMP pathway and a taste receptor homolog." Nat Neurosci 13(6): 715-722.

Liu, S., E. Schulze and R. Baumeister (2012). "Temperature- and touch-sensitive neurons couple CNG and TRPV channel activities to control heat avoidance in *Caenorhabditis elegans*." PLoS One 7(3): e32360.

Luo, L., Q. Wen, J. Ren, M. Hendricks, M. Gershow, Y. Qin, J. Greenwood, E. R. Soucy, M. Klein, H. K. Smith-Parker, A. C. Calvo, D. A. Colon-Ramos, A. D. Samuel and Y. Zhang (2014). "Dynamic encoding of perception, memory, and movement in a *C. elegans* chemotaxis circuit." Neuron 82(5): 1115-1128.

Mains, R. E. and P. H. Patterson (1973). "Primary cultures of dissociated sympathetic neurons. I. Establishment of long-term growth in culture and studies of differentiated properties." J Cell Biol 59(2 Pt 1): 329-345.

Mains, R. E. and P. H. Patterson (1973). "Primary cultures of dissociated sympathetic neurons. II. Initial studies on catecholamine metabolism." J Cell Biol 59(2 Pt 1): 346-360.

Mains, R. E. and P. H. Patterson (1973). "Primary cultures of dissociated sympathetic neurons. III. Changes in metabolism with age in culture." J Cell Biol 59(2 Pt 1): 361-366.

Maricq, A. V., E. Peckol, M. Driscoll and C. I. Bargmann (1995). "Mechanosensory signalling in *C. elegans* mediated by the GLR-1 glutamate receptor." Nature 378(6552): 78-81.

McIntire, S. L., E. Jorgensen, J. Kaplan and H. R. Horvitz (1993). "The GABAergic nervous system of *Caenorhabditis elegans*." Nature 364(6435): 337-341.

McKay, S. J., R. Johnsen, J. Khattra, J. Asano, D. L. Baillie, S. Chan, N. Dube, L. Fang, B. Goszczynski, E. Ha, E. Halfnight, R. Hollebakken, P. Huang, K. Hung, V.

Jensen, S. J. Jones, H. Kai, D. Li, A. Mah, M. Marra, J. McGhee, R. Newbury, A. Pouzyrev, D. L. Riddle, E. Sonnhammer, H. Tian, D. Tu, J. R. Tyson, G. Vatcher, A. Warner, K. Wong, Z. Zhao and D. G. Moerman (2003). "Gene expression profiling of cells, tissues, and developmental stages of the nematode *C. elegans*." Cold Spring Harb Symp Quant Biol 68: 159-169.

Mellem, J. E., P. J. Brockie, Y. Zheng, D. M. Madsen and A. V. Maricq (2002). "Decoding of polymodal sensory stimuli by postsynaptic glutamate receptors in *C. elegans*." Neuron 36(5): 933-944.

Mello, C. C., J. M. Kramer, D. Stinchcomb and V. Ambros (1991). "Efficient gene transfer in C.elegans: extrachromosomal maintenance and integration of transforming sequences." EMBO J 10(12): 3959-3970.

Meredith, M. A., J. W. Nemitz and B. E. Stein (1987). "Determinants of multisensory integration in superior colliculus neurons. I. Temporal factors." J Neurosci 7(10): 3215-3229.

Meredith, M. A. and B. E. Stein (1986). "Spatial factors determine the activity of multisensory neurons in cat superior colliculus." Brain Res 365(2): 350-354.

Miller, A. C., T. R. Thiele, S. Faumont, M. L. Moravec and S. R. Lockery (2005). "Step-response analysis of chemotaxis in *Caenorhabditis elegans*." J Neurosci 25(13): 3369-3378.

Mills, H., R. Wragg, V. Hapiak, M. Castelletto, J. Zahratka, G. Harris, P. Summers, A.

Korchnak, W. Law, B. Bamber and R. Komuniecki (2012). "Monoamines and neuropeptides interact to inhibit aversive behaviour in *Caenorhabditis elegans*." EMBO J 31(3): 667-678.

Mori, I. and Y. Ohshima (1995). "Neural regulation of thermotaxis in *Caenorhabditis elegans*." Nature 376(6538): 344-348.

Mueller-Pfeiffer, C., M. Schick, T. Schulte-Vels, R. O'Gorman, L. Michels, C. Martin-Soelch, J. R. Blair, M. Rufer, U. Schnyder, T. Zeffiro and G. Hasler (2013). "Atypical visual processing in posttraumatic stress disorder." Neuroimage Clin 3: 531-538.

Mulderry, P. K. (1994). "Neuropeptide expression by newborn and adult rat sensory neurons in culture: effects of nerve growth factor and other neurotrophic factors." Neuroscience 59(3): 673-688.

Nakata, K., B. Abrams, B. Grill, A. Goncharov, X. Huang, A. D. Chisholm and Y. Jin (2005). "Regulation of a DLK-1 and p38 MAP kinase pathway by the ubiquitin ligase RPM-1 is required for presynaptic development." Cell 120(3): 407-420.

Nawa, H., S. Nakanishi and P. H. Patterson (1991). "Recombinant cholinergic differentiation factor (leukemia inhibitory factor) regulates sympathetic neuron phenotype by alterations in the size and amounts of neuropeptide mRNAs." J Neurochem 56(6): 2147-2150.

Nawa, H. and P. H. Patterson (1990). "Separation and partial characterization of

neuropeptide-inducing factors in heart cell conditioned medium." Neuron 4(2): 269-277.

O'Hagan, R. and M. Chalfie (2006). "Mechanosensation in *Caenorhabditis elegans*." Int Rev Neurobiol 69: 169-203.

O'Lague, P. H., K. Obata, P. Claude, E. J. Furshpan and D. D. Potter (1974). "Evidence for cholinergic synapses between dissociated rat sympathetic neurons in cell culture." Proc Natl Acad Sci U S A 71(9): 3602-3606.

Oda, S., M. Tomioka and Y. Iino (2011). "Neuronal plasticity regulated by the insulin-like signaling pathway underlies salt chemotaxis learning in *Caenorhabditis elegans*." J Neurophysiol 106(1): 301-308.

Ohnishi, N., A. Kuhara, F. Nakamura, Y. Okochi and I. Mori (2011). "Bidirectional regulation of thermotaxis by glutamate transmissions in *Caenorhabditis elegans*." EMBO J 30(7): 1376-1388.

Ojemann, G. A., J. Schoenfield-McNeill and D. P. Corina (2002). "Anatomic subdivisions in human temporal cortical neuronal activity related to recent verbal memory." Nat Neurosci 5(1): 64-71.

Okochi, Y., K. D. Kimura, A. Ohta and I. Mori (2005). "Diverse regulation of sensory signaling by *C. elegans* nPKC-epsilon/eta TTX-4." EMBO J 24(12): 2127-2137.

Ortiz, C. O., S. Faumont, J. Takayama, H. K. Ahmed, A. D. Goldsmith, R. Pocock, K. E. McCormick, H. Kunimoto, Y. Iino, S. Lockery and O. Hobert (2009).

"Lateralized gustatory behavior of *C. elegans* is controlled by specific receptor-type guanylyl cyclases." Curr Biol 19(12): 996-1004.

Parush, S., H. Sohmer, A. Steinberg and M. Kaitz (2007). "Somatosensory function in boys with ADHD and tactile defensiveness." Physiol Behav 90(4): 553-558.

Patterson, P. H. and L. L. Chun (1974). "The influence of non-neuronal cells on catecholamine and acetylcholine synthesis and accumulation in cultures of dissociated sympathetic neurons." Proc Natl Acad Sci U S A 71(9): 3607-3610.

Perkins, L. A., E. M. Hedgecock, J. N. Thomson and J. G. Culotti (1986). "Mutant sensory cilia in the nematode *Caenorhabditis elegans*." Dev Biol 117(2): 456-487.

Pierce-Shimomura, J. T., S. Faumont, M. R. Gaston, B. J. Pearson and S. R. Lockery (2001). "The homeobox gene *lim-6* is required for distinct chemosensory representations in *C. elegans*." Nature 410(6829): 694-698.

Piggott, B. J., J. Liu, Z. Feng, S. A. Wescott and X. Z. Xu (2011). "The neural circuits and synaptic mechanisms underlying motor initiation in *C. elegans*." Cell 147(4): 922-933.

Pirri, J. K., A. D. McPherson, J. L. Donnelly, M. M. Francis and M. J. Alkema (2009). "A tyramine-gated chloride channel coordinates distinct motor programs of a *Caenorhabditis elegans* escape response." Neuron 62(4): 526-538.

Pocock, R. and O. Hobert (2010). "Hypoxia activates a latent circuit for processing

gustatory information in *C. elegans*." Nat Neurosci 13(5): 610-614.

Pokala, N., Q. Liu, A. Gordus and C. I. Bargmann (2014). "Inducible and titratable silencing of *Caenorhabditis elegans* neurons in vivo with histamine-gated chloride channels." Proc Natl Acad Sci U S A 111(7): 2770-2775.

Putrenko, I., M. Zakikhani and J. A. Dent (2005). "A family of acetylcholine-gated chloride channel subunits in *Caenorhabditis elegans*." J Biol Chem 280(8): 6392-6398.

Rand, J. B. and R. L. Russell (1984). "Choline acetyltransferase-deficient mutants of the nematode *Caenorhabditis elegans*." Genetics 106(2): 227-248.

Rao, M. S., S. C. Landis and P. H. Patterson (1990). "The cholinergic neuronal differentiation factor from heart cell conditioned medium is different from the cholinergic factors in sciatic nerve and spinal cord." Dev Biol 139(1): 65-74.

Rao, M. S., S. Tyrrell, S. C. Landis and P. H. Patterson (1992). "Effects of ciliary neurotrophic factor (CNTF) and depolarization on neuropeptide expression in cultured sympathetic neurons." Dev Biol 150(2): 281-293.

Reese, T. S. (1965). "Olfactory Cilia in the Frog." J Cell Biol 25(2): 209-230.

Rizzuto, D. S., A. N. Mamelak, W. W. Sutherling, I. Fineman and R. A. Andersen (2005). "Spatial selectivity in human ventrolateral prefrontal cortex." Nat Neurosci 8(4): 415-417.

Roayaie, K., J. G. Crump, A. Sagasti and C. I. Bargmann (1998). "The G alpha protein ODR-3 mediates olfactory and nociceptive function and controls cilium morphogenesis in *C. elegans* olfactory neurons." Neuron 20(1): 55-67.

Rostaing, P., R. M. Weimer, E. M. Jorgensen, A. Triller and J. L. Bessereau (2004). "Preservation of immunoreactivity and fine structure of adult *C. elegans* tissues using high-pressure freezing." J Histochem Cytochem 52(1): 1-12.

Saadat, S., M. Sendtner and H. Rohrer (1989). "Ciliary neurotrophic factor induces cholinergic differentiation of rat sympathetic neurons in culture." J Cell Biol 108(5): 1807-1816.

Sambongi, Y., T. Nagae, Y. Liu, T. Yoshimizu, K. Takeda, Y. Wada and M. Futai (1999). "Sensing of cadmium and copper ions by externally exposed ADL, ASE, and ASH neurons elicits avoidance response in *Caenorhabditis elegans*." Neuroreport 10(4): 753-757.

Sambongi, Y., K. Takeda, T. Wakabayashi, I. Ueda, Y. Wada and M. Futai (2000). "*Caenorhabditis elegans* senses protons through amphid chemosensory neurons: proton signals elicit avoidance behavior." Neuroreport 11(10): 2229-2232.

Sawin, E. R., R. Ranganathan and H. R. Horvitz (2000). "*C. elegans* locomotory rate is modulated by the environment through a dopaminergic pathway and by experience through a serotonergic pathway." Neuron 26(3): 619-631.

Schafer, W. R. and C. J. Kenyon (1995). "A calcium-channel homologue required for

adaptation to dopamine and serotonin in *Caenorhabditis elegans*." Nature 375(6526): 73-78.

Schiller, P. H., J. H. Sandell and J. H. Maunsell (1986). "Functions of the ON and OFF channels of the visual system." Nature 322(6082): 824-825.

Schroder, E., M. Byse and J. Satin (2009). "L-type calcium channel C terminus autoregulates transcription." Circ Res 104(12): 1373-1381.

Segalat, L., D. A. Elkes and J. M. Kaplan (1995). "Modulation of serotonin-controlled behaviors by Go in *Caenorhabditis elegans*." Science 267(5204): 1648-1651.

Shingai, R. (2000). "Durations and frequencies of free locomotion in wild type and GABAergic mutants of *Caenorhabditis elegans*." Neurosci Res 38(1): 71-83.

Shingai, R., H. Ichijo, T. Wakabayashi, H. Tanaka and T. Ogurusu (2014). "Chemotaxis behavior toward an odor is regulated by constant sodium chloride stimulus in *Caenorhabditis elegans*." Neurosci Res 81-82: 51-54.

Skora, S. and M. Zimmer (2013). "Life(span) in balance: oxygen fuels a sophisticated neural network for lifespan homeostasis in *C. elegans*." EMBO J 32(11): 1499-1501.

Snutch, T. P., J. Peloquin, E. Mathews and J. E. McRory (2000). Molecular Properties of Voltage-Gated Calcium Channels. Austin, TX, Landes Bioscience.

Spitzer, N. C. (2015). "Neurotransmitter Switching? No Surprise." Neuron 86(5): 1131-

1144.

Stein, C., J. D. Clark, U. Oh, M. R. Vasko, G. L. Wilcox, A. C. Overland, T. W. Vanderah and R. H. Spencer (2009). "Peripheral mechanisms of pain and analgesia." Brain Res Rev 60(1): 90-113.

Stevenson, R. A., J. K. Siemann, B. C. Schneider, H. E. Eberly, T. G. Woynaroski, S. M. Camarata and M. T. Wallace (2014). "Multisensory temporal integration in autism spectrum disorders." J Neurosci 34(3): 691-697.

Stone, D. M., M. Grillo, F. L. Margolis, T. H. Joh and H. Baker (1991). "Differential effect of functional olfactory bulb deafferentation on tyrosine hydroxylase and glutamic acid decarboxylase messenger RNA levels in rodent juxtaglomerular neurons." J Comp Neurol 311(2): 223-233.

Su, C. Y., K. Menuz, J. Reisert and J. R. Carlson (2012). "Non-synaptic inhibition between grouped neurons in an olfactory circuit." Nature 492(7427): 66-71.

Sulston, J., Z. Du, K. Thomas, R. Wilson, L. Hillier, R. Staden, N. Halloran, P. Green, J. Thierry-Mieg, L. Qiu and et al. (1992). "The *C. elegans* genome sequencing project: a beginning." Nature 356(6364): 37-41.

Sulston, J. E. and H. R. Horvitz (1977). "Post-embryonic cell lineages of the nematode, *Caenorhabditis elegans*." Dev Biol 56(1): 110-156.

Sulston, J. E., E. Schierenberg, J. G. White and J. N. Thomson (1983). "The embryonic cell lineage of the nematode *Caenorhabditis elegans*." Dev Biol 100(1): 64-119.

Summers, P. J., R. M. Layne, A. C. Ortega, G. P. Harris, B. A. Bamber and R. W. Komuniecki (2015). "Multiple Sensory Inputs Are Extensively Integrated to Modulate Nociception in *C. elegans*." J Neurosci 35(28): 10331-10342.

Suzuki, H., T. R. Thiele, S. Faumont, M. Ezcurra, S. R. Lockery and W. R. Schafer (2008). "Functional asymmetry in *Caenorhabditis elegans* taste neurons and its computational role in chemotaxis." Nature 454(7200): 114-117.

Takamori, S., J. S. Rhee, C. Rosenmund and R. Jahn (2000). "Identification of a vesicular glutamate transporter that defines a glutamatergic phenotype in neurons." Nature 407(6801): 189-194.

Tande, D., G. Hoglinger, T. Debeir, N. Freundlieb, E. C. Hirsch and C. Francois (2006). "New striatal dopamine neurons in MPTP-treated macaques result from a phenotypic shift and not neurogenesis." Brain 129(Pt 5): 1194-1200.

Tavernarakis, N., W. Shreffler, S. Wang and M. Driscoll (1997). "unc-8, a DEG/ENaC family member, encodes a subunit of a candidate mechanically gated channel that modulates *C. elegans* locomotion." Neuron 18(1): 107-119.

Thiele, T. R., S. Faumont and S. R. Lockery (2009). "The neural network for chemotaxis to tastants in *Caenorhabditis elegans* is specialized for temporal differentiation." J Neurosci 29(38): 11904-11911.

Tian, L., T. Jiang, M. Liang, Y. Zang, Y. He, M. Sui and Y. Wang (2008). "Enhanced resting-state brain activities in ADHD patients: a fMRI study." Brain Dev 30(5):

342-348.

Tobin, D., D. Madsen, A. Kahn-Kirby, E. Peckol, G. Moulder, R. Barstead, A. Maricq and C. Bargmann (2002). "Combinatorial expression of TRPV channel proteins defines their sensory functions and subcellular localization in *C. elegans* neurons." Neuron 35(2): 307-318.

Tomioka, M., T. Adachi, H. Suzuki, H. Kunitomo, W. R. Schafer and Y. Iino (2006). "The insulin/PI 3-kinase pathway regulates salt chemotaxis learning in *Caenorhabditis elegans*." Neuron 51(5): 613-625.

Troemel, E. R., J. H. Chou, N. D. Dwyer, H. A. Colbert and C. I. Bargmann (1995). "Divergent seven transmembrane receptors are candidate chemosensory receptors in *C. elegans*." Cell 83(2): 207-218.

Troemel, E. R., A. Sagasti and C. I. Bargmann (1999). "Lateral signaling mediated by axon contact and calcium entry regulates asymmetric odorant receptor expression in *C. elegans*." Cell 99(4): 387-398.

Tsalik, E. L. and O. Hobert (2003). "Functional mapping of neurons that control locomotory behavior in *Caenorhabditis elegans*." J Neurobiol 56(2): 178-197.

Vassilatis, D. K., J. P. Arena, R. H. Plasterk, H. A. Wilkinson, J. M. Schaeffer, D. F. Cully and L. H. Van der Ploeg (1997). "Genetic and biochemical evidence for a novel avermectin-sensitive chloride channel in *Caenorhabditis elegans*. Isolation and characterization." J Biol Chem 272(52): 33167-33174.

Von Stetina, S. E., M. Treinin and D. M. Miller, 3rd (2006). "The motor circuit." Int Rev Neurobiol 69: 125-167.

Vowels, J. J. and J. H. Thomas (1994). "Multiple chemosensory defects in *daf-11* and *daf-21* mutants of *Caenorhabditis elegans*." Genetics 138(2): 303-316.

Wakabayashi, T., I. Kitagawa and R. Shingai (2004). "Neurons regulating the duration of forward locomotion in *Caenorhabditis elegans*." Neurosci Res 50(1): 103-111.

Walicke, P. A., R. B. Campenot and P. H. Patterson (1977). "Determination of transmitter function by neuronal activity." Proc Natl Acad Sci U S A 74(12): 5767-5771.

Walicke, P. A. and P. H. Patterson (1981). "On the role of cyclic nucleotides in the transmitter choice made by cultured sympathetic neurons." J Neurosci 1(4): 333-342.

Ward, S., N. Thomson, J. G. White and S. Brenner (1975). "Electron microscopical reconstruction of the anterior sensory anatomy of the nematode *Caenorhabditis elegans*.?2UU." J Comp Neurol 160(3): 313-337.

Ware, R. W., D. Clark, K. Crossland and R. L. Russell (1975). "The nerve ring of the nematode *Caenorhabditis elegans*: Sensory input and motor output." The Journal of Comparative Neurology 162(1): 71-110.

Webber, W. A. and J. Lee (1975). "Fine structure of mammalian renal cilia." Anat Rec 182(3): 339-343.

Weimann, J. M., P. Meyrand and E. Marder (1991). "Neurons that form multiple pattern generators: identification and multiple activity patterns of gastric/pyloric neurons in the crab stomatogastric system." J Neurophysiol 65(1): 111-122.

Weimer, R. M. and E. M. Jorgensen (2003). "Controversies in synaptic vesicle exocytosis." J Cell Sci 116(Pt 18): 3661-3666.

Wes, P. D. and C. I. Bargmann (2001). "*C. elegans* odour discrimination requires asymmetric diversity in olfactory neurons." Nature 410(6829): 698-701.

White, J. G., E. Southgate, J. N. Thomson and S. Brenner (1976). "The structure of the ventral nerve cord of *Caenorhabditis elegans*." Philos Trans R Soc Lond B Biol Sci 275(938): 327-348.

White, J. G., E. Southgate, J. N. Thomson and S. Brenner (1983). "Factors that determine connectivity in the nervous system of *Caenorhabditis elegans*." Cold Spring Harb Symp Quant Biol 48 Pt 2: 633-640.

White, J. G., E. Southgate, J. N. Thomson and S. Brenner (1986). "The structure of the nervous system of the nematode *Caenorhabditis elegans*." Philos Trans R Soc Lond B Biol Sci 314(1165): 1-340.

Williams, P. D. (Unpublished).

Williams, Z. M., G. Bush, S. L. Rauch, G. R. Cosgrove and E. N. Eskandar (2004). "Human anterior cingulate neurons and the integration of monetary reward with motor responses." Nat Neurosci 7(12): 1370-1375.

Wragg, R. T., V. Hapiak, S. B. Miller, G. P. Harris, J. Gray, P. R. Komuniecki and R. W. Komuniecki (2007). "Tyramine and octopamine independently inhibit serotonin-stimulated aversive behaviors in *Caenorhabditis elegans* through two novel amine receptors." J Neurosci 27(49): 13402-13412.

Xiong, W. H., E. C. Solessio and K. W. Yau (1998). "An unusual cGMP pathway underlying depolarizing light response of the vertebrate parietal-eye photoreceptor." Nat Neurosci 1(5): 359-365.

Yamamori, T., K. Fukada, R. Aebersold, S. Korsching, M. J. Fann and P. H. Patterson (1989). "The cholinergic neuronal differentiation factor from heart cells is identical to leukemia inhibitory factor." Science 246(4936): 1412-1416.

Yang, B., J. D. Slonimsky and S. J. Birren (2002). "A rapid switch in sympathetic neurotransmitter release properties mediated by the p75 receptor." Nat Neurosci 5(6): 539-545.

Yang, X. L. (2004). "Characterization of receptors for glutamate and GABA in retinal neurons." Prog Neurobiol 73(2): 127-150.

Zahratka, J. (Unpublished). Unpublished.

Zahratka, J. A., P. D. Williams, P. J. Summers, R. W. Komuniecki and B. A. Bamber (2015). "Serotonin differentially modulates Ca2+ transients and depolarization in a *C. elegans* nociceptor." J Neurophysiol 113(4): 1041-1050.

Zhang, X. and R. H. Cote (2005). "cGMP signaling in vertebrate retinal photoreceptor

cells." Front Biosci 10: 1191-1204.

Zhao, H. and M. L. Nonet (2000). "A retrograde signal is involved in activity-dependent remodeling at a *C. elegans* neuromuscular junction." Development 127(6): 1253-1266.

Zhen, M. and Y. Jin (2004). "Presynaptic terminal differentiation: transport and assembly." Curr Opin Neurobiol 14(3): 280-287.

Zheng, Y., P. J. Brockie, J. E. Mellem, D. M. Madsen and A. V. Maricq (1999). "Neuronal control of locomotion in *C. elegans* is modified by a dominant mutation in the GLR-1 ionotropic glutamate receptor." Neuron 24(2): 347-361.

Zimmer, M., J. M. Gray, N. Pokala, A. J. Chang, D. S. Karow, M. A. Marletta, M. L. Hudson, D. B. Morton, N. Chronis and C. I. Bargmann (2009). "Neurons detect increases and decreases in oxygen levels using distinct guanylate cyclases." Neuron 61(6): 865-879.

Appendix A

Supplementary Data for Chapter 3

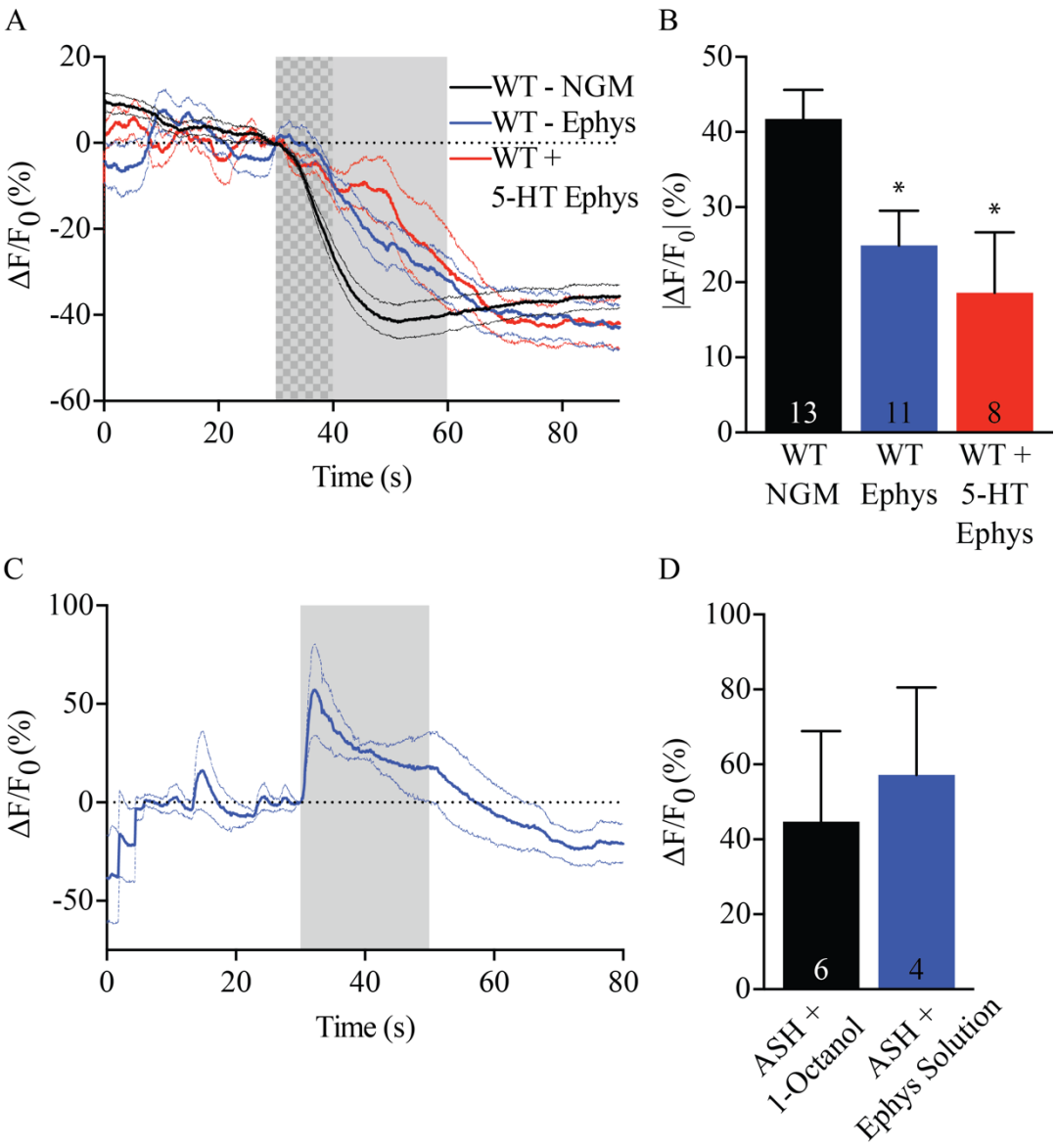

Figure A-1. High NaCl alters sensory-evoked responses. A. Trace averages of 1-octanol-evoked iCa^{2+} transients in the AIBs of wild-type animals. WT - NGM animals received a 10 s exposure (checkered region) and WT - Ephys and WT + 5-HT - Ephys animals received a 30 s exposure (checkered + uniform region). B. Comparison of 1-octanol-evoked iCa^{2+} changes from (A) when WT - NGM is maximally decreased. Data are presented as mean ± SEM and were analyzed by two-tailed Student's *t* test with

Welch's correction. *$p<0.05$, significantly different from wild-type animals under identical conditions. Numbers within bars indicate *n*. C. Trace average of Ephys solution-evoked iCa^{2+} transients in the ASHs of wild-type animals in NGM solution. D. Comparison of the maximum 1-octanol-evoked ASH iCa^{2+} changes from Figure 4A, B and maximum Ephy solution-evoked iCa^{2+} changes from (C). Data are presented as mean ± SEM and were analyzed by two-tailed Student's *t* test with Welch's correction. There is not a significant difference from wild-type 1-octanol-evoked ASH iCa^{2+} changes Numbers within bars indicate *n*.

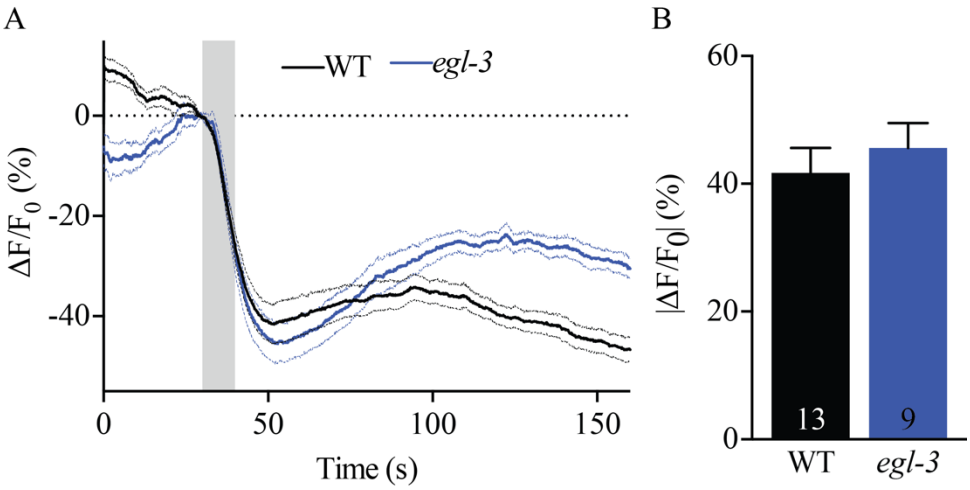

Figure A-2. The EGL-3-processed peptides do not contribute to 1-octanol inhibition of AIB iCa^{2+}. A. Trace averages of 100% 1-octanol-evoked iCa^{2+} transients in the AIBs of wild-type and null animals. B. Comparison of the absolute value of maximum 1-octanol-evoked iCa^{2+} changes, which were all decreases, from (A). Data are presented as mean ± SEM and were analyzed by two-tailed Student's *t* test with Welch's correction. There is not a significant difference from wild-type animals under identical conditions. Numbers within bars indicate *n*.